

ออกซิเดชันของกลีเซอรอลด้วยตัวเร่งปฏิกิริยาทองรองรับบนซิลิกา



นายวิชัย ใบนำเงิน

สถาบันวิทยบริการ  
จุฬาลงกรณ์มหาวิทยาลัย

วิทยานิพนธ์นี้เป็นส่วนหนึ่งของการศึกษาตามหลักสูตรปริญญาวิทยาศาสตรมหาบัณฑิต

สาขาวิชาปิโตรเคมีและวิทยาศาสตร์พอลิเมอร์

คณะวิทยาศาสตร์ จุฬาลงกรณ์มหาวิทยาลัย

ปีการศึกษา 2551

ลิขสิทธิ์ของจุฬาลงกรณ์มหาวิทยาลัย

**GLYCEROL OXIDATION BY SILICA SUPPORTED GOLD CATALYSTS**



**Mr. Taweechai Bainumngern**

**A Thesis Submitted in Partial Fulfillment of the Requirements  
for the Degree of Master of Science Program in Petrochemistry and Polymer Science**

**Faculty of Science**

**Chulalongkorn University**


**Academic Year 2008**

**Copyright of Chulalongkorn University**

Thesis Title           GLYCEROL OXIDATION BY SILICA SUPPORTED  
                                  GOLD CATALYSTS  
By                         Mr. Taweechai Bainumngern  
Field of Study         Petrochemistry and Polymer Science  
Advisor                 Assistant Professor Chawalit Ngamcharussrivichai, Ph.D.  
Co-Advisor            Nipaka Sukpirom, Ph.D.

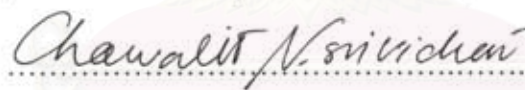
---


Accepted by the Faculty of Science, Chulalongkorn University in Partial  
Fulfillment of the Requirements for the Master's Degree


  
..... Dean of the Faculty of Science  
(Professor Supot Hannongbua, Dr.rer.nat.)

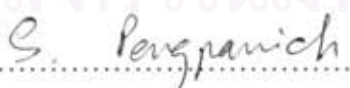
#### THESIS COMMITTEE

  
..... Chairman  
(Professor Pattarapan Prasassarakich, Ph.D.)

  
..... Advisor  
(Assistant Professor Chawalit Ngamcharussrivichai, Ph.D.)

  
..... Co-Advisor  
(Nipaka Sukpirom, Ph.D.)

  
..... Examiner  
(Associate Professor Wimonrat Trakarnpruk, Ph.D.)

  
..... External Examiner  
(Sitthiphong Pengpanich, Ph.D.)

ทวิชัย ไบน้ำเงิน: ออกซิเดชันของกลีเซอรอลด้วยตัวเร่งปฏิกิริยาทองรองรับบนซิลิกา. (GLYCEROL OXIDATION BY SILICA SUPPORTED GOLD CATALYSTS) อ.ที่  
 ปรีกษาวิทยานิพนธ์หลัก: ผศ.ดร. ชวลิต งามจรัสศรีวิชัย, อ.ที่ปรีกษาวิทยานิพนธ์ร่วม: ดร.  
 นิปกา สุขภิรมย์ 86 หน้า.

งานวิจัยนี้ศึกษาการเตรียม วิเคราะห์และประสิทธิภาพตัวเร่งปฏิกิริยา ทองบนซิลิกานชนิด  
 ต่างๆ โดยได้ทำการปรับเปลี่ยนหมู่ฟังก์ชันของซิลิกาและสังเคราะห์ SBA-15 และ MCM-41 ตัวเร่ง  
 ปฏิกิริยาทองสามารถเตรียมได้จากเทคนิค อิมพรีกเนชัน (impregnation) โดยใช้ฟอร์มัลดีไฮด์เป็น  
 ตัวรีดิวซ์เชิงเอเจนต์ และเทคนิคอิม โมบิไลเซชัน (immobilization) นำตัวเร่งปฏิกิริยาที่เตรียม ได้มาใช้  
 เร่งในปฏิกิริยาออกซิเดชันของกลีเซอรอล โดยที่วัสดุรองรับซิลิกา, SBA-15 และ MCM-41 ที่ผ่าน  
 การปรับเปลี่ยนหมู่ฟังก์ชันสามารถเตรียมเป็นตัวเร่งปฏิกิริยาทองบนวัสดุรองรับ ได้อย่างมี  
 ประสิทธิภาพโดยการควบคุมพีเอชในเทคนิคอิม โมบิไลเซชัน ผลที่ได้มีปริมาณทองที่สูงและได้  
 อนุภาคทองขนาดนาโน การควบคุมพีเอชของสารละลายในปฏิกิริยาทำได้โดยเติม โซเดียมไฮดรอก  
 ไซด์ในปริมาณที่เหมาะสมเพื่อช่วยปรับปรุงร้อยละการเปลี่ยนของกลีเซอรอล ส่วนการทำปฏิกิริยา  
 ออกซิเดชันของกลีเซอรอลพบว่าเมื่อเวลาผ่านไป กรดกลีเซอริกที่ได้จะเปลี่ยนไปเป็นผลิตภัณฑ์  
 อื่นๆ ผลของการควบคุมพีเอชพบว่าที่พีเอช 11 จะมีความจำเพาะต่อการเกิดกรดกลีเซอริกที่เสถียร  
 มากกว่าที่พีเอช 12 และผลของการใช้แก๊สออกซิเจนที่เพิ่มขึ้น ทำให้ได้ร้อยละการเปลี่ยนแปลงของ  
 กลีเซอรอล เพิ่มขึ้นแต่จะมีผลน้อยกว่าการเปลี่ยนแปลงของพีเอชในสารละลายในปฏิกิริยา  
 ออกซิเดชันของกลีเซอรอล

## สถาบันวิทยบริการ จุฬาลงกรณ์มหาวิทยาลัย

สาขาวิชา ปิโตรเคมีและวิทยาศาสตร์พอลิเมอร์ ลายมือชื่อนิสิต ..... ทวิชัย ไบน้ำเงิน .....

ปีการศึกษา .....2551..... ลายมือชื่อ อ. ที่ปรีกษาวิทยานิพนธ์หลัก .....  
 ลายมือชื่อ อ. ที่ปรีกษาวิทยานิพนธ์ร่วม ..... สุเมธ งามจรัสศรีวิชัย .....

## 497 23023 23 : MAJOR PETROCHEMISTRY AND POLYMER SCIENCE

KEYWORDS : MODIFIED SILICA GEL / AMIDOXIME / GOLD NANOPARTICLES

TAWEECHAI BAINUMNGERN: GLYCEROL OXIDATION BY SILICA SUPPORTED GOLD CATALYSTS. ADVISOR: ASST.PROF. CHAWALIT NGAMCHARUSSRIVICHAH, Ph.D., CO-ADVISER: NIPAKA SUKPIROM, Ph.D., 86 pp.

This thesis has studied the preparation, characterization and performance test of various supported gold catalysts. The preparation has been focused on immobilization of gold on amido-amidoxime functionalized SiO<sub>2</sub> and mesoporous materials, i.e. MCM-41 and SBA-15. The conventional impregnation method using HCOH as a reducing agent was applied for comparison. The catalytic performance of supported nanogold was investigated in the liquid phase oxidation of glycerol using molecular oxygen at atmospheric pressure. Amido-SiO<sub>2</sub>, Amido-MCM-41 and Amido-SBA-15 supported Au catalysts were successfully prepared through the pH-controlling immobilization method, resulting in the high gold content and the formation of gold particles with nanosize. Controlling pH of reaction mixture by addition of a suitable amount of NaOH solution improved the glycerol conversion. The pH was optimized at 11 since it maintained the glyceric acid selectivity at a high value. The glycerol conversion was slightly enhanced by increasing the flow rate of O<sub>2</sub>. It seems that this influence affected the reaction at much less extent than the pH of reaction solution.

สถาบันวิทยบริการ  
จุฬาลงกรณ์มหาวิทยาลัย

Field of Study: ...Petrochemistry and Polymer Science... Student's Signature: *Taweechai Bainumngern*

Academic Year: .....2008..... Advisor's Signature: *Chawalit Ngsrivichai*

Co-Advisor's Signature: *Nipaka Sukpirom*



## ACKNOWLEDGEMENTS

The author would like to express my gratitude and appreciation to my advisor, Assistant Professor Dr. Chawalit Ngamcharussrivichai and co-Adviser, Dr. Nipaka Sukpirom for guidance, support and supervision during this study. The author is grateful to my thesis committees Professor Pattarapan Prasassarakich; Assistant Professor Wimonrat Trakarnpruk; Dr. Sitthiphong Pengpanich for their comments and suggestions.

Many thanks go to Assistant Professor Dr. Apichat Imyim for guidance, support and supervision during this study and Dr. Nipaka Sukpirom for suggestions on solving some research problems.

The author is also thank National Center of Excellence for Petroleum, Petrochemicals and Advanced Materials. (NCE-PPAM) and the author would like to thank National Nanotechnology Center (NANOTEC), Thailand.

Finally, the author would like to especially thank my family members for their love, kindness and support throughout the entire education.

สถาบันวิทยบริการ  
จุฬาลงกรณ์มหาวิทยาลัย

# CONTENTS

	<b>page</b>
ABSTRACT (THAI).....	iv
ABSTRACT (ENGLISH).....	v
ACKNOWLEDGEMENTS.....	vi
CONTENTS.....	vii
LIST OF TABLES.....	x
LIST OF FIGURES.....	xi
LIST OF SCHEMES .....	xiii
LIST OF ABBREVIATIONS.....	xiv
<b>CHAPTER I INTRODUCTION.....</b>	<b>1</b>
1.1 Statement of the problem.....	1
1.2 Objective of this research .....	2
1.3 Scope of the research.....	2
<b>CHAPTER II THEORY AND LITERATURE REVIEW.....</b>	
2.1 Properties of gold.....	3
2.1.1 Colloidal Gold .....	3
2.1.2 Gold's Properties at the Nanoscale .....	4
2.1.3 Crystal structure and morphology .....	4
2.2 Catalytic properties of gold .....	5
2.3 Preparation supported catalysts.....	6
2.3.1 Preparation of active gold catalysts .....	7
2.3.1.1 Preparation of gold nanoparticles .....	8
2.3.2 Removal of chloride .....	8
2.4 Application of gold nanoparticles.....	9
2.4.1 Catalyst .....	9
2.4.2 The catalytic activities of metals.....	10
2.5 Particle size and sensitivity of gold catalysts towards reaction condition .....	10

	<b>page</b>
2.6 Interaction of oxygen with gold .....	11
2.7 Oxidation of alcohol .....	11
2.7.1 Oxidizing Agents .....	12
2.7.2 Homogeneous catalyst .....	13
2.7.3 Heterogeneous catalyst .....	14
2.8 Oxidation of a triol: glycerol .....	15
2.9 Literature review.....	16
<b>CHAPTER III EXPERIMENTAL.....</b>	
3.1 Chemicals.....	19
3.1.1 Chemicals.....	19
3.1.2 Reagents.....	20
3.2 Analytical instruments.....	21
3.3 Characterization of nanogold and determination of gold content.....	22
3.3.1 X-ray diffractometry (XRD) .....	22
3.3.2 X-ray fluorescence spectrometry (XRF).....	23
3.3.3 Transmission electron microscopy (TEM).....	24
3.3.4 BET Surface Area & Pore Size Distribution Analysis .....	25
3.3.5 High performance liquid chromatography (HPLC).....	27
3.4 Substrate preparation .....	28
3.4.1 Synthesis of amido-amidoxime functionalized silica.....	28
3.4.2 Synthesis of SBA-15 .....	29
3.4.3 Synthesis of MCM-41 .....	29
3.5 Preparation of gold nanoparticles.....	30
3.5.1 Preparation procedures .....	30
3.6 Characterization of silica .....	30
3.7 Batch method.....	31
3.8 Oxidation glycerol to glyceric acid .....	30
3.8.1 Result of method verification .....	32
3.8.2 Influence of various supported Au catalysts on glycerol oxidation.....	32



	<b>page</b>
<b>CHAPTER IV RESULTS AND DISCUSSION.....</b>	
4.1 Characterization of amido-amidoxime functionalized silica.....	34
4.1.1 Determination of surface functional groups .....	34
4.1.2 Elemental analysis .....	35
4.2 Characterization of supported gold catalysts .....	35
4.2.1 Effect of supported gold catalysts .....	37
4.2.2 Effect of pH during immobilization .....	39
4.3 Oxidation of glycerol with molecular oxygen .....	40
4.3.1 Influence of reaction time .....	40
4.3.2 Influence of NaOH/glycerol ratio .....	42
4.3.3 Influence of pH controlling .....	43
4.3.4 Influence of O <sub>2</sub> flow rate .....	44
4.3.5 Influence of support types .....	46
4.3.5.1 Influence of Amido-amidoxime functionalized SBA-15 ...	46
4.3.5.2 Influence of various support types .....	47
4.3.6 Influence of calcinations .....	48
4.3.6.1 Influence of calcination of Au/Amido-SiO <sub>2</sub> .....	48
4.3.6.2 Influence of calcinations of Au/Amido-MCM-41 .....	50
4.3.7 Influence of pH during immobilization of Au .....	51
<b>CHAPTER V CONCLUSION AND RECOMMENDATION.....</b>	
5.1 Conclusions .....	53
5.2 Recommendation .....	54
<b>REFERENCES.....</b>	<b>55</b>
<b>APPENDICES</b>	
APPENDIX A .....	60
APPENDIX B .....	64
APPENDIX C .....	80
APPENDIX D .....	81
<b>VITA.....</b>	<b>86</b>

**LIST OF TABLES**

<b>TABLE</b>		<b>PAGE</b>
3.1	Chemical list	19
3.2	Analytical instruments	21
3.3	Conditions for analysis of reaction products by using High Performance Liquid Chromatographic (HPLC)	31
4.1	Elemental composition of functionalized silica	35
4.2	Physicochemical properties of supported Au catalysts	36
4.3	Calculated turnover number (TON)	37
4.4	Glycerol oxidation over various supported Au catalysts	40
4.5	Glycerol conversion and glyceric acid selectivity over Au/Amido-SiO <sub>2</sub> at different pH controlling	44
4.6	Glycerol conversion and product distribution in the oxidation of glycerol with different O <sub>2</sub> flow rate over Au/Amido-SiO <sub>2</sub> catalyst	45
4.7	Glycerol conversion and glyceric acid selectivity over Au/SBA-15 and Au/Amido-SBA-15 catalyst	47
4.8	Glycerol oxidation over various supported Au catalysts	48
4.9	Glycerol conversion and glyceric acid selectivity over Au/Amido-SiO <sub>2</sub> catalyst calcined at different temperatures	50
4.10	Glycerol oxidation and glyceric acid selectivity over Au/Amido-MCM-41 catalysts	51
4.11	Glycerol oxidation over various supported Au catalysts	52

## LIST OF FIGURES

FIGURE	PAGE
2.1 Comparison of (a) truncated octahedron, (b) icosahedron, (c) Marks decahedron and (d) cuboctahedron	5
2.2 The oxidation of alcohols	11
2.3 Oxidation alternatives.	13
2.4 The catalytic cycle for the reaction of $A + B \rightarrow C$ .	14
2.5 Reaction network of the glycerol oxidation.	16
3.1 Diffraction of X-rays by a crystal.	22
3.2 Energy dispersive X-ray fluorescence spectrometer	23
3.3 The synthetic pathway of Amido-SiO <sub>2</sub> .	28
3.4 Calibration curve for glycerol solution.	32
4.1 FT-IR spectra of SiO <sub>2</sub> , AP-SiO <sub>2</sub> , CA-SiO <sub>2</sub> and Ami-SiO <sub>2</sub> in KBr.	34
4.2 TEM micrographs of supported gold catalysts.	37
4.3 TEM micrograph of Amido-SiO <sub>2</sub> and gold nanoparticles at different pH	38
4.4 Dependence of (a) glycerol conversion and (b) glyceric acid selectivity on time in the oxidation of glycerol at different supported gold catalysts. Without pH adjustment	40
4.5 Influence of NaOH/glycerol molar ratios on the glycerol conversion and the glyceric acid selectivity in the oxidation of glycerol over Au/C	41
4.6 Dependence of (a) glycerol conversion and (b) glyceric acid selectivity on time in the oxidation of glycerol over Au/Amido-SiO <sub>2</sub> immobilized at different pH.	42
4.7 Dependence of (a) glycerol conversion and (b) glyceric acid selectivity on time in the oxidation of glycerol over Au/Amido-SiO <sub>2</sub> immobilized at different O <sub>2</sub> flow rate.	44
4.8 Dependence of (a) glycerol conversion and (b) glyceric acid selectivity on time in the oxidation of glycerol compare with Au/SBA-15 and Au/Amido-SBA-15.	45

FIGURE	PAGE
4.9 Dependence of (a) glycerol conversion and (b) glyceric acid selectivity on time in the oxidation of glycerol Au/Amido-SiO <sub>2</sub> calcined at different temperature.	48
4.10 Dependence of (a) glycerol conversion and (b) glyceric acid selectivity on time in the oxidation of glycerol over Au/Amido-SiO <sub>2</sub> immobilized at different pH.	51



สถาบันวิทยบริการ  
จุฬาลงกรณ์มหาวิทยาลัย

**LIST OF SCHEME**

<b>SCHEME</b>	<b>PAGE</b>
2.1 Potential areas within automotive systems for using nanoparticulated gold catalysts	9
3.1 Schematic diagram of transmission electron microscope.	24
3.2 Schematic diagrams of BET Surface Area and Pore Structure	25
3.3 Schematic diagram of high performance liquid chromatography.	27



สถาบันวิทยบริการ  
จุฬาลงกรณ์มหาวิทยาลัย



## LIST OF ABBREVIATIONS

°C	degree Celsius
cm <sup>-1</sup>	unit of wavenumber
g	gram(s)
h	hour(s)
mL	milliliter
mmol	millimole
% wt	Percent by weight
ATM	ammonium tetrathiomolybdate
ASTM	The American Society for Testing and Material
BET	Brunauer-Emmett-Teller method
EDX	energy dispersive x-ray
FID	flame ionization detector
HPLC	high performance liquid chromatograph
SEM	scanning electron microscope
SRGO	straight run gas oil
XRD	x-ray diffraction
XRF	x-ray fluorescence

สถาบันวิทยบริการ  
จุฬาลงกรณ์มหาวิทยาลัย

# CHAPTER I

## INTRODUCTION

### 1.1 Statement of the problem

Nowadays, glycerol has attracted much attention as a bio-sustainable starting material for syntheses of a large number of valuable compounds, such as dihydroxyacetone, glyceric acid, and glyceraldehyde, because of its availability, low cost and high functionality. Glycerol is increasingly produced as a by-product from the syntheses of biodiesel and other oleochemicals. Oxidation reaction is of industrial importance for converting glycerol to such a high-value added chemical. Based on the conventional process involving stoichiometric oxidants, e.g. permanganate or chromic acid, a significant amount of various by-products is formed. An environmentally friendly alternative is the oxidation in the presence of a heterogeneous catalyst and molecular oxygen [1].

Gold catalysts operating in the aqueous phase also have been shown to be highly active for the oxidation of various alcohols and, in particular, glycerol. Conversion of glycerol is of interest because it is a byproduct of biodiesel production from plant and animal oils. A major surplus of glycerol has resulted from rapid expansion of biodiesel production capacity around the world. The oxidation of glycerol over Au catalysts is one possible route for using this bio-renewable feedstock [2-3]. In the present work, we have focused our attention on the syntheses of valuable chemicals via the heterogeneously catalyzed liquid-phase oxidation of glycerol under atmospheric pressure by fine tuning between catalyst design and reaction conditions. Different kinds of supports, including activated carbon, silica gel ( $\text{SiO}_2$ ), amidoxime-functionalised silica gel (Amido- $\text{SiO}_2$ ) were used for the preparation of nanogold catalysts. The influences of catalyst preparation methods and reaction conditions, concomitantly with the catalyst characterizations, have been investigated to optimize the conversion and the product selectivity.

Several studies have reported various gold nanoparticles supported on different carbons (carbon black, activated carbon and graphite) and oxides ( $\text{TiO}_2$ ,  $\text{MgO}$  and  $\text{Al}_2\text{O}_3$ ) were active.

In this work, silica was functionalized with amido-amidoxime functional group and used to study the optimized condition for oxidation of glycerol

### 1.2 Objective of this research

1. To prepare amidoxime functionalised silica supported gold catalysts.
2. To study the effect of reaction conditions on the production of glyceric acid from glycerol oxidation over the supported gold catalysts.

### 1.3 Scope of the research

The scope of this research is the synthesis of amidoxime functionalised silica and used as support for the preparation of nano-sized gold catalysts. The prepared catalysts were characterized by XRD, XRF, TEM, CHN and N<sub>2</sub> adsorption-desorption measurement techniques. To investigate effect of reaction of glycerol oxidation i.e. the effect of reaction time, the effect of NaOH/glycerol molar ratios. Then the synthesized silica is brought to find suitable condition for oxidation of glycerol.



สถาบันวิทยบริการ  
จุฬาลงกรณ์มหาวิทยาลัย

## CHAPTER II

### THEORY AND LITERATURE REVIEWS

#### 2.1 Properties of gold

There are a few chemical substances that can attack gold: the most notable is called aqua regia (literally, 'royal water') and is made from a mixture of hydrochloric acid and nitric acid. This is sometimes used for etching a gold surface. Another is sodium cyanide (NaCN) which is used in the extraction of gold from ore. These are unusual, though, and in general, gold is safe from attack by most chemicals. Both metallic gold and gold compounds were useful in several aspects. The density of gold ( $19.3 \text{ gcm}^{-3}$ ) depends on both its atomic mass and the crystal structure [4]. This makes gold rather heavy compared to some other common materials. For example, aluminium has a density of  $2.7 \text{ gcm}^{-3}$  and even steel's density is only  $7.87 \text{ gcm}^{-3}$ . The melting point of pure gold is  $1064^\circ\text{C}$ , although when alloyed with other elements such as silver or copper the gold alloy will melt over a range of temperatures. The boiling point of gold, when gold transforms from the liquid to gaseous state, is  $2860^\circ\text{C}$ . The ability of gold to efficiently transfer heat and electricity is bettered only by copper and silver, but unlike these metals gold does not tarnish, making it indispensable in electronics.

##### 2.1.1 Colloidal Gold

Colloidal gold, which consists of gold nanoparticles, has been known since ancient times, and was originally used as a method of staining glass. It is produced from tetrachlorogold(III) acid by, firstly, addition of alkali, whereupon successive replacement of chlorine atoms by hydroxyl groups occurs, to form the unstable tetrahydroxygold(III) ion,  $[\text{Au}(\text{OH})_4]^-$ .



This is used as a test for all gold compounds, because they are all easily reduced in alkaline solution to metallic gold which, being in colloidal form, may appear red, blue or intermediate colors due to light scattering. Nowadays, colloidal gold finds application in a wide variety of areas, including medicine, electronics, and nanotechnology. In the medical fields, an interesting application of gold nanoparticles is in 'immunogold labeling' of antibodies, for detection of antigens under the electron microscope [5].

### **2.1.2 Gold's Properties at the Nanoscale**

The color of gold nanoparticles may range from red through purple to blue and almost black. This is due to a change in their absorption spectrum on the formation of aggregates. A melting point of gold nanoparticle is shrunken from that of bulk gold. The reason for this phenomenon is the huge increase in surface area of gold nanoparticles. It is important to draw a distinction between the properties of gold in the bulk form and those properties it exhibits when present in the form of tiny nanoparticles. The unique properties of gold at the nanoscale lead to its use in a growing number of applications including colloids for biomedical marking and catalysts in chemical processing and pollution control.

### **2.1.3 Crystal structure and morphology**

In the bulk form gold has the face centred cubic (fcc) structure which is closest-packed. Naturally-occurring macro-crystals of native gold exhibit the highly symmetrical cubic, octahedral or rhombododecahedral crystal forms associated with this crystal structure [6]. However, there is debate and even confusion in the literature regarding the structure and external form of nano-particles of gold [7], arising no doubt from the difficulties inherent in trying to physically characterize such tiny objects. As a result, several attempts have been made to predict the structure of gold nanoparticles using molecular dynamics or other calculations. However, there is not yet complete agreement between the results of the calculations and of the experimental measurements, with conflicting claims being made for icosahedral or



decahedral quasi-crystal structures, amorphous structures, or octahedra, cuboctahedra and truncated octahedra based on fcc packing. . Some shapes of gold nanoparticles are shown in Figure 2.1 [8]. The surface plasmon band (SPB) of gold nanoparticle is a characteristic electronic property which exhibits a broad absorption band in the visible region around 520 nm due to the crystalline structure of gold nanoparticle. The SPB is the result from the collective oscillation of the electron cloud at the surface of nanoparticles that is correlated with the electromagnetic field of the incoming light.

The crystalline structure of gold at the nanoscale differs from the bulk one. Several attempts have been made to predict the structure of gold nanoparticles by calculation. In general, the results from calculations are not completely in agreement, either with each other or with the results of experimental techniques

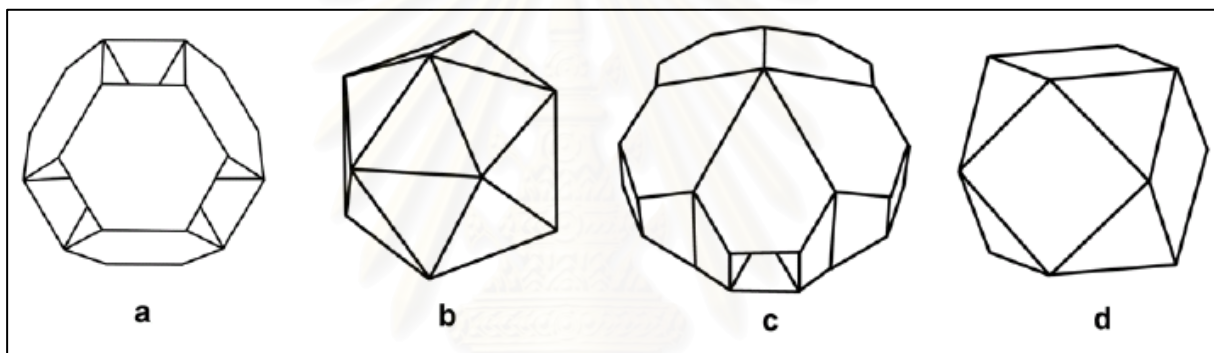


**Figure 2.1** Comparison of (a) truncated octahedron, (b) icosahedron, (c) Marks decahedron and (d) cuboctahedron [8].

## 2.2 Catalytic properties of gold

Gold has traditionally been regarded as inactive as a catalytic metal. However, the advent of nanoparticulate gold on high surface area oxide supports has demonstrated its high catalytic activity in many chemical reactions. Gold is active as a heterogeneous catalyst in both gas and liquid phases, and complexes catalyze reactions homogeneously in solution. Many of the reactions being studied will lead to new application areas for catalysis by gold in pollution control, chemical processing, sensors and fuel cell technology.

### **2.3 Preparation supported catalysts**

There are three different methods for the preparation of supported nanogold catalysts, (a) Impregnation (b) Coprecipitation (c) Deposition-precipitation

#### **(a) Impregnation**

Impregnating methods used to seal porosity in metal castings, powder metal parts, and electrical components are typically performed by one of four different processes. Choosing the best process depends on a variety of factors such as: (i) number and size of parts to be impregnated, (ii) material used to produce the part, (iii) size and amount of porosity contained in the parts, (iv) desired sealing results, (v) economics [9].

Impregnation method can be divided into two types;

##### **(i) Wet Impregnation**

This method can be prepared by adding an excess amount of metal salt solution into supports. The composition of the solution will be changed slowly as the metal is absorbed on the surface. Thus, the metal content on the support will not be equal to the initial content in the solution. Besides, the release of support debris in the solution might form a mud, which makes it difficult to separate from the catalyst.

##### **(ii) Dry Impregnation or Impregnation to incipient wetness**

This method is favored for industrial catalysts because the solution of metal salt will be dispersed by spraying on supports. The volume of solution should be equal to the pore volume of support in order to control the amount of active component. The required catalyst was obtained after drying and calcinations step.

### **(b) Coprecipitation**

Solutions of salt of the catalytically active material and of the support are prepared, to which a precipitating agent is added, such as NaOH or NaHCO<sub>3</sub>. As a result hydroxides or hydroxyl salts precipitate and form a homogeneous mixture that is filtered off. Removal of CO<sub>2</sub> and water during drying and calcinations, and of oxygen during reduction, yields a porous catalyst. The process is difficult to control; it is essential to keep the solution homogeneous to allow the two components to precipitate simultaneously, and variations of pH throughout the solution should be avoided

### **(c) Deposition-precipitation**

The deposition-precipitation method is that small crystallites of metal hydroxide or carbonate precipitate from solution, preferably by heterogeneous nucleation at the interface between liquid and support. To this end the support powder is suspended in the metal solution, and a base is added to raise the pH. As the pH must be homogeneous throughout the solution, efficient stirring is required, which, however, poses problems in large volumes, as well as in porous systems.

#### **2.3.1 Preparation of active gold catalysts**

In general, the widely used catalysts based on the platinum group metals are produced by impregnating a porous ceramic substrate with a solution of metal salt, followed by drying, and then thermal decomposition to produce a dispersion of metallic particles loaded onto a meso-porous oxide or other support. In addition, optimum use of such catalysts generally requires some form of chemical reduction of the metallic particle immediately prior to use. As a general observation, attempts to prepare active gold-based catalysts by this route produce indifferent results [10]. It has become abundantly evident that gold only becomes catalytically active in very particular instances. However, one fact that is agreed is that active gold catalysts may be reliably produced by attaching nanoparticles of gold to the surface of particular transition metal oxides by co-precipitating the transition metal and the gold (possibly

in the form of thermally unstable hydroxides or carbonates) followed by a calcinations treatment, or by deposition-precipitating the  $\text{Au}(\text{OH})_3$  onto a previously synthesised oxide substrate, followed by a calcination treatment. Details of the preparation techniques for successful catalysts vary widely between laboratories, with the effects of aging, stirring, washing, order in which reactants are added, temperature, concentration of reactants, and calcining conditions.

### **2.3.1.1 Preparation of gold nanoparticles**

For metal nanoparticles, their physical and chemical properties are dependent of their size and shape. Thus, controlling the morphology and size of nanoparticles are important which achieved by varying stabilizer, reducing agent and all the conditions. Currently, the various methods of synthesis nanoparticles are explored. The preparation of gold nanoparticles has received considerable attention due to their interesting application. Gold nanoparticles could be synthesized in aqueous solution by the chemical reduction. Gold nanoparticles can be formed by using some special substances present in both solid and solution forms. The reaction between the substances and Au (III) is often a redox reaction which changes the oxidation state of gold from 3 to 0 (gold nanoparticles). The reducing agents have been utilized for the reduction of gold (III) to gold nanoparticles. Typical reducing agents for the preparation of gold nanoparticles include  $\text{NaBH}_4$ , citrate salts and hydroxylamine [11-14].

### **2.3.2 Removal of chloride**

After preparation of supported of gold catalyst, the presence of chloride was still contained chloride in its coordination sphere. It might be sintered to form rather large gold particles during calcinations. Thus, for most catalysts, the residual Cl was removed by washing with  $\text{NaOH}$ ,  $\text{NH}_4\text{OH}$ , or water until the washings contained no chloride.

## 2.4 Application of gold nanoparticles

The properties of gold nanoparticles are ensuring that gold is a candidate material for nanotechnology applications in the diverse areas of electronics, catalysis, biomedical and coating. The applications have found in many different field of science.

### 2.4.1 Catalyst

Recently gold is used as a catalyst in chemical processing. In the field of selective oxidation, Dow Chemical Company has patented the selective production of propene oxide by the epoxidation of propene in the presence of hydrogen and gold on  $\text{TiO}_2/\text{SiO}_2$  catalyst [15]. Gold nanoparticles have been used in pollution control and fuel cell. The basis of fuel cell energy generation is believed that there are significant opportunities for gold catalysts in automotive industry [16]. The automotive systems for using gold nanoparticles are shown in Table 2.2. The ability of gold to oxidize CO and remove  $\text{NO}_x$  compounds offers scope for air quality improvement and control of malodors. They can apply in buildings, transport or other applications.

**Scheme 2.1** Potential areas within automotive systems for using nanoparticulated gold catalysts

Automotive Power Source	Application for Gold Based Catalysts	Reaction (s)	Main Characteristic of Supports Gold Nanoparticulate Catalyst
Fuel cell	Fuel processing System for clean $\text{H}_2$ production	Water gas shift reaction for $\text{H}_2$ production	High activity at low Temperature
		Preferential oxidation of CO for $\text{H}_2$ clean up	High activity at low Temperature
		Methanol decomposition for $\text{H}_2$ production	High activity
	Fuel cell catalyst	Oxidation removal of CO From $\text{H}_2$	Improvement in electrical conductivity
Diesel Engine	Component of TWC For diesel engine Emission control	CO and HC Combustion and $\text{NO}_x$ reduction HC	Low temperature activity (and high for $\text{NO}_x$ reduction)
Petrol Engine	Low light off catalyst For petrol engine	CO and HC combustion	Low temperature activity



### **2.4.2 The catalytic activities of metals**

The kinds of reactions catalysed by various types of solid are determined by the ability of the surface to convert the reactants into adsorbed forms that are conducive to making the desired products. So, for example, the metals of groups 8-10 are particularly adept at reactions that require the dissociation of hydrogen molecules, i.e. hydrogenolysis. Metals of group 11 have the reputation of adsorbing hydrogen only weakly, and they are not therefore versatile catalysts for reactions needing hydrogen atoms. The base metals are useless for oxidations because they so readily become oxidized and it is only the noble metals of these Groups that are useful oxidation catalysts, and then it is generally for non-selective or deep oxidation. Many transition metal oxides make splendid selective oxidation catalysts, and some of them, and particularly mixtures of them, are renowned for catalyzing the selective oxidation of alkenes, alkanes and aromatic molecules [17].

### **2.5 Particle size and sensitivity of gold catalysts towards reaction condition**

The size of gold particles is a very important parameter in obtaining active catalysts for many reactions [18,19]. The perceived importance of particle size for determining the catalytic activity of gold for some if not all reactions requires us to examine carefully how the physical properties vary with this parameter. The method of preparation strongly influences the particle size. Activity depends not only on the obvious variables (method, type of support, gold particle size and preparation method). On particle size effect of supported gold catalysts in liquid phase oxidation reaction has already been reported [20]. There is general agreement that small gold particle show higher activities with smaller gold particle size. Moreover, the mean gold particle size influences not only the catalytic activity but also the selectivity of the catalyst.

## 2.6 Interaction of oxygen with gold

There have been many attempts over the years to establish under what conditions if any molecular oxygen is chemisorbed by gold. The consensus is that under ambient conditions of temperature and pressure it does not take place on massive gold, so that much of the reported work has had the intention of delimiting the range of conditions under which it does not.

## 2.7 Oxidation of alcohol

The conversion of alcohols into aldehydes and ketones is one of the most common and most useful transformations available to the synthetic organic chemist. The general features of this oxidation reaction are outlined in Figure 2.2 [21].

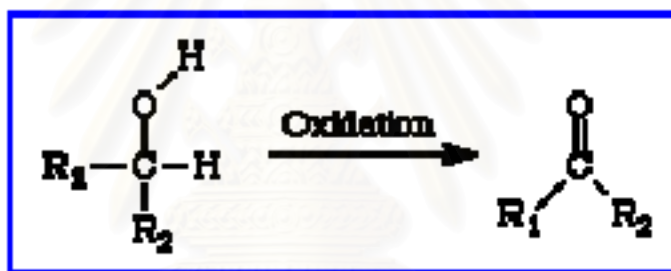
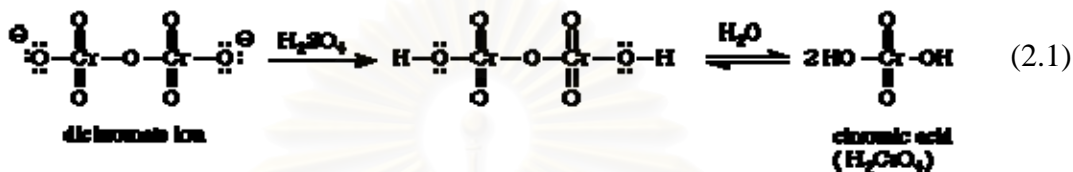


**Figure 2.2** The oxidation of alcohols.

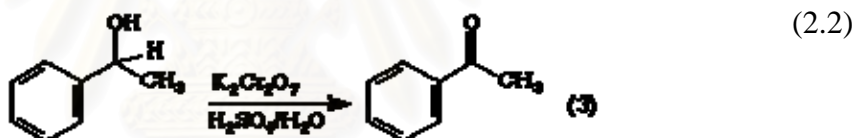
A synonym for the oxidation of alcohols, dehydrogenation, suggests the structural feature that is required for this process: H-C-O-H. The OH group must be attached to a carbon atom that is bonded to at least one hydrogen atom. In other words, oxidation of alcohols involves the 1,2-elimination of "the elements of" dihydrogen, H and H.

### 2.7.1 Oxidizing Agents

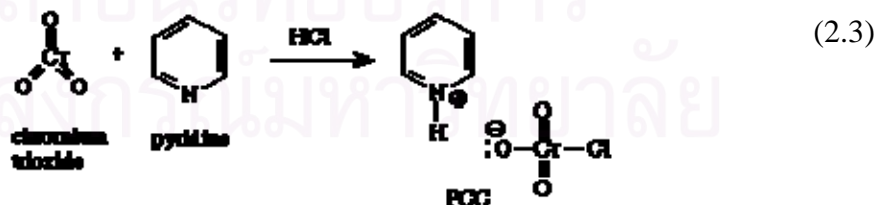
There is a wide variety of reagents that are used for the oxidation of alcohols. Two of the most common are chromic acid,  $\text{H}_2\text{Cr}_2\text{O}_7$ , and pyridinium chlorochromate, PCC [22]. Chromic acid is prepared by treatment of sodium or potassium dichromate with aqueous sulfuric acid.



Chromic acid is most commonly used to oxidize  $2^\circ$  alcohols to ketones. One example is given in Equation 2.1.



Pyridinium chlorochromate is made by mixing chromium trioxide with pyridine and hydrochloric acid as indicated in Equation 2.2. The oxidizing component of PCC is the chlorochromate anion,  $\text{CrClO}_3^-$ .



PCC was developed especially for the oxidation of  $1^\circ$  alcohols to aldehydes, a transformation which is difficult to accomplish using chromic acid because aldehydes react rapidly with aqueous chromic acid to produce carboxylic acids.

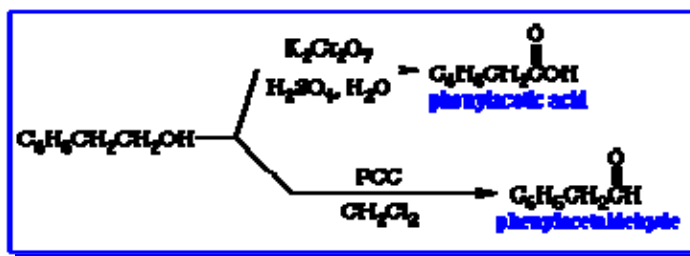


**Figure 2.3** compares the oxidation of 2-phenylethanol by chromic acid and PCC.

### 2.7.2 Homogeneous catalyst

In a homogeneous reaction, the catalyst is in the same phase as the reactants. A major obstacle to the commercialization of homogeneous catalysts is that they are often difficult to separate from the reaction products and the solvent. We are attempting to tackle this in a number of different ways. This is a solution reaction that you may well only meet in the context of catalysis, Persulphate ions (peroxodisulphate ions),  $S_2O_8^{2-}$ , are very powerful oxidising agents. Iodide ions are very easily oxidised to iodine. And yet the reaction between them in solution in water is very slow [23].



The reaction needs a collision between two negative ions. Repulsion is going to get seriously in the way of that. The catalysed reaction avoids that problem completely. The catalyst can be either iron(II) or iron(III) ions which are added to the same solution. This is another good example of the use of transition metal compounds as catalysts because of their ability to change oxidation state. For the sake of argument, we'll take the catalyst to be iron(II) ions. As you will see shortly, it doesn't actually matter whether you use iron(II) or iron(III) ions. The persulphate ions oxidise the iron(II) ions to iron(III) ions. In the process the persulphate ions are reduced to sulphate ions.



The iron(III) ions are strong enough oxidising agents to oxidise iodide ions to iodine. In the process, they are reduced back to iron(II) ions again.



Both of these individual stages in the overall reaction involve collision between positive and negative ions. This will be much more likely to be successful than collision between two negative ions in the uncatalysed reaction. What happens if you use iron(III) ions as the catalyst instead of iron(II) ions? The reactions simply happen in a different order.

### 2.7.3 Heterogeneous catalyst

In a heterogeneous reaction, the catalyst is in a different phase from the reactants. One or more of the reactants are adsorbed on to the surface of the catalyst at active sites. Adsorption is where something sticks to a surface. It isn't the same as absorption where one substance is taken up within the structure of another. An active site is a part of the surface which is particularly good at adsorbing things and helping them to react. There is some sort of interaction between the surface of the catalyst and the reactant molecules which makes them more reactive. This might involve an actual reaction with the surface, or some weakening of the bonds in the attached molecules. The reaction happens. At this stage, both of the reactant molecules might be attached to the surface, or one might be attached and hit by the other one moving freely in the gas or liquid. The product molecules are desorbed (Figure 2.4).

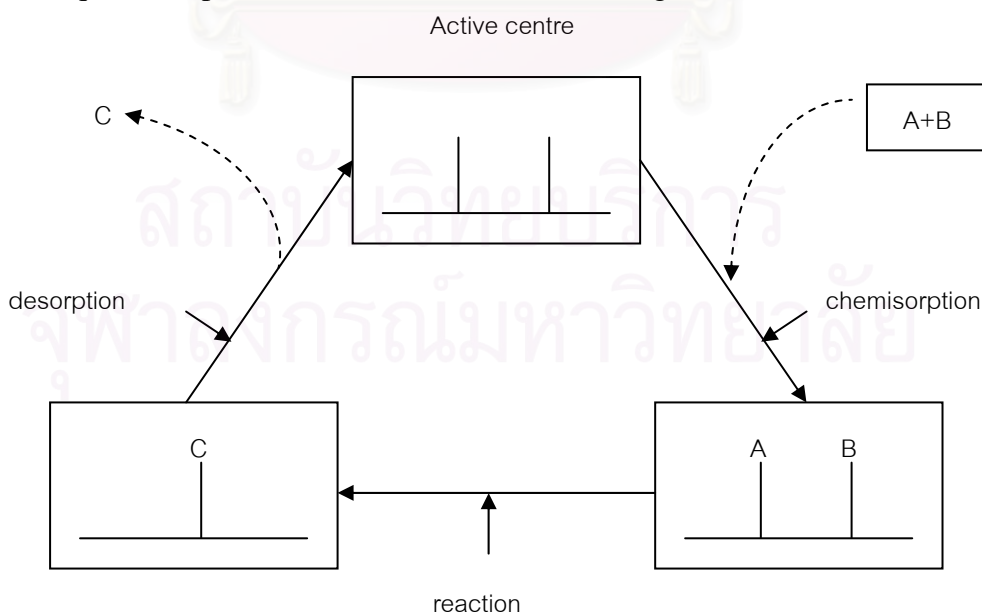


**Figure 2.4** The catalytic cycle for the reaction of  $\text{A} + \text{B} \rightarrow \text{C}$ .

Desorption simply means that the product molecules break away. This leaves the active site available for a new set of molecules to attach to and react. A good catalyst needs to adsorb the reactant molecules strongly enough for them to react, but not so strongly that the product molecules stick more or less permanently to the surface. Silver, for example, isn't a good catalyst because it doesn't form strong enough attachments with reactant molecules. Tungsten, on the other hand, isn't a good catalyst because it adsorbs too strongly. Metals like platinum and nickel make good catalysts because they adsorb strongly enough to hold and activate the reactants, but not so strongly that the products can't break away [24].

### **2.8 Oxidation of a triol: glycerol**

The oxidation of glycerol leads to a complex reaction pathway and a large number of products can be obtained (Fig. 2.5). Oxidation reaction is of industrial importance for converting glycerol to such a high-value added chemical. Based on the conventional process involving stoichiometric oxidants, e.g. permanganate or chromic acid, a significant amount of various by-products is formed. An environmentally friendly alternative is the oxidation in the presence of a heterogeneous catalyst and molecular oxygen [25].



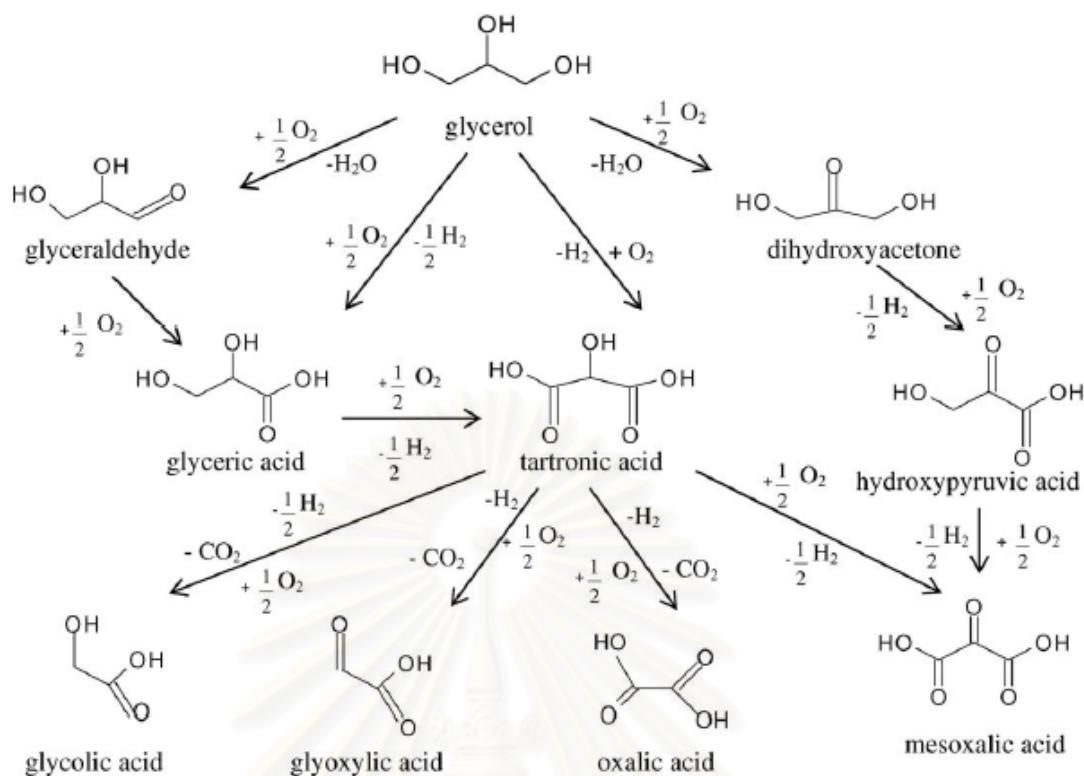


**Figure 2.5** Reaction network of the glycerol oxidation.

Much attention has therefore been paid to the effects of catalyst composition and operating conditions on product selectivities. These are closely connected in the sense that optimum conditions depend somewhat on the type of catalyst being used.

## 2.9 Literature review

In 1995, Garcia, R. *et al.* [26] also studied the transesterification of triglycerides extracted from oilseeds to obtain biodiesel fuel yields up to 14% by weight of glycerol as by-product. The liquid-phase oxidation of glycerol with air on platinum catalysts was investigated to prepare valuable oxidation products such as glyceric acid or dihydroxyacetone. The effect of the pH (pH range 2-11) and of different metal catalysts was studied. The selectivity to glyceric acid can be as high as 70% at 100% conversion on Pd/C at pH 11. On Pt/C catalyst, glyceric acid was still the main product (55% selectivity)

In 1997, Gallezot, P. [27] also studied the oxidation of glyoxal to glyoxylic acid, glucose to gluconic acid and glycerol to various oxygenated derivatives were conducted in water at 60°C in the presence of carbon-supported palladium or platinum catalysts. Bismuth promoter, deposited on the platinum metals by redox reaction, improves the catalyst activity by preventing over-oxidation of the metal surface and favors the oxidation of secondary alcohol functions into keto-derivatives. At higher reaction temperatures, platinum catalysts produce C-C bond rupture with the formation of carboxylic acids with smaller chains. Thus, cyclohexanol was converted into C<sub>6</sub>, C<sub>5</sub>, and C<sub>4</sub> diacids with a 45% selectivity to adipic acid on Pt/C catalysts at 150°C.

In 2000, Bianchi, C., Prati, L. *et al.* [28] also studied Au/C and Au/oxide (Al<sub>2</sub>O<sub>3</sub>, TiO<sub>2</sub>) which were compared in the liquid phase oxidation of glycols and a different trend in reactivity revealed. On the oxides the activity of supported gold increases by decreasing particle size, whereas on carbon maximum activity is achieved with gold particle mean diameter around 7–8 nm. XPS revealed that in the latter case activity depends not only on the size of the gold particle but also on its surface concentration.

In 2003, Hutchings, J. *et al.* [29] also studied the oxidation of aqueous solutions of glycerol and discussed for Pd, Pt and Au nanoparticles supported on graphite and activated carbon. The oxidation in a batch reactor at 60 °C and 1 bar pressure using air as oxidant was initially investigated. Under these conditions, supported Pd and Pt catalysts give some selectivity to glyceric acid, but the main reaction products are considered to be non-desired C<sub>1</sub> by-products, e.g. CO<sub>2</sub>, HCHO and HCOOH. In addition, under these conditions, supported Au catalysts were totally inactive. Using an autoclave with pure oxygen at 3 bar pressure gave a significant improvement in reactivity and, for Pt and Au catalysts, the formation of C<sub>1</sub> by-products was eliminated when NaOH was added. In particular, it was noted that, in the absence of NaOH, the Au/C catalyst was inactive. For 1 wt.% Au/graphite or activated carbon, 100% selectivity to glyceric acid at high conversion was readily achieved.

In 2004, Prati, L. *et al.* [30] also studied the experimental conditions to optimise glycerate production with selected catalysts, with particular regard to the effect of the NaOH/glycerol ratio, glycerol concentration, temperature, and glycerol/catalyst ratio. The best result was 92% selectivity to glycerate at full conversion, obtained by oxidising glycerol at 30 °C, with a NaOH/glycerol ratio of 4, a glycerol/Au = 500, and 0.3 M concentration.

In 2007, Claus, L. *et al.* [31] also studied the promotor effect of platinum on Au/C catalysts which were examined and it could be shown that the presence of Pt increases not only the catalyst activity but also the selectivity. By promoting the gold catalysts with platinum the selectivity to dihydroxyacetone could be increased from 26% (Au/C) to 36% (Au-Pt/C).



สถาบันวิทยบริการ  
จุฬาลงกรณ์มหาวิทยาลัย

## CHAPTER III

### EXPERIMENTAL

#### 3.1 Chemicals

##### 3.1.1 Chemicals

All chemicals used were analytical grade and commercially available from the suppliers listed in Table 3.1.

**Table 3.1** Chemical list

Chemicals	Suppliers
(3-aminopropyl) triethoxysilane	Fluka
Calcium hydride	Fluka
Dichloromethane (commercial reagent grade, 37%)	ZEN POINT
Ethanol	MERCK
Ethanol (commercial reagent grade, 37%)	U&V
Hydrochloric acid (analytical reagent grade, 37%)	MERCK
Hydroxylammonium chloride	MERCK
Methyl cyanoacetate	Fluka
Potassium hydroxide	MERCK
Silica gel (60 mesh)	MERCK
Single element standard solution for Au(III) (1000 mg L <sup>-1</sup> )	Fisher Scientific
Sodium hydroxide	MERCK
Sulfuric acid (analytical reagent grade, 95-97%)	MERCK
Toluene	Fisher Scientific
Glycerol	MERCK
Glyceraldehyde	Fluka
Dihydroxyacetone	MERCK
Activated charcoal	Sigma-Aldrich

---

<b>Chemicals</b>	<b>Suppliers</b>
Glyceric acid	MERCK
Hydroxypyruvic acid	Fluka
Glycolic acid	MERCK
Glyoxylic acid	Fluka
Oxalic acid	MERCK

---

### **3.1.2 Reagents**

#### **(a) Aqua regia solution**

The aqua regia was prepared by mixing conc. HCl and conc. HNO<sub>3</sub> at the ratio of 3:1 v/v.

#### **(b) Dried toluene solution**

Toluene and calcium hydride were added to 1000 mL two-neck round bottom flask and refluxed under nitrogen atmosphere for 4 hours.

#### **(c) Sulfuric acid solutions**

Hydrochloric acid (0.01 and 1 M) for pH adjustment were prepared by subsequent dilutions from the concentrated solution.

#### **(d) Sodium hydroxide solution**

Sodium hydroxide solution (0.05 and 1 M) for pH adjustment of hydroxylamine solution was prepared by dissolving the appropriate amount of NaOH in DI water.

จุฬาลงกรณ์มหาวิทยาลัย

### 3.2 Analytical instruments

The instruments used in this study were listed in Table 3.2

**Table 3.2** Analytical instruments

Analytical instruments <i>and Model (Manufacturer)</i>	Purpose
1. CHN analyzer <i>CHN-2000 (Leco)</i>	The percentage determination of carbon, nitrogen and oxygen of organic compounds
2. Fourier transform infrared spectrometer (FT-IR) <i>Impact 410 (Nicolet)</i>	Characterization of functional groups
3. X-ray diffractometer (XRD) <i>DMAX 2200/Ultima+ (Rigaku)</i>	Pattern crystallites analysis
4. High performance liquid chromatography (HPLC) <i>Lc-10ADvp (Shimadzu)</i>	Separate, identify, and quantify compounds
5. Transmission electron microscope (TEM) <i>JEM-2001</i>	Particle size analysis of gold nanoparticle
6. X-ray fluorescence spectrometer (XRF) <i>Midex (Spectro)</i>	Elemental analysis on silica
7. Surface Area and Porosity Analyzer (BET) <i>Micromeritic ASAP 2020</i>	Measurement of surface area and pore size
8. pH meter <i>pH 211 (Hanna instruments)</i>	pH measurement



### 3.3 Characterization of nanogold and determination of gold content

Gold ions or gold complexes are always present in liquid phase, especially in aqueous solution, They are usually determined by atomic spectrometry. While gold nanoparticles are characterized by different techniques such as X-ray diffractometry (XRD) and transmission electron microscopy (TEM).

#### 3.3.1 X-ray diffractometry (XRD) [32]

When an X-ray beam strikes a surface of crystalline sample at an angle  $\theta$ , a portion of the radiation is scattered by the layer of atoms at the surface. The effect of scattering from the regularly spaced centers of the crystal is a diffraction of the beam. The data of X-ray diffraction indicates that the spacing between layers of atoms and the scattering centers must be spatially distributed in a higher regular way. The diffraction of X-rays by crystals is shown in Figure 3.1.

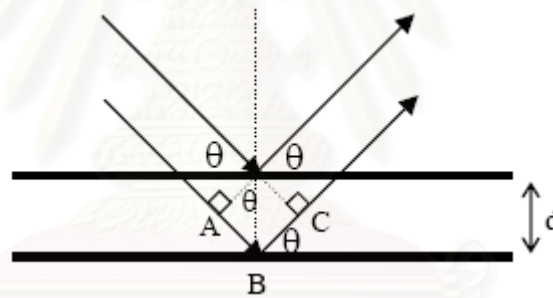


**Figure 3.1** Diffraction of X-rays by a crystal.

A narrow beam strikes the crystal surface at angle  $\theta$ ; scattering occurs as a consequence of interaction of the radiation with atoms located at B. The distance was calculated from formula (2.1).

$$AB + BC = n\lambda \quad (3.1)$$

The scattered radiation will be in phase, and the crystal will appear to reflect the X-radiation. It is investigated with formula (2.2).

$$AB = BC = d \sin\theta \quad (3.2)$$

Thus the condition for constructive interference of the beam at angle  $\theta$  is expressed by the formula (2.3), called Bragg's law.

$$2 d \sin\theta = n\lambda \quad \text{Bragg's law} \quad (3.3)$$

Where n = an integer

- $d$  = interplanar distance of the crystal ( $\text{\AA}$ ;  $1 \text{\AA} = 10^{-10} \text{ m}$ )  
 $\theta$  = angle between X-ray and crystal planes (degree)  
 $\lambda$  = wavelength ( $\text{\AA}$ )

### 3.3.2 X-ray fluorescence spectrometry [33]

An X-radiation (fluorescence) emission of each element is detected in XRF technique. There are two ways for the detection of the fluorescence intensity or energy, i.e. wavelength dispersive (WDX) and energy dispersive (EDX) technique. In EDX, the energy of a characteristic X-ray is adapted by a detector and output data reports in the relative of intensity and electron volt (eV). An energy dispersive XRF spectrometer diagram is shown in Figure 3.2.

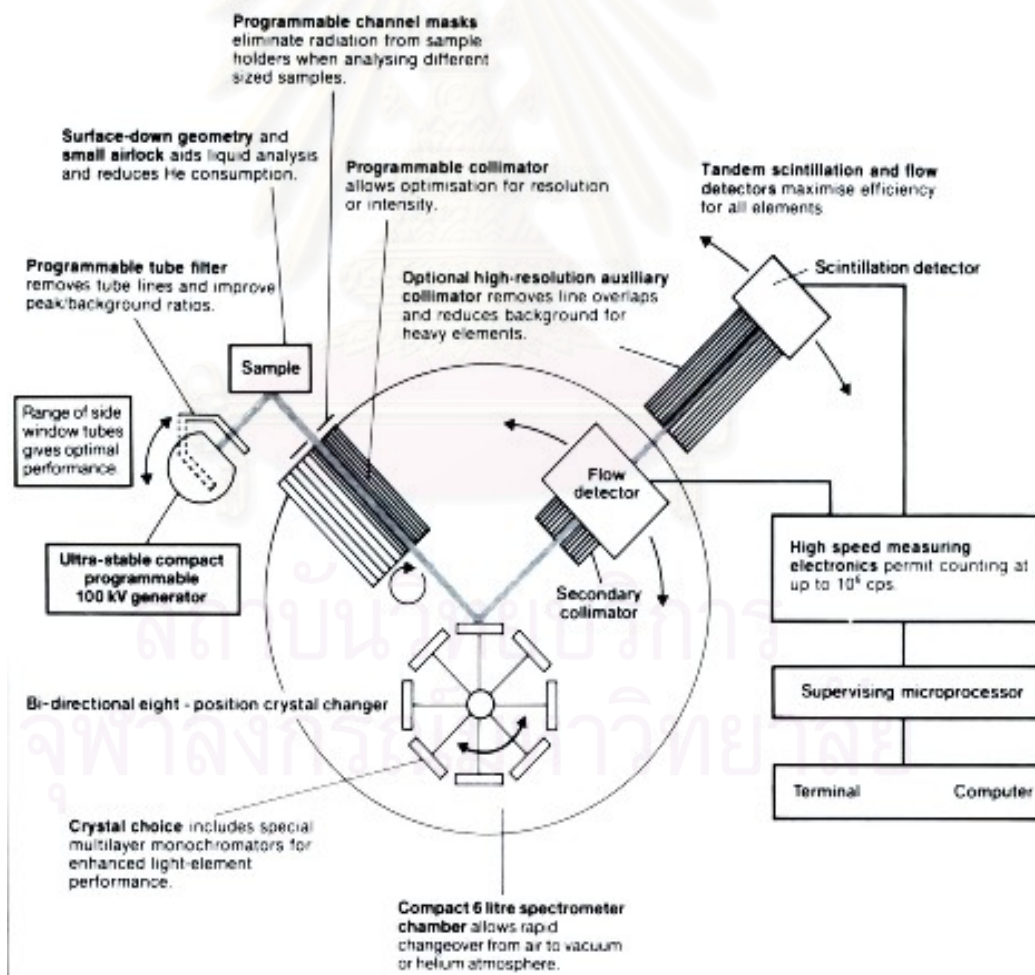
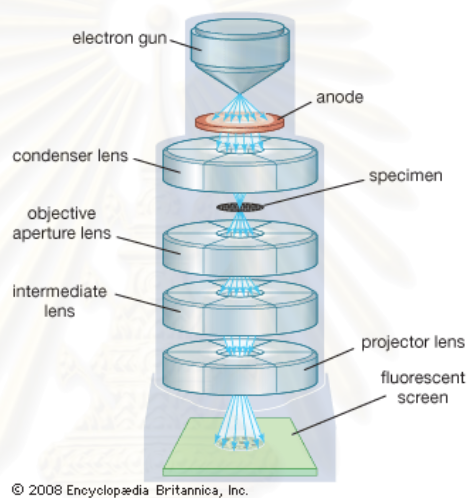


**Figure 3.2** Energy dispersive X-ray fluorescence spectrometer.

### 3.3.3 Transmission electron microscopy (TEM) [34]

A schematic TEM instrument is shown in Figure 3.3. High energy electron beam passes through a condenser lens to produce parallel rays, which affect the sample. The transmitted beam represents a two-dimensional image of the sample which is subsequently magnified by electron optics. It produces a so-called bright field image. Typical operating conditions of a TEM instrument are 100-200 keV,  $10^{-6}$  mbar vacuum, 1 nm resolution and a magnification of  $10^5$  to  $10^6$



**Scheme 3.1** Schematic diagram of transmission electron microscope.

Furthermore, TEM technique is used to determine particles size of gold nanoparticles. The reduced gold nanoparticles have a broad distribution of size and shapes. An average particle size can be calculated by a formula (3.4) [35]

$$d_s = \frac{\sum n_i d_i^3}{\sum n_i d_i^2} \quad (3.4)$$

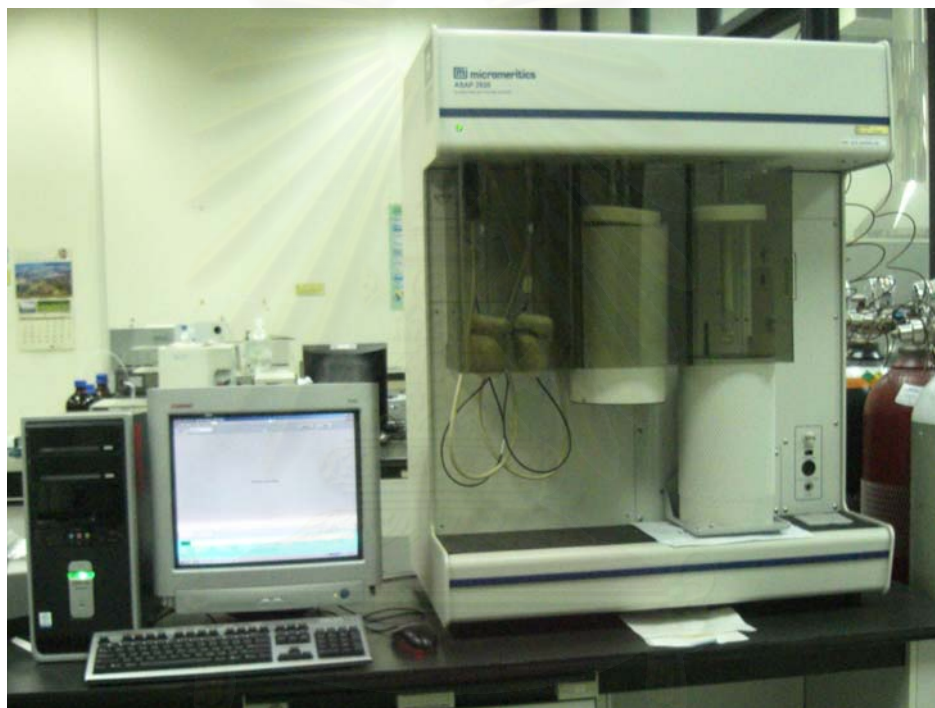
where  $d_s$  = the average particle diameter

$d_i$  = particle diameter

$n_i$  = amount particle

### 3.3.4 BET Surface Area & Pore Size Distribution Analysis [36]

BET theory is a rule for the physical adsorption of gas molecules on a solid surface and serves as the basis for an important analysis technique for the measurement of the specific surface area of a material. The concept of the theory is an extension of the Langmuir theory, which is a theory for monolayer molecular adsorption, to multilayer adsorption with the following hypotheses: (a) gas molecules physically adsorb on a solid in layers infinitely; (b) there is no interaction between each adsorption layer; and (c) the Langmuir theory can be applied to each layer.



**Scheme 3.2** Schematic diagrams of BET Surface Area and Pore Structure.

The resulting BET equation is expressed by (3.5)

$$\frac{1}{v \left[ \left( \frac{P_0}{P} \right) - 1 \right]} = \frac{c - 1}{v_m c} \left( \frac{P}{P_0} \right) + \frac{1}{v_m c} \quad (3.5)$$

$P$  and  $P_0$  are the equilibrium and the saturation pressure of adsorbates at the temperature of adsorption,  $v$  is the adsorbed gas quantity (for example, in volume

units), and  $v_m$  is the monolayer adsorbed gas quantity.  $c$  is the BET constant, which is expressed by (3.6):

$$c = \exp\left(\frac{E_1 - E_L}{RT}\right) \quad (3.6)$$

$E_1$  is the heat of adsorption for the first layer, and  $E_L$  is that for the second and higher layers and is equal to the heat of liquefaction. Equation (3.5) is an adsorption isotherm and can be plotted as a straight line with  $1 / v[(P_0 / P) - 1]$  on the y-axis and  $\phi = P / P_0$  on the x-axis according to experimental results. This plot is called a BET plot. The linear relationship of this equation is maintained only in the range of  $0.05 < P / P_0 < 0.35$ . The value of the slope  $A$  and the y-intercept  $I$  of the line are used to calculate the monolayer adsorbed gas quantity  $v_m$  and the BET constant  $c$ . The following equations can be used:

$$v_m = \frac{1}{A + I} \quad (3.7)$$

$$c = 1 + \frac{A}{I} \quad (3.8)$$

The BET method is widely used in surface science for the calculation of surface areas of solids by physical adsorption of gas molecules. A total surface area  $S_{total}$  and a specific surface area  $S$  are evaluated by the following equations:

$$S_{BET,total} = \frac{(v_m N s)}{V} \quad (3.9)$$

$N$ : Avogadro's number,

$s$ : adsorption cross section,

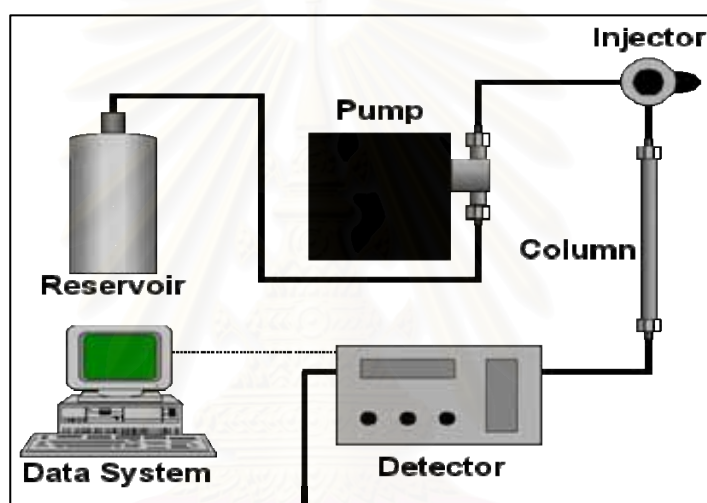
$V$ : molar volume of adsorbent gas

$a$ : molar weight of adsorbed species



### 3.3.5 High performance liquid chromatography (HPLC) [37]

High-performance liquid chromatography (or High pressure liquid chromatography, HPLC) is a form of column chromatography used frequently in biochemistry and analytical chemistry to separate, identify, and quantify compounds. HPLC utilizes a column that holds chromatographic packing material (stationary phase), a pump that moves the mobile phase(s) through the column, and a detector that shows the retention times of the molecules. Retention time varies depending on the interactions between the stationary phase, the molecules being analyzed, and the solvent(s) used.



**Scheme 3.3** Schematic diagram of high performance liquid chromatography.



### 3.4 Substrate preparation

#### 3.4.1 Synthesis of amido-amidoxime functionalized silica

Synthesis of amido-amidoxime functionalized silica gel (Amido-SiO<sub>2</sub>) was carried out in a 250-mL two-neck round bottom flask according to Sirikanjanawanit [38]. Firstly, 25 g of silica gel in dried toluene was refluxed at 90-100 °C under stirring and nitrogen atmosphere. After 1 h, 3-aminopropyltriethoxysilane was added and the mixture was continuously refluxed for 24 h. The solid was filtered and washed three times with dichloromethane, designated as AP-SiO<sub>2</sub>. In the second step, AP-SiO<sub>2</sub> was then refluxed with dried toluene at 90-100 °C for 1 h. Subsequently, 6.2 g methylcyano acetate was added. The mixture was refluxed under nitrogen atmosphere for 24 h. The solid was filtered and washed three times with ethanol and twice with dichloromethane. It was designated as CA-SiO<sub>2</sub>. Finally CA-SiO<sub>2</sub> was added into a mixture of ethanol and hydroxylamine solution (prepared by mixing hydroxylamine hydrochloride with sodium hydroxide in deionized water and adjusted pH to 7 with 1 M HCl and 1 M NaOH). The mixture was again refluxed at 78 °C under nitrogen atmosphere for 24 h. The resultant solid was recovered by filtration and sequentially washing with deionized water, ethanol and dichloromethane. The final product, amido-amidoxime silica (Amido-SiO<sub>2</sub>), was kept in desiccators. Figure 3.3 summarizes the synthetic pathway for Amido-SiO<sub>2</sub> support.

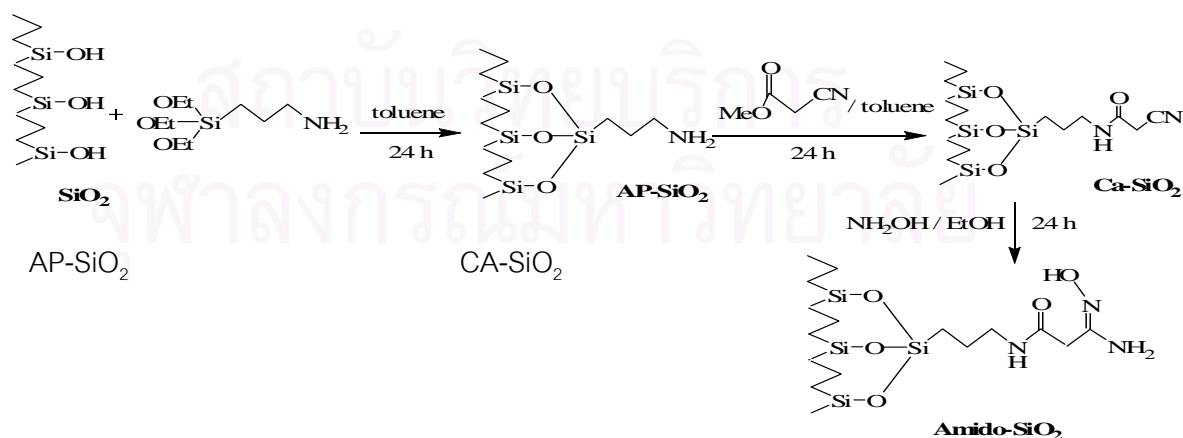


**Figure 3.3** The synthetic pathway of Amido-SiO<sub>2</sub>.

### 3.4.2 Synthesis of SBA-15

SBA-15 was synthesized according to Jin et al. [39] by using Pluronic 123 (poly(ethylene oxide)-poly(propylene oxide)- poly(ethylene oxide) EO<sub>20</sub>PO<sub>70</sub>EO<sub>20</sub>, P123) triblock copolymer as the template and tetraethyl orthosilicate (TEOS) as the silicate source. In a typical synthesis, 4 g of Pluronic 123 was dissolved in a mixture of 116.28 mL of deionized water and 8.76 g of HCl under vigorous stirring at 40 °C followed by the addition of 8.52 g of TEOS. The resultant mixture was maintained at the same temperature for 24 h. Subsequently, it was submitted to a hydrothermal treatment at 100 °C for 1 day. After recovery of the solid product by filtration, it was dried at 100 °C for 1 day. Finally, the dried solid was calcined in a muffle furnace at 400 °C for 6 h in order to remove the template.

### 3.4.3 Synthesis of MCM-41

MCM-41 was synthesized according to Puanngam et al. [40] by using Ludox HS-40 35 g 3 g were dissolved in a solution containing NaOH 117 g in distilled water at temperature 80 °C for 2 h. The solution is then mixed with a solution of hexadecyltrimethylammonium bromide [C<sub>16</sub>H<sub>33</sub>(CH<sub>3</sub>)<sub>3</sub>NBR 14.3 g] in distilled water 37.5 mL until a clear solution is obtained. The pH of the gel mixture was adjusted to 11 with H<sub>2</sub>SO<sub>4</sub> then the gel mixture was stirred for 2 h and finally the mixture was transferred into a Teflon-lined autoclave and kept at 100 °C under static conditions for 3 days. The solid material obtained was separated by centrifugation at 3000 rpm for 30 min. and washed well with distilled water, until the solution shows a neutral pH then dried in air at 100 °C overnight. Finally the resulting material was calcined at 540 °C for 6 h

### 3.5 Preparation of gold nanoparticles

#### 3.5.1 Preparation procedures

There are two different methods for the preparation of supported nanogold catalysts, (a) impregnation method using formaldehyde (HCHO) as a reducing agent and (b) immobilization of gold nanoparticles on Amido-SiO<sub>2</sub> support. The amount of Au loading was maintained at 1 wt.%.

(a) Impregnation - Four catalysts were prepared as reported elsewhere [28] using activated carbon (C), silica gel (SiO<sub>2</sub>), SBA-15 and MCM-41 as the supports. Typically, a slurry of support was prepared by suspending 3 g of a support in 200 mL of deionized water. A solution of HAuCl<sub>4</sub> (2.6 mL, 20 mg Au/mL) was added into the slurry. The resulting mixture was refluxed for 2 h. After cooling the mixture, HCHO solution was added and then refluxed again for 2 h. The solid particles were recovered by filtration, followed by washing with deionized water, drying, and calcination at 150 °C for 6 h. The resultant catalysts were designated as Au/C, Au/SiO<sub>2</sub>, Au/SBA-15 and Au/MCM-41.

(b) Immobilization - Immobilization of gold nanoparticles on Amido-SiO<sub>2</sub> was typically prepared by mixing 0.4 g of Amido-SiO<sub>2</sub> with 100 mL of Au (III) solution (40 mg Au/L). The pH of slurry was controlled at 3 adjusted by 1.0 M NaOH and 1.0 M HCl. The slurry was continuously stirred for 30 min at ambient temperature. The solid was then separated by centrifugal at 3,000 rpm for 10 min. The resulting solid was dried in an oven at 100 °C for 2 h. The resultant catalyst was designated as Au/Amido-SiO<sub>2</sub>.

### 3.6 Characterization of silica

The functionalized silica was characterized with FT-IR techniques.

#### Fourier transform infrared spectrometer (FT-IR)

Infrared spectra were recorded from 400 to 4000 cm<sup>-1</sup> in transmittance mode by KBr pellet technique.

### 3.7 Batch method

The effect of various parameters such as various reaction time, NaOH/glycerol, pH control, O<sub>2</sub> flow rate, support types, calcination and pH during immobilization was investigated by batch method, and all experiments were performed in 250-mL three-neck round bottom flask.

### 3.8 Oxidation glycerol to glyceric acid

The glycerol oxidation was performed in a 250-mL three-neck round bottom flask using molecular oxygen as the oxidant. Typically, the reaction was carried out in a water bath at 60 °C and ambient pressure. A catalyst was added into a 1.0 M aqueous solution of glycerol. After purging the system with inert gas, oxygen was introduced to the reaction mixture at the rate of 300 mL/min. The progress of reaction was followed by taking reaction liquid (0.5 mL) at regular time intervals during 3 h of reaction course and analyzing with a SHIMADZA LC-10 AD vp high performance liquid chromatograph (HPLC) equipped with an ion-exchange column (Aminex HPX-87H) and a refractive index (RI) and a UV detector. In the HPLC analysis, the liquid sample was diluted with the eluent (0.01 M H<sub>2</sub>SO<sub>4</sub>) with a dilution factor of 30. The HPLC method was developed and the optimum condition is reported in Table 3.3. The chromatograms of standard solution are shown in APPENDIX D.

**Table 3.3** Conditions for analysis of reaction products by using High Performance Liquid Chromatographic (HPLC)

Setting Parameter	Desired Conditions
Analytical column	ion exchange column (Aminex HPX-87H)
Mobile phase	H <sub>2</sub> SO <sub>4</sub> (0.01 M)
Flow rate	0.5 mL/min
Injection volume	10 µl
Detector	UV and RI detector
Wavelength	245 nm

### 3.8.1 Result of method verification

To quantify the glycerol conversion in the field test using a HPLC the known concentrations of glycerol solution (0.5-1.5 M) were prepared and injected into the HPLC. A solution of acetic acid (0.625 M) was used as the external standard. Relative areas of peaks correspondently to glycerol and acetic acid, obtained from HPLC chromatograms, were plotted with molar ratios of glycerol/acetic acid (Figure 3.7) The relationship was fitted with a linear equation (Eq.(4.1)).

$$Y = 0.3724 - 0.0042 \quad (4.1)$$

$$R^2 = 0.9994 \quad (4.2)$$

The linear plot was obtained with good correlation coefficient (0.9994). The curve was used to calculate amount of compounds after sample preparation as described in Section 4.4.1.

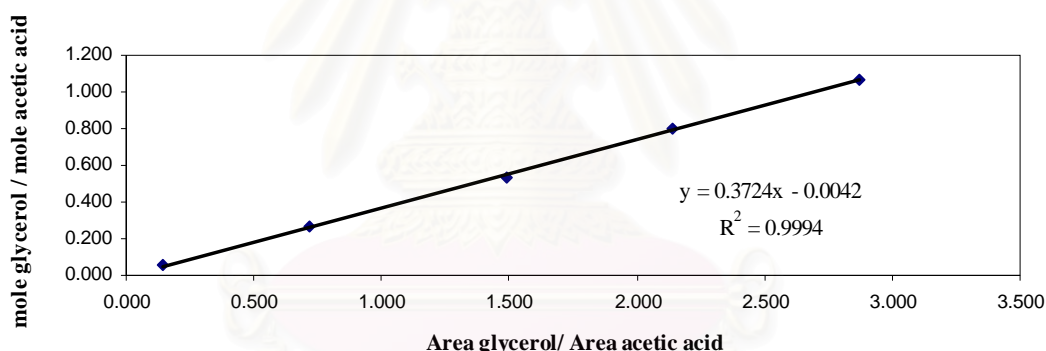


**Figure 3.4** Calibration curve for glycerol solution.

### 3.8.2 Influence of various supported Au catalysts on glycerol oxidation

The glycerol oxidation was performed in a 250-mL three-neck round bottom flask using molecular oxygen as the oxidant. Typically, the reaction was carried out in a water bath at 60 °C and ambient pressure. A various supported Au catalysts (Au/C, Au/SiO<sub>2</sub>, Au/Amido-SiO<sub>2</sub>, Au/SBA-15, Au/Amido-SBA-15, Au/MCM-41 and Au/Amido-MCM-41) were added into a 1.0 M aqueous solution of glycerol. After purging the system with inert gas, oxygen was introduced to the reaction mixture at the rate of 300 mL/min. The progress of reaction was followed by taking reaction liquid (0.5 mL) at regular time intervals during 3 h of reaction course. This project

various different condition such as; Influence of reaction time, NaOH/glycerol ratio, pH controlling, glycerol concentration, O<sub>2</sub> flow rate, support types, calcinations and pH during immobilization of Au



สถาบันวิทยบริการ  
จุฬาลงกรณ์มหาวิทยาลัย



## CHAPTER IV

### RESULTS AND DISCUSSION

#### 4.1 Characterization of amidoxime functionalized silica

The functionalized silica was characterized by elemental analysis, FT-IR spectroscopy. The results of which are shown below.

##### 4.1.1 Determination of surface functional groups.

The FT-IR spectra of the original silica and functionalized silica are illustrated in Figure 4.1. In all case, the characteristic peaks of silica appeared at around  $1,100\text{ cm}^{-1}$  due to Si-O stretching and at  $786$  and  $450\text{ cm}^{-1}$  correspond to Si-O-Si stretching. The FT-IR spectra of the functionalized silica obtained from each synthesis step (i.e. AP-SiO<sub>2</sub>, CA-SiO<sub>2</sub> and Ami-SiO<sub>2</sub>) revealed a corresponding transformation from AP-SiO<sub>2</sub> (C-H stretching at  $2,953\text{ cm}^{-1}$  and N-H bending at  $1,600\text{ cm}^{-1}$ ) to CA-SiO<sub>2</sub> (C-N stretching  $1,343\text{ cm}^{-1}$  and C≡N stretching at  $2,248\text{ cm}^{-1}$ ) and finally to Amido-SiO<sub>2</sub> (C=N stretching at  $1,628\text{ cm}^{-1}$ ). These results further confirmed the successful syntheses of the proposed functionalized silica.

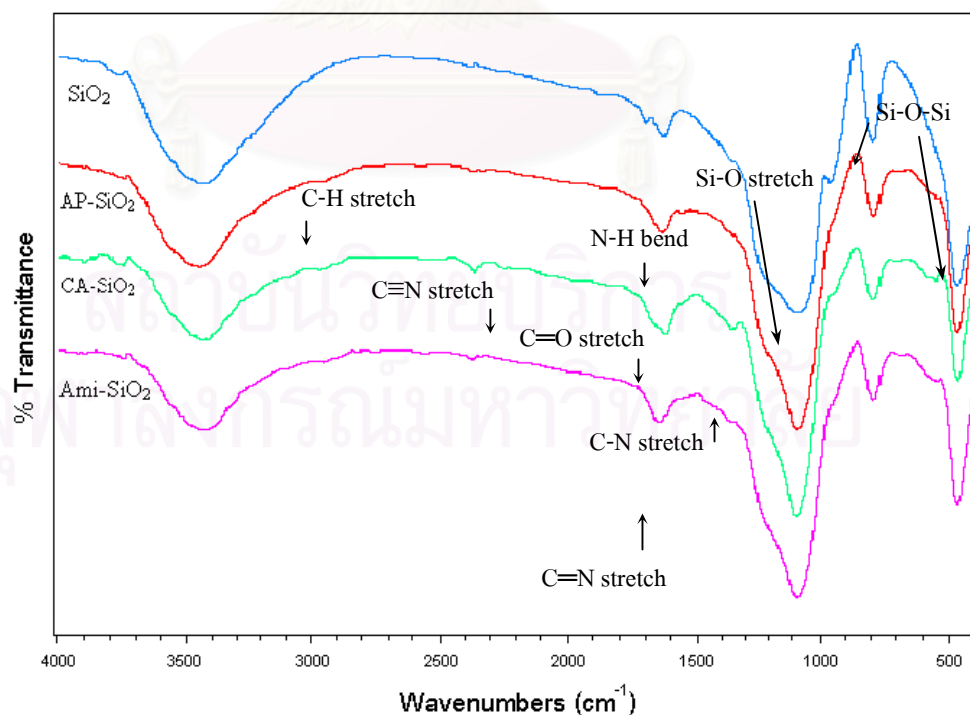


**Figure 4.1** FT-IR spectra of SiO<sub>2</sub>, AP-SiO<sub>2</sub>, CA-SiO<sub>2</sub> and Amido-SiO<sub>2</sub>.

### 4.1.2 Elemental analysis (EA)

The elemental analyses of functionalized silica modification step. The results are shown in Table 4.2.

**Table 4.1** Elemental composition of functionalized silica

Catalyst		%C	%H	%N	C/N ratio
Au/Amido-SiO <sub>2</sub>	exp	5.62	1.94	1.91	3.43
a) Cf: C <sub>6</sub> H <sub>12</sub> N <sub>3</sub> O <sub>5</sub> Si	cal	2.19	0.36	1.28	2.00
Au/Amido-SBA-15	exp	4.59	4.66	1.62	3.30
a) Cf: C <sub>6</sub> H <sub>12</sub> N <sub>3</sub> O <sub>5</sub> Si	cal	2.19	0.36	1.28	2.00
Au/Amido-MCM-41	exp	6.43	2.09	2.64	2.84
a) Cf: C <sub>6</sub> H <sub>12</sub> N <sub>3</sub> O <sub>5</sub> Si	cal	2.19	0.36	1.28	2.00

a) calculated from chemical structure, exp = experimental value, cal = calculated value.

The presence of C, H and N atoms in the functionalized silica, which was modified by introduced organic molecules, was compared with the structure of all types of silica. The experimental values and calculated values of percentage of C, H and N were compared. It was clearly observed that the experimental values were significantly higher than that of the calculated values, which probably cause from an incompleteness in each step of the synthesis (Figure 3.3). The first step, amine group was immobilized on silica gel and then cyano group was immobilized on silica gel in the second step, which was linked to the aminopropyl silica *via* the amide linkage. The cyanoamido silica was converted to the amidoxime group using hydroxylamine hydrochloride. Accordingly, if there are any incompleteness of the 2 steps as mentioned, C/N ratio increase. The increase of C/N ratio was due to the loss of nitro group, which containing in oxime and amide group.

## 4.2 Characterization of supported gold catalysts

Pure SiO<sub>2</sub> with weakly acid surface has less electronic interaction with Au ions, yielding the low Au content. Table 4.2 summarizes gold content, mean diameter of gold

nanoparticles, and textural properties of different supported Au catalysts. It was found that loading gold by the immobilization on amido-amidoxime group is an effective method since it is likely that gold supported on the functionalized silica was higher than that on the parent silica supports. The presence of three electron-donating nitrogen atoms facilitates capturing Au (III) ions simultaneously with reducing the ions to Au<sup>0</sup>.

**Table 4.2** Physicochemical properties of supported Au catalysts

Catalyst	Au content <sup>a</sup> (wt%)	$\bar{d}_{\text{Au}}^{\text{b}}$ (nm)	$S_{\text{BET}}^{\text{c}}$ (m <sup>2</sup> g <sup>-1</sup> )	$V_{\text{avg}}^{\text{d}}$ (cm <sup>3</sup> g <sup>-1</sup> )	$D_{\text{avg}}^{\text{e}}$ (nm)
Au/C	0.6	27.1	646	0.341	4.83
Au/SiO <sub>2</sub>	0.4	23.7	631	0.966	4.63
Au/Amido-SiO <sub>2</sub>	0.8	18.3	305	0.448	4.25
Au/MCM-41	0.7	19.5	760	0.381	5.42
Au/Amido-MCM-41	0.8	4.5	382	0.195	3.31
Au/SBA-15	0.6	5.36	892	1.226	5.99
Au/Amido-SBA-15	0.4	11.6	287	0.589	7.29

<sup>a</sup> Determined by XRF analysis. <sup>b</sup> Diameter of Au particles determined by TEM analysis. <sup>c</sup> BET surface area. <sup>d</sup> Average pore volume. <sup>e</sup> Average pore diameter.

BET specific surface area, average pore size diameter and average pore volume of the supported gold catalysts obtained by the nitrogen physisorption method, are also shown in Table 4.2. The pore diameter ( $D_{\text{avg}}$ ), specific surface area and pore volume decreased upon the introduction of organic functional group. The specific surface area and the pore volume of micropores sharply decrease, while those of mesopores decreased with the introduction of the modify functional groups in the beginning. This indicates that the modify functional group was decreased surface area of the pore structure of the supported gold catalysts.

Table 4.3 shows calculated turnover number of gold nanoparticles supported on different substrates. It can be seen that Au/C catalyst exhibited the highest turnover number. The higher turnover number of Au/C catalyst gave higher amount of undesired products. The higher glyceric acid selectivity found when using Au/SBA-

15 and Au/Amido-MCM-41 as the catalyst (Table 4.8) should be due to the smaller Au particle size compared to Au/C.

**Table 4.3 Calculated turnover number (TON)**

Catalyst	TON
Au/C	44.8
Au/SiO <sub>2</sub>	29.1
Au/Amido-SiO <sub>2</sub>	37.6
Au/MCM-41	21.1
Au/Amido-MCM-41	24.0
Au/SBA-15	32.0
Au/Amido-SBA-15	19.0

The calculation of turnover number is shown in APPENDIX A.

#### 4.2.1 Effect of supported gold catalysts

The presence of gold nanoparticles with different sizes on the supported on gold catalysts were confirmed by TEM micrographs as illustrated in Figure 4.2. The average particle size was calculated according to Eq. (3.4).

สถาบันวิทยบริการ  
จุฬาลงกรณ์มหาวิทยาลัย

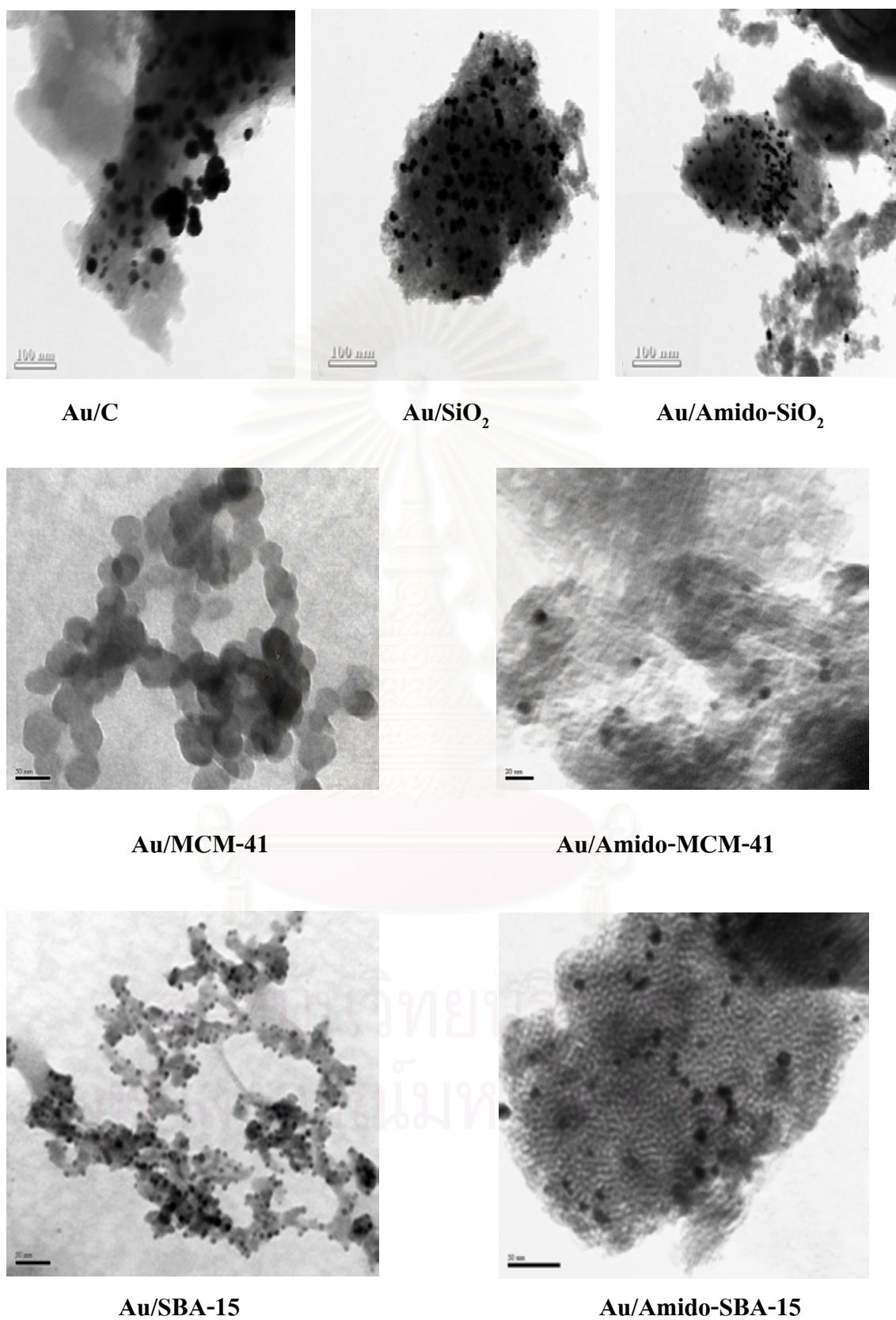


**Figure 4.2** TEM micrographs of supported gold catalysts.

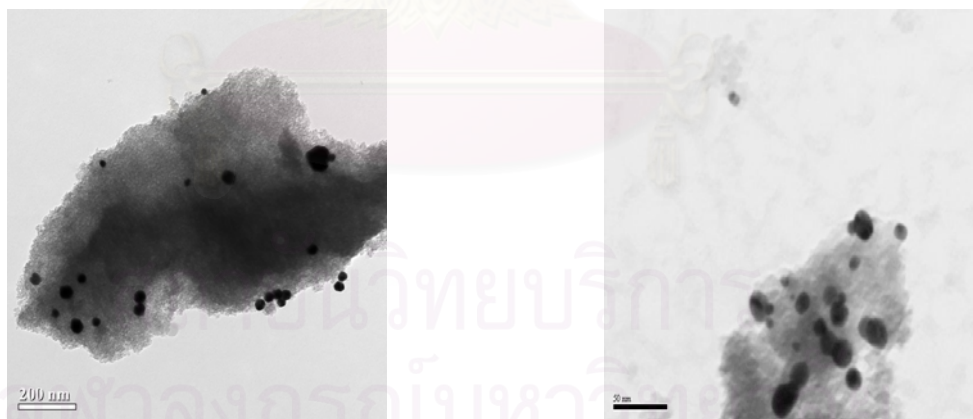


The strong reducing characteristics of amido-amidoxime group should retard the agglomeration of Au ions on the support surface, resulting in the smallest gold particles. Activated carbon is referred to as the most appropriate support for the preparation of Au catalysts [41]. The complexity of surface functional groups and a high surface area of activated carbon promoted loading of gold particles with the sizes of 1-10 nm.

However, the TEM analysis indicated that Au/C possessed larger gold particle sizes than those reported in the literature [42]. It should be ascribed to relatively weak reducing strength of HCHO, compared to THPC or NaHB<sub>4</sub>.

#### 4.2.2 Effect of pH during immobilization

Figure 4.3 shows TEM micrographs of gold nanoparticles supported on the amidoxime functionalized silica. Comparing to the light color of Amido-SiO<sub>2</sub> amorphous phase, the dark cubic crystals of nanogold with different sizes were clearly presented. On the phase of pH 3 and 6 were bearing the sizes within the approximate range of 5-30 nm. Comparing particle sizes of gold catalyst between pH of 3 and pH of 6, the immobilization of gold on functionalized silica under pH of 6 promoted the generation of gold particles with smaller sizes.



**Au-pH 3, 18±9 nm**

**Au-pH 6, 10±4 nm**

**Figure 4.3** TEM micrographs of Amido-SiO<sub>2</sub> and gold nanoparticles at different pH.



### 4.3 Oxidation of glycerol with molecular oxygen

Catalytic performance of synthesized supported Au catalysts in the oxidation of glycerol with molecular oxygen was investigated under batch conditions. The influence of reaction conditions including amount of base (represented as the NaOH/glycerol ratio), O<sub>2</sub> flow rate and reaction time on the glycerol conversion and the product selectivity were studied. The catalyst characterizations described in the previous parts have been referred to explain the results observed. Influence of effect reaction time, temp., NaOH/glycerol, pH control. Glycerol concentration, O<sub>2</sub> flow rate, support types, calcination and pH during immobilization of Au

#### 4.3.1 Influence of reaction time

Table 4.3 shows the results of glycerol oxidation catalyzed by different supported Au catalysts. It can be seen that Au/C catalyst exhibited the highest glycerol conversion, although it possessed relatively large gold particle sizes (Table 4.2).

**Table 4.4** Glycerol oxidation over various supported Au catalysts

Catalyst	Glycerol conversion (mol %)	Product selectivity (mol %)					
		GLYA	GOA	GLA	OLA	DHA	Unknown
Au/C	16.8	61.7	-	12.1	5.4	16.0	4.8
Au/SiO <sub>2</sub>	8.8	79.5	1.6	4.4	2.7	6.5	5.3
Au/Amido-SiO <sub>2</sub>	9.1	77.3	-	4.9	7.2	8.1	2.5

<sup>a</sup> Reaction conditions: glycerol/Au, 3500 (mol/mol); O<sub>2</sub> flow rate, 300 mL/min; NaOH/glycerol ratio, 4; temp., 60 °C; time, 3 h.

<sup>b</sup> GLYA = Glyceric acid, GOA = Glyoxylic acid, GLA = Glycolic acid, OLA = Oxalic acid, and DHA = Dihydroxyacetone.

The major product found in all cases was glyceric acid. Glyoxylic acid, glycolic acid, oxalic acid and dihydroxyacetone were present as the minor products. In fact, glyceric acid, a high value chemical for pharmaceutical and cosmetic applications, is a product from the oxidation of an  $\alpha$ -hydroxyl group located far left or right of glycerol molecule, while dihydroxyacetone is formed by oxidizing  $\beta$ -hydroxyl group at the center of the molecule. It was reported earlier that supported Au catalyst is selective for glyceric acid production, whereas dihydroxyacetone is selectively synthesized by using supported

Pt catalyst. Other by-products are generated *via* the successive oxidation of glyceric acid which illustrated in Figure 2.5 [42].

It can be seen that Au/SiO<sub>2</sub> and Au/Amido-SiO<sub>2</sub> are more selective than Au/C catalyst. The higher activity of Au/C resulted in the successive oxidation of glyceric acid formerly produced to glycolic acid and oxalic acid. Moreover, Au/C catalyst gave higher amount of dihydroxyacetone. The higher glyceric acid selectivity found when using Au/SiO<sub>2</sub> and Au/Amido-SiO<sub>2</sub> as the catalyst should be due to the smaller Au particle (Table 4.2) sizes compared to Au/C. Bianci et al. [26] observed an increase in the selectivity to glyceric acid with decreasing the particle size of gold (8-9 nm). The relatively large gold particles also induced the formation of dihydroxyacetone.

Figure 4.4 reveals the effect of reaction time on the glycerol conversion (Figure 2a) and the selectivity to glyceric acid (Figure 2b). The conversion increased linearly with prolongation of the reaction time. The higher activity of Au/C resulted in a fast decrease in the selectivity to glyceric acid due to the formation of dihydroxyacetone.

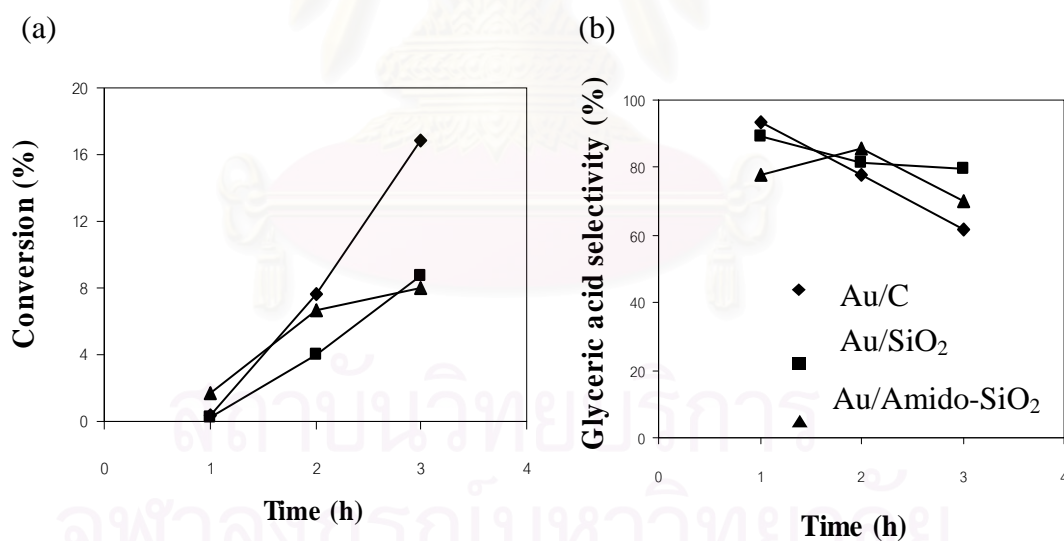


**Figure 4.4** Dependence of (a) glycerol conversion and (b) glyceric acid selectivity on time in the oxidation of glycerol at different supported gold catalysts. Without pH adjustment. Reaction conditions: glycerol/Au, 3500 (mol/mol); O<sub>2</sub> flow rate, 300 mL/min; NaOH/glycerol ratio, 4; temp., 60 °C.

Their electron structure may be modified during the reaction. Although Au/SiO<sub>2</sub> and Au/Amido-SiO<sub>2</sub> were much less active, they exhibited more selectivity to glyceric acid. It should be related to the smaller Au particle sizes as mentioned above.

### 4.3.2 Influence of NaOH/glycerol molar ratios

The oxidation of glycerol is normally initiated by abstracting a proton from a hydroxyl group of the glycerol molecule by a base, so-called oxidative dehydrogenation. For this purpose, a strong base is required and normally NaOH is used. In this section, the effects of NaOH/glycerol ratios were investigated, which illustrated in Figure 4.5. The higher the base concentration is used, the greater the rate of glycerol is converted to the other products [40]. The highest conversion of 49.8 % can be achieved at the NaOH/glycerol molar ratio of 4. However, the selectivity to glyceric acid was dropped sharply when increasing the ratio due to the successive oxidation of glyceric acid to other products. Moreover, it was found that the formation of dihydroxyacetone was enhanced. This result suggests an alteration of reaction mechanism depended on the amount of base. The present investigation indicated that the base concentration is more crucial factor than reaction time to determine the glycerol conversion and the selectivity to glyceric acid. After study of NaOH/glycerol ratios, the optimum pH condition was investigated to use in the next section.

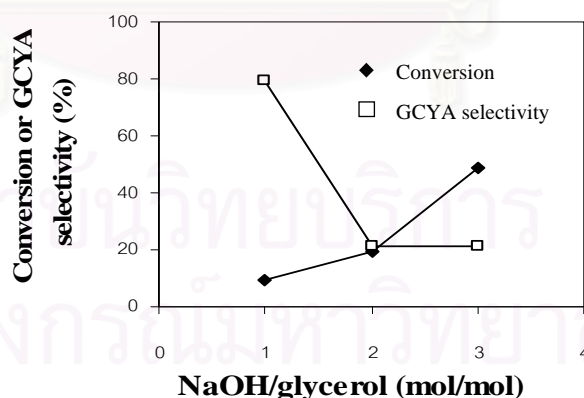


**Figure 4.5** Influence of NaOH/glycerol molar ratios on the glycerol conversion and the glyceric acid selectivity in the oxidation of glycerol over Au/C  
 Reaction conditions: glycerol/Au, 3500 (mol/mol); O<sub>2</sub> flow rate, 300 mL/min; temp., 60 °C; time, 3 h.

### 4.3.3 Influence of pH control

Figure 4.6 reveals the effect of pH controlling on the glycerol conversion (Figure 4.6 a) and the selectivity to glyceric acid (Figure 4.6 b). The pH of reaction mixture was controlled by timely adding 0.5 M NaOH solution. It can be seen that with increasing the solution pH from 10 to 12, the conversion was increased. It should be due to an increased in the deprotonation of  $\alpha$ -hydroxy group form glycerol molecular [41]. Controlling pH of reaction mixture by addition of a suitable amount of NaOH solution improved the glycerol conversion. The control pH of 11 was likely to stabilize the reaction system since the selectivity to glyceric acid was not severely dropped (Table 4.4). Too high solution pH promoted the formation of undesired products. Therefore, the suitable pH of the solution was 11, which probably due to this pH condition was not affected to a deprotonation of glyceric acid. However, the reaction mixture will be controlled at this pH in all experiments.

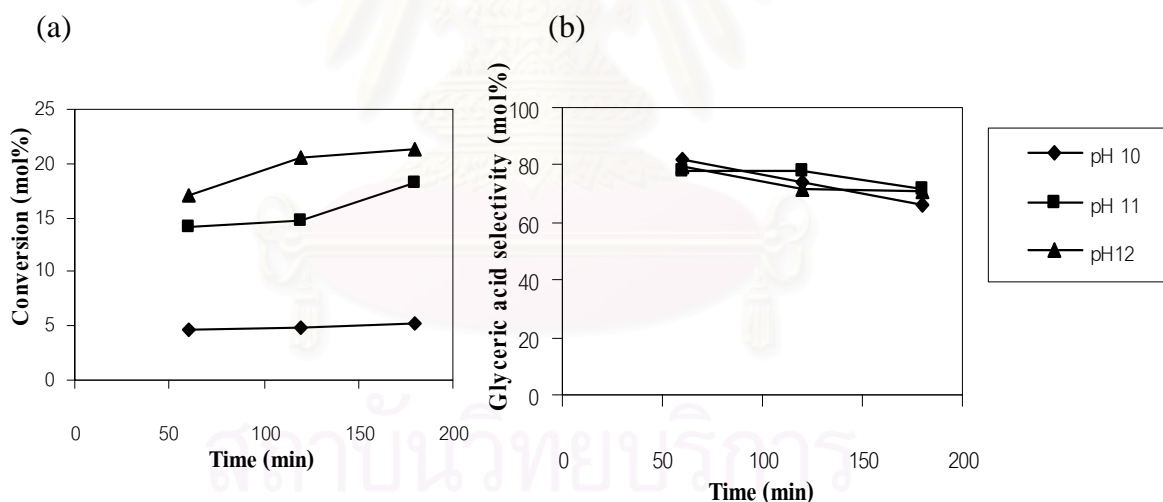


**Figure 4.6** Dependence of (a) glycerol conversion and (b) glyceric acid selectivity on time in the oxidation of glycerol over Au/Amido-SiO<sub>2</sub> immobilized at different pH of reaction mixture. Reaction conditions: glycerol/Au, 3500 (mol/mol); O<sub>2</sub> flow rate, 300 mL/min; solution pH, 11; temp., 60 °C.

**Table 4.5** Glycerol conversion and glyceric acid selectivity over Au/Amido-SiO<sub>2</sub> at different pH controlling

Catalyst	Reaction time (min)	Glycerol conversion <sup>a</sup> (mol %)	Product selectivity <sup>b</sup> (mol %)					
			GLYA	GOA	GLA	OLA	DHA	Unknown
Au/Amido-SiO <sub>2</sub> solution pH =10	60	4.7	82.0	4.6	1.6	4.9	3.5	3.3
	120	4.9	74.2	3.8	14.3	3.2	2.5	1.9
	180	5.2	66.5	10.0	4.0	9.5	5.8	4.2
Au/Amido-SiO <sub>2</sub> solution pH =11	60	14.1	78.1	4.9	2.8	4.9	6.1	3.2
	120	14.8	78.0	4.6	3.6	4.7	6.4	2.7
	180	18.3	71.5	5.3	4.2	6.0	9.2	3.8
Au/Amido-SiO <sub>2</sub> solution pH =12	60	17.1	79.6	5.1	4.5	4.3	4.7	1.8
	120	20.5	71.4	5.6	5.0	7.8	8	2.2
	180	21.2	70.6	3.4	6.6	7.5	8.9	3.0

<sup>a</sup> Reaction conditions: glycerol/Au, 3500 (mol/mol); temp, 60 °C.

<sup>b</sup> GLYA = Glyceric acid, GOA = Glyoxylic acid, GLA = Glycolic acid, OLA = Oxalic acid, and DHA = Dihydroxyacetone.

#### 4.3.4 Influence of O<sub>2</sub> flow rate

Figure 4.7 reveals the effect of O<sub>2</sub> flow rate on the glycerol conversion (Figure 4.7 a) and the selectivity to glyceric acid (Figure 4.7 b) with increasing the flow rate of O<sub>2</sub> from 100 to 300 mL/min, the conversion was increased. It should be due to an increase in the number of oxygen required for the reaction. However, the oxidation of glycerol was compared upon further increasing the O<sub>2</sub> flow. Too high flow rate of O<sub>2</sub> may cause the occurrence of large bubbles, which may disturb mass transfer in the mixture reaction. The presences of large bubbles were greatly disturbance of a contact between solid and aqueous solution. Thus, the glycerol conversion was dropped by increasing the too high flow rate of O<sub>2</sub> at 500 mL/min. It can be shown that the selectivity to glyceric acid and the distribution of other products (Table 4.5) were not much altered.

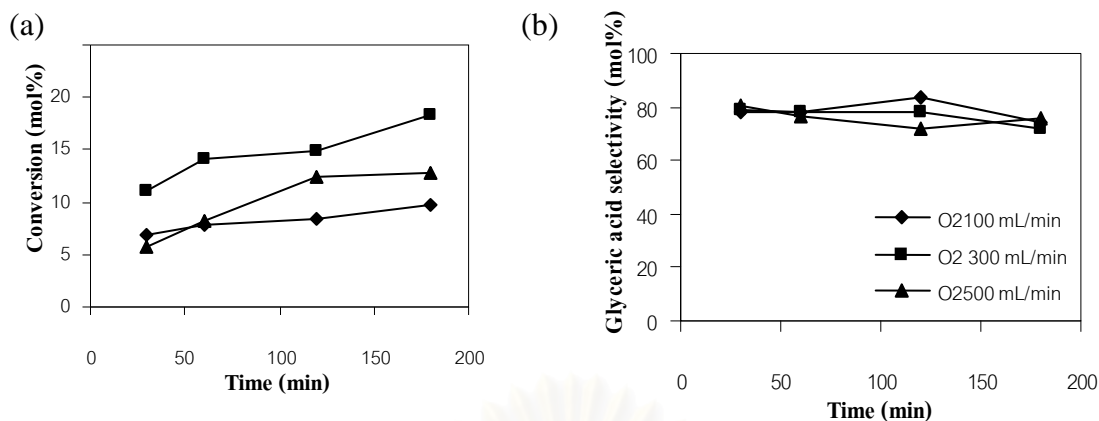


**Figure 4.7** Dependence of (a) glycerol conversion and (b) glyceric acid selectivity on time in the oxidation of glycerol over Au/Amido-SiO<sub>2</sub> immobilized at different O<sub>2</sub> flow rate. Reaction conditions: glycerol/Au, 3500 (mol/mol); O<sub>2</sub> flow rate, 300 mL/min; solution pH, 11; temp., 60 °C.

**Table 4.6** Glycerol conversion and product distribution in the oxidation of glycerol with different O<sub>2</sub> flow rate over Au/Amido-SiO<sub>2</sub> catalyst

O <sub>2</sub> flow rate (mL min <sup>-1</sup> )	Reaction time (min)	Glycerol conversion <sup>a</sup> (mol %)	Product selectivity <sup>b</sup> (mol %)					
			GLYA	GOA	GLA	OLA	DHA	Unknown
100	30	6.8	77.8	7.9	2.9	8.0	3.6	7.8
	60	7.8	78.0	4.0	2.2	3.5	2.4	28.9
	120	8.4	83.9	3.8	1.7	3.8	1.8	0.0
	180	9.8	74.3	7.3	3.9	7.5	5.1	2.0
300	30	11.1	78.8	4.3	3.2	4.3	5.1	4.4
	60	14.1	78.1	4.9	2.8	4.9	6.1	3.2
	120	14.8	78.0	4.6	3.6	4.7	6.4	2.7
	180	18.3	71.5	5.3	4.2	6.0	9.2	3.8
500	30	5.7	80.4	5.5	3.5	5.0	2.9	2.9
	60	8.3	76.9	7.3	4.7	4.8	4.8	2.3
	120	12.4	71.8	6.7	4.9	6.4	5.7	4.8
	180	12.8	75.9	5.3	5.8	6.0	5.2	1.8

<sup>a</sup> Reaction conditions: glycerol/Au, 3500 (mol/mol); solution pH, 11; temp., 60 °C.

<sup>b</sup> GLYA = Glyceric acid, GOA = Glyoxylic acid, GLA = Glycolic acid, OLA = Oxalic acid, and DHA = Dihydroxyacetone.



### 4.3.5 Influence of support types

#### 4.3.5.1 Influence of Amido-amidoxime functionalized SBA-15

Influence of Amido-amidoxime functionalized SBA-15, Under comparable experimental conditions the catalysts Au/SBA-15 and Au/Amido-SBA-15; Au/SBA-15 show higher conversion with smaller gold particle size (Table 4.2). Moreover, the mean gold particle size influences not only the catalytic activity but also the selectivity of the catalyst. The selectivity is increased with decreasing gold particle size. With smaller gold particle size (Au/SBA-15 catalyst,  $d_{Au}^b = 5.36$  nm), a decrease of the selectivity to glyceric acid was observed. Furthermore, from Table 4.2, it is obvious that with the smallest gold particle size the highest selectivity to glyceric acid was obtained.

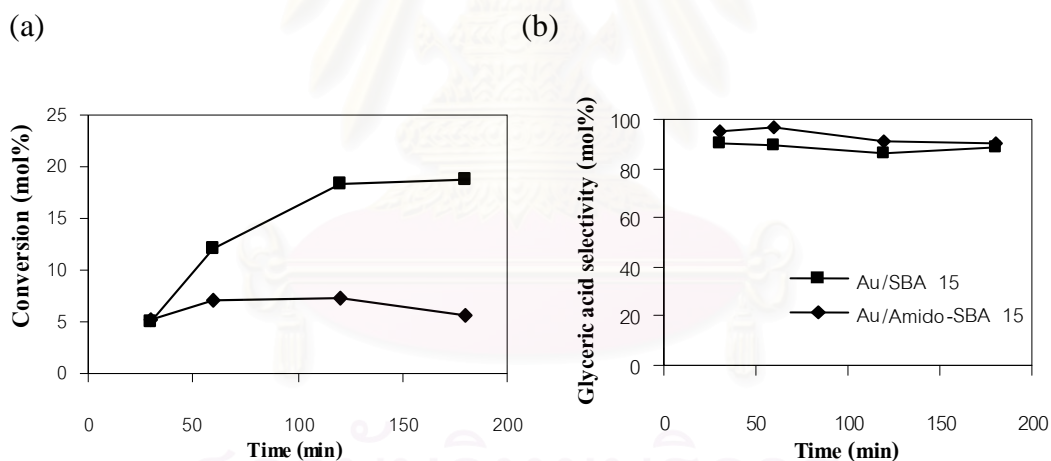


**Figure 4.8** Dependence of (a) glycerol conversion and (b) glyceric acid selectivity on time in the oxidation of glycerol compare with Au/SBA-15 and Au/Amido-SBA-15.

Reaction conditions: glycerol/Au, 3500 (mol/mol); O<sub>2</sub> flow rate, 300 mL/min; solution pH, 11; temp., 60 °C.

**Table 4.7** Glycerol conversion and glyceric acid selectivity over Au/SBA-15 and Au/Amido-SBA-15 catalysts

Catalyst	Reaction time(min)	Glycerol conversion <sup>a</sup> (mol %)	Product selectivity <sup>b</sup> (mol %)					
			GLYA	GOA	GLA	OLA	DHA	Unknown
Au/ SBA-15	30	5.0	90.4	0.6	0.0	3.0	0.0	6.1
	60	12.0	89.5	0.0	0.0	2.9	0.0	7.7
	120	18.3	86.5	0.0	0.0	2.8	0.0	10.7
	180	18.7	88.9	0.0	0.0	2.1	0.0	8.9
Au/Amido-SBA-15	30	5.3	94.9	0.3	0	1.6	0.7	2.5
	60	7.1	96.6	0.3	0	2.3	0.6	0.4
	120	7.3	90.8	1.3	0.2	4	2.2	1.5
	180	5.7	90.3	0.6	0	3.7	1.3	4.3

<sup>a</sup> Reaction conditions: glycerol/Au, 3500 (mol/mol); O<sub>2</sub> flow rate, 300 mL/min; solution pH, 11; temp., 60 °C.

<sup>b</sup> GLYA = Glyceric acid, GOA = Glyoxylic acid, GLA = Glycolic acid, OLA = Oxalic acid, and DHA = Dihydroxyacetone.

#### 4.3.5.2 Influence of various support types

Table 4.7 shows the results of glycerol oxidation catalyzed by gold nano particles supported on different substrates. The support types did not only influence the physicochemical properties of nanogold catalysts, but also altered the oxidation performance. The relationship between the nanosize of gold particles and the initial rate of glycerol oxidation can be found. The differences in the surface and textural properties of supports, more or less, affected the oxidation of glycerol. With smaller gold particle size (Table 4.2), the glycerol conversion and initial rate was increased, while the selectivity to glyceric acid was gradually decreased due to the formation of subsequent oxidized products.

**Table 4.8** Glycerol oxidation over various supported Au catalysts

Catalyst	Initial rate (mmol min <sup>-1</sup> g <sup>-1</sup> )	Glycerol conversion <sup>a</sup> (mol %)	Product selectivity <sup>b</sup> (mol %)			
			GLYA	OLA	DHA	Others <sup>c</sup>
Au/SiO <sub>2</sub>	2.96	10.9	94.6	2.1	1	3.2
Au/Amido-SiO <sub>2</sub>	3.83	14.1	78.1	6.0	9.2	3.2
Au/MCM-41	2.14	7.9	89.5	1.2	0.3	7.7
Au/Amido-MCM-41	2.44	9.0	96.6	5.2	6.8	1.3
Au/SBA-15	3.26	12.0	91.4	2.1	0.0	8.5
Au/Amido-SBA-15	1.93	7.1	87.8	3.7	1.3	4.4

<sup>a</sup> Reaction conditions: glycerol/Au, 3500 (mol/mol); O<sub>2</sub> flow rate, 300 mL/min; solution pH, 11; temp., 60 °C; time, 1 h.

<sup>b</sup> GLYA = Glyceric acid, GOA = Glyoxylic acid, GLA = Glycolic acid, OLA = Oxalic acid, and DHA = Dihydroxyacetone.

<sup>c</sup> Others = GOA + GLA + Unknown

### 4.3.6 Influence of calcination supported gold catalysts

#### 4.3.6.1 Influence of calcination of Au/Amido-SiO<sub>2</sub>

The oxidation of glycerol to glyceric acid was investigated on Au/Amido-SiO<sub>2</sub> catalysts under pH controlling conditions. Figure 4.9 gives the product distribution obtained at pH 11 at which the higher reaction rates were measured. In this section, a calcination of Au/Amido-SiO<sub>2</sub> catalyst between 300 and 500 °C for 2 h was studied. The investigation of effects of calcinations Au/Amido-SiO<sub>2</sub> catalyst is illustrated in Figure 4.9. The calcination of Amido-silica supported Au catalysts improved the glycerol conversion and the glyceric acid selectivity. At 500 °C, the organo-functional groups were burnt off, probably resulted in the formation of smaller gold particles. The surface silanol groups ( $\equiv\text{Si-OH}$ ) recovered after the calcination should enhance the adsorption of glycerol molecules.

The higher the calcination temperature for Au/Amido-SiO<sub>2</sub> is used, the greater the selectivity to glyceric acid increased. The highest glyceric acid selectivity of 96.5 % can be achieved at the calcinations Au/Amido-SiO<sub>2</sub> at 500 °C. However, the

selectivity to glyceric acid was dropped sharply with prolonging the reaction time. Moreover, it was found that the formation of dihydroxyacetone was enhanced.

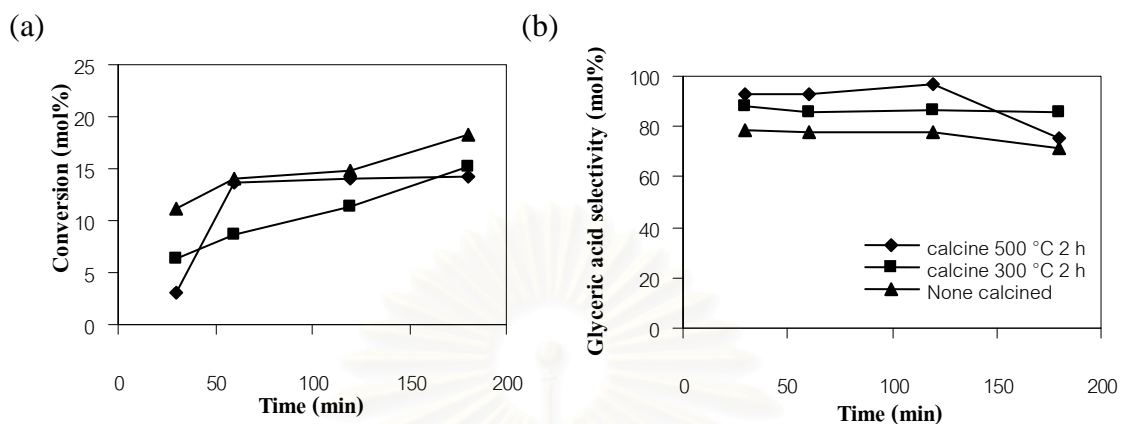


**Figure 4.9** Dependence of (a) glycerol conversion and (b) glyceric acid selectivity on time in the oxidation of glycerol over Au/Amido-SiO<sub>2</sub> calcined at different temperatures. Reaction conditions: glycerol/Au, 3500 (mol/mol); O<sub>2</sub> flow rate, 300 mL/min; solution pH, 11; temp., 60 °C.

**Table 4.9** Glycerol conversion and glyceric acid selectivity over Au/Amido-SiO<sub>2</sub> calcined at different temperatures.

Catalyst	Reaction time (min)	Glycerol conversion <sup>a</sup> (mol %)	Product selectivity <sup>b</sup> (mol %)					
			GLYA	GOA	GLA	OLA	DHA	Unknown
Au/Amido-SiO <sub>2</sub> non calcined	30	11.1	78.8	4.3	3.2	4.3	5.1	4.4
	60	14.1	78.1	4.9	2.8	4.9	6.1	3.2
	120	14.8	78.0	4.6	3.6	4.7	6.4	2.7
	180	18.3	71.5	5.3	4.2	6.0	9.2	3.8
Au/Amido-SiO <sub>2</sub> calcined at 300 °C, 2 h	30	6.4	87.8	2.5	1.6	3.9	0.3	3.8
	60	8.7	86.0	2.3	2.6	3.3	0.5	5.3
	120	11.3	86.7	1	2.2	4	0.5	5.8
	180	15.2	85.9	1	2.2	4.3	0.6	6.1
Au/Amido-SiO <sub>2</sub> Calcined at 500 °C 2 h	30	3.1	93.2	0.3	0	1.6	0.3	4.6
	60	13.7	92.6	1.6	0	1.6	0	4.3
	120	14.0	96.5	0.9	0	0.8	0	1.8
	180	14.2	75.3	7	1.8	4.5	1.6	9.7

<sup>a</sup> Reaction conditions: glycerol/Au, 3500 (mol/mol); O<sub>2</sub> flow rate, 300 mL/min; solution pH, 11; temp., 60 °C.

<sup>b</sup> GLYA = Glyceric acid, GOA = Glyoxylic acid, GLA = Glycolic acid, OLA = Oxalic acid, and DHA = Dihydroxyacetone.

#### 4.3.6.2 Influence of calcinations of Au/Amido-MCM-41

Au/Amido-MCM-41 catalyst, in table 4.9, was compared between calcined Au/Amido-MCM-41 catalyst and uncalcined catalyst. The calcined Au/Amido-MCM-41 catalyst showed higher conversion than uncalcined catalyst. The highest glyceric acid selectivity of 94.3 % can be achieved the calcination of Au/Amido-SiO<sub>2</sub> catalyst at 500 °C. However, the selectivity to glyceric acid was dropped sharply with prolonging the reaction time because oxidation of glyceric acid to other products.

**Table 4.10** Glycerol oxidation and glyceric acid selectivity over Au/Amido-MCM-41 catalysts

Catalyst	Reaction time (min)	Glycerol conversion <sup>a</sup> (mol %)	Product selectivity <sup>b</sup> (mol %)					
			GLYA	GOA	GLA	OLA	DHA	Unknown
Au/Amido-MCM-41 non calcined	30	2.6	92.9	0.6	0.0	2.1	0.0	4.3
	60	7.6	93.1	0.3	0.0	2.5	0.0	4.1
	120	9.0	87.8	0.8	0.0	3.7	3.7	3.9
	180	10.5	81.1	0.0	0.9	5.2	6.8	6.0
Au/Amido-MCM-41 (calcined at 500°C, 2 h)	30	5.7	94.3	0.5	0.0	1.7	0.0	3.5
	60	10.3	93.8	0.1	0.0	2.3	0.0	3.7
	120	11.5	91.2	0.5	0.0	3.1	2.6	2.7
	180	14.0	85.7	0.0	0.6	4.3	4.9	4.4

<sup>a</sup> Reaction conditions: glycerol/Au, 3500 (mol/mol); O<sub>2</sub> flow rate, 300 mL/min; solution pH, 11; temp., 60 °C.

<sup>b</sup> GLYA = Glyceric acid, GOA = Glyoxylic acid, GLA = Glycolic acid, OLA = Oxalic acid, and DHA = Dihydroxyacetone.

#### 4.3.7 Influence of pH during immobilization of Au

Figure 4.10 and Table 4.10 show the result obtained from the glycerol oxidation over Au/Amido-SiO<sub>2</sub> prepared via immobilization of Au at pH of 3 and 6. When using the Au (III) solution with pH of 6, the catalyst exhibited higher activity and selectivity to glyceric acid. The higher selectivity to dihydroxyacetone was observed on Au/Amido-SiO<sub>2</sub> immobilized at pH of 3. These results showed the presence of gold nanoparticles with different sizes as indicated by TEM analysis (Figure 4.3). The immobilization at pH of 6 provided the catalysts with the smaller size of gold particles, so that the oxidation was promoted towards the formation of glyceric acid. If gold particle sizes were smaller than that of pH of 6, they can be selective to dihydroxyacetone. This phenomenon was an undesirable reaction, because it directly affected the decrease of desirable products according to Demirel et al. [31].



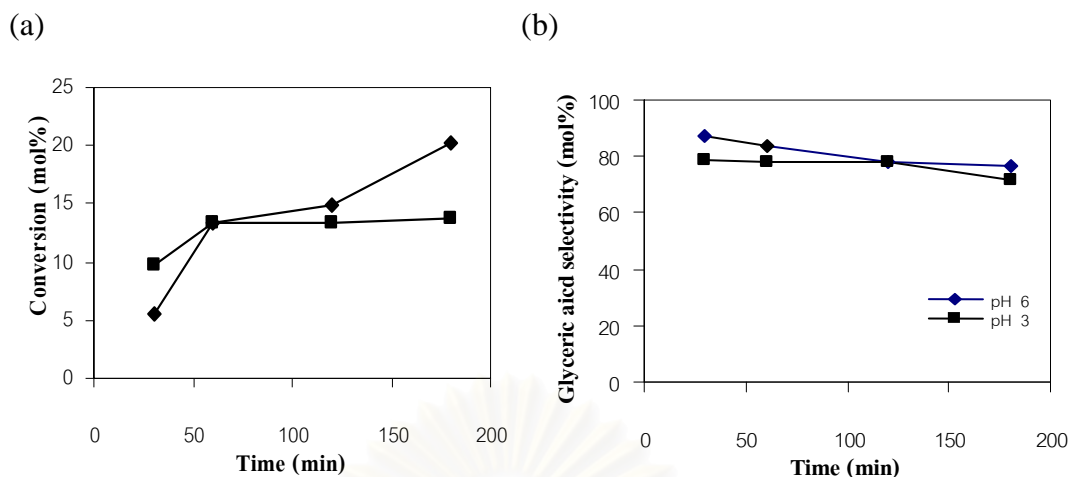


**Figure 4.10** Dependence of (a) glycerol conversion and (b) glyceric acid selectivity on time in the oxidation of glycerol over Au/Amido-SiO<sub>2</sub> immobilized at different pH. Reaction conditions: glycerol/Au, 3500 (mol/mol); O<sub>2</sub> flow rate, 300 mL/min; solution pH, 11; temp., 60 °C.

**Table 4.11** Glycerol conversion and glyceric acid selectivity over Au/Amido-SiO<sub>2</sub> at different pH during immobilization of Au

Catalyst	Reaction time (min)	Glycerol conversion <sup>a</sup> (mol %)	Product selectivity <sup>b</sup> (mol %)					
			GLYA	GOA	GLA	OLA	DHA	Unknown
Au/Amido-SiO <sub>2</sub> Au(III) solution pH 3	30	11.1	78.8	4.3	3.2	4.3	5.1	4.4
	60	14.1	78.1	4.9	2.8	4.9	6.1	3.2
	120	14.8	78.0	4.6	3.6	4.7	6.4	2.7
	180	18.3	71.5	5.3	4.2	6.0	9.2	3.8
Au/Amido-SiO <sub>2</sub> Au(III) solution pH 6	30	5.6	87.4	1.5	0.9	3.2	1.9	5.3
	60	13.4	83.5	1.7	2.6	3.2	2.4	6.8
	120	14.9	78.3	2.4	4.3	4.0	4.6	6.6
	180	20.2	76.9	2.4	5.6	4.0	5.4	5.8

<sup>a</sup> Reaction conditions: glycerol/Au, 3500 (mol/mol); solution pH, 11; temp, 60 °C.

<sup>b</sup> GLYA = Glyceric acid, GOA = Glyoxylic acid, GLA = Glycolic acid, OLA = Oxalic acid, and DHA = Dihydroxyacetone.

## CHAPTER V

### CONCLUSION AND RECOMMENDATION

#### 5.1 Conclusions

This thesis has studied the preparation, characterization and performance test of various supported gold catalysts. The preparation has been focused on immobilization of gold on amido-amidoxime functionalized SiO<sub>2</sub> and mesoporous materials, i.e. MCM-41 and SBA-15. The conventional impregnation method using HCOH as a reducing agent was applied for comparison. Various characterization techniques were used to reveal physicochemical properties of the synthesized catalysts. The catalytic performance of supported nanogold was investigated in the liquid phase oxidation of glycerol using molecular oxygen at atmospheric pressure. From the present study, the following conclusions can be made;

- Amido-amidoxime functionalized silica gel, MCM-41 and SBA-15, designated as Amido-SiO<sub>2</sub>, Amido-MCM-41 and Amido-SBA-15, respectively, supported Au catalysts were successfully prepared through the pH-controlling immobilization method.
- The presence of three electron-donating nitrogen atoms in the amido-amidoxime group with strong reducing characteristics facilitates capturing Au (III) ions simultaneously with reducing the ions to Au<sup>0</sup>, resulting in the high gold content and the formation of gold particles with nanosize, respectively.
- The immobilization of gold on functionalized silica under pH of 6 promoted the generation of gold particles with smaller sizes that are more catalytically active for the oxidative conversion of glycerol.
- With increasing the reaction time, the glycerol conversion was increased, while the selectivity to glyceric acid was gradually decreased due to the formation of subsequent oxidized products.
- The oxidation of glycerol was effectively promoted by increasing the ratio of NaOH/glycerol. However, the high amount of base enhanced the generation of undesired byproducts.

- Controlling pH of reaction mixture by addition of a suitable amount of NaOH solution improved the glycerol conversion. The pH was optimized at 11 since it maintained the glyceric acid selectivity at a high value.
- The glycerol conversion was slightly enhanced by increasing the flow rate of O<sub>2</sub>. It seems that this influence affected the reaction at much less extent than the pH of reaction solution.
- The support types did not only influence the physicochemical properties of nanogold catalysts, but also alter the oxidation performance. The relationship between the nanosize of gold particles and the initial rate of glycerol oxidation can be found. The differences in the surface and textural properties of supports, more or less, affected the oxidation of glycerol.
- The calcination of Amido-silica supported Au catalysts improved the glycerol conversion and the glyceric acid selectivity. At 500 °C, the organo-functional groups were burnt off, probably resulted in the formation of smaller gold particles. The surface silanol groups ( $\equiv\text{Si-OH}$ ) recovered after the calcination should enhance the adsorption of glycerol molecules.

## 5.2 Recommendation

The present study reported that mesoporous silica supported gold nanoparticles are selective catalysts for the production of glyceric acid via the glycerol oxidation. However, due to a low yield of the desired product, an attempt to increase the glycerol conversion should be made by promoting the generation of active oxygen. This can be done by performing the reaction under oxygen pressures of 3 – 5 bars. Moreover, the reaction mechanism for the catalytic glycerol oxidation on surface of gold should be investigated to obtain informative knowledge for further catalyst development.

## REFERENCES

- [1] Garcia, R., Besson, M., Gallezot, P. Chemoselective Catalytic Oxidation of Glycerol with Air on Platinum Metals. *Applied Catalysis A* 127: 165-176 (1995).
- [2] Gallezot, P. Selective Oxidation with Air on Metal Catalysts. *Catalysis Today* 37: 405-418 (1997).
- [3] Biella, S., Prati, L., Rossi, M. Selective Oxidation of D-Glucose on Gold Catalyst. *Journal of Catalysis* 206: 242-247 (2002).
- [4] *Properties of gold* [online]. Available from: [http://www.utilisegold.com/uses\\_applications/properties\\_of\\_gold/](http://www.utilisegold.com/uses_applications/properties_of_gold/) [2007, December 14].
- [5] Turkevich, J. Colloidal Gold. Part I. *Gold Bull.*, 18: 3 (1985)
- [6] Hao, Z.; Guo, Z. Y. and Liang, Y. Support Supported gold catalysts used for ozone decomposition and simultaneous elimination of ozone and carbon monoxide at ambient temperature. *Applied Catalysis B Environmental* 33: 217-222. (2001).
- [7] *Catalytic Synthesis of carbon Nanotubes* [online]. Available from: <http://cobweb.ecn.purdue.edu/~catalyst/Carbon%20Nanotubes/Catalytic%20Nanotubes/Catalytic%20Synthesis%20of%20Carbon%20Nanotubes.htm> [2007, December 14].
- [8] Greenwood, N. N.; and Earnshaw, A. Chemistry of the elements. UK: Butterworth-Heinemann, (1997).
- [9] *Impregnation* [online]. Available from: <http://www.impco-inc.com/page209.html> [2007, December 14].
- [10] Puddephatt, R. J.; and Vittal, J. J. Gold: inorganic & coordinate chemistry. Encyclopedia of Inorganic Chemistry. Chichester UK: John Wiley & Sons, 1320-1331. (1994)
- [11] Pal, A.; Pal, T.; Stokes, D. L.; and Vo-Dinh, T. Photochemically prepared gold nanoparticles: A substrate for surface *Current Science* 84: 1342-1345. (2003).
- [12] Corti, C. W.; and Holliday, R. J. Commercial aspects of gold applications: from materials science to chemical science. *Gold Bull* 37: 1-2. (2004).

- [13] Stremstoerfer, G.; et al. Autocatalytic deposition of gold and palladium onto n-GaAs in acidic media. *Journal of the Electrochemical Society* 135 2881-2886. (1988).
- [14] Patungwasa, W.; and Hodak, J. H. pH tunable morphology of the gold nanoparticles produced by citrate reduction. *Materials Chemistry and Physics*: 108 45-54. (2008).
- [15] Corti, C. W.; and Holliday, R. J. Commercial aspects of gold applications: from materials science to chemical science. *Gold Bull* 37 1-2. (2004).
- [16] Hao, Z.; Guo, Z. Y. and Liang, Y. Support Supported gold catalysts used for ozone decomposition and simultaneous elimination of ozone and carbon monoxide at ambient temperature. *Applied Catalysis B Environmental*: 33 217-222. (2001).
- [17] Sarkas, H.; Arnold, A. An investigation of catalytic activity in mixed metal oxide nanophase materials. *Z. Phys. D* 26, 46-50 (1993).
- [18] G.C. Bond and D.T. Thompson, *Gold Bull* 33 41. (2000).
- [19] Pillai, U., Deevi S., Highly active gold-ceria catalyst for the room temperature oxidation of carbon monoxide. *Appl. Catal. A Gen.* 299: 266-273 (2006).
- [20] Bianchi, C., Porta, F., Prati, L., Rossi, M. Selective Liquid Phase Oxidation Using Gold Catalysts. *Topics in Catalysis* 14: 231-236 (2000).
- [21] *Oxidation of alcohol* [online]. Available from: <http://www.chemguide.co.uk/organicprops/alcohols/oxidation.html> [2007, December 14].
- [22] *Heterogeneous catalysts* [online]. Available from: <http://www.science.uwaterloo.ca/~cchieh/cact/applychem/heterocat.html> [2007, December 14].
- [23] *Homogeneous catalyst* [online]. Available from: <http://www.chemguide.co.uk/physical/catalysis/introduction.html> [2007, December 14].
- [24] *Heterogeneous catalyst* [online]. Available from: <http://www.science.uwaterloo.ca/~cchieh/cact/applychem/heterocat.html> [2007, December 14].
- [25] Hutchings, J., McMorn P. Oxidation of glycerol using supported Pt, Pd and Au catalysts. *Phys. Chem. Chem. Phys.* 5: 1429–1436 (2003).



- [26] Demirel, S., Lucas, M., Claus, P. Liquid phase oxidation of glycerol over carbon supported gold catalysts. *Catalysis Today* 102-103: 166-172 (2005).
- [27] Gallezot, P. Selective Oxidation with Air on Metal Catalysts. *Catalysis Today* 37: 405-418 (1997).
- [28] Bianchi, C., Porta, F., Prati, L., Rossi, M. Selective Liquid Phase Oxidation Using Gold Catalysts. *Topics in Catalysis* 14: 231-236 (2000).
- [29] Hutchings, J., McMorn P. Oxidation of glycerol using supported Pt, Pd and Au catalysts. *Phys. Chem. Chem. Phys.* 5: 1429–1436 (2003).
- [30] Bianchi, C., Canton, P., Dimitratos, N. Selective Oxidation of Glycerol to Sodium Glycerate with Gold-on Carbon Catalyst: An Insight into Reaction Selectivity. *Journal of Catalysis* 224: 397-403 (2004).
- [31] Demirel, S., Lehnert, K. Use of renewables for the production of chemicals: Glycerol oxidation over carbon supported gold catalysts. *Applied Catalysis B Environmental* 70: 637–643 (2007).
- [32] *X-ray powder Diffractometer* [online]. Available from: [http://www.tint.or.th/adv/phys\\_oap/XRD.pdf](http://www.tint.or.th/adv/phys_oap/XRD.pdf) [2008, March 24].
- [33] Christian, G. D. and O'Reilly, J. E. *Instrument Analysis*. Vol. 2. (n.d.): Allyn and Bacon, 1986.
- [34] *Transmission Electron Microscope* [online]. Available from: [http://nobelprize.org/educational\\_games/physics/microscopes/tem/index.html](http://nobelprize.org/educational_games/physics/microscopes/tem/index.html) [2008, March 24]
- [35] Jin, Y.; Wang, P.; and Yin, D.; et. al. Gold nanoparticles prepared by sonochemical method in thiol-functionalized ionic liquid. *Colloids Surface A Physicochemical and Engineering Aspects* 302: 366-370. (2007).
- [36] *BET Surface Area* [online]. Available from: [http://en.wikipedia.org/wiki/BET\\_theory](http://en.wikipedia.org/wiki/BET_theory) [2008, March 24]
- [37] *High performance liquid chromatography* [online]. Available from: <http://www.answers.com/topic/high-performance-liquid-chromatography> [2008, March 24]
- [38] Sirikanjanawanit, N. Preparation of gold nanoparticles from jewelry industry wastewater by amido-amidoxime functionalized silica, Master's thesis of Science Program in Chemistry, Faculty of Science, Chulalongkorn university: (2007)



- [39] Jin, Y.; Wang, P.; and Yin, D.; et al. Selective Solid-Phase Extraction of  $\alpha$ -Tocopherol by Functionalized Ionic Liquid-modified Mesoporous SBA-15 Adsorbent. *Analytical Sciences* 24: 1245-1250 (2008).
- [40] Puanggam, M, Unob, F. Preparation and use of chemically modified MCM-41 and silica gel as selective adsorbents for Hg (II) ions. *Journal of Hazardous Materials* 49: 1635-1638 (2007).
- [41] Bianci, C., Canton, P., Dimitratos, N. Selective oxidation of glycerol to sodium glycerate with gold-on carbon catalyst: an Insight into reaction selectivity. *Journal of Catalysis* 224: 397-403 (2004).
- [42] Bianchi, C., Porta, F., Prati, L., Rossi, M. Selective liquid phase oxidation using gold catalysts. *Topics in Catalysis*, 14: 231-236 (2000).



สถาบันวิทยบริการ  
จุฬาลงกรณ์มหาวิทยาลัย



**APPENDICES**

สถาบันวิทยบริการ  
จุฬาลงกรณ์มหาวิทยาลัย

## APPENDICES

### Appendix A Definitions, and Calculations

The glycerol conversion and percent selectivity of each component can be analysis by the calibration curve glycerol.

The conversion is defined as:

$$\% \text{ Conversion} = \frac{\text{Mole reactant in} - \text{Mole reactant out}}{\text{Mole reactant in}} \times 100 \quad (\text{B.1})$$

The first selectivity is defined as:

$$\% \text{ Selectivity} = \frac{\text{Area of product}}{\text{Total Area of all products}} \times 100 \quad (\text{B.2})$$

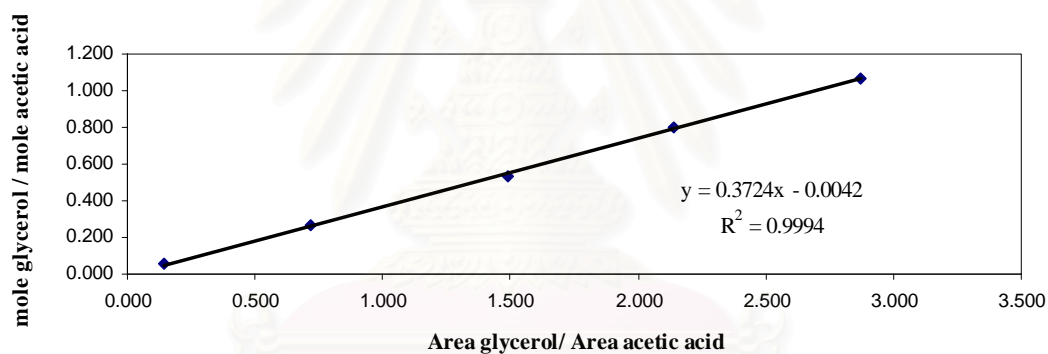


**Figure A-1** Calibration curve of glycerol used in this work

สถาบันวิทยบริการ  
จุฬาลงกรณ์มหาวิทยาลัย

**Percentages of C, H and N is calculated as:**

$$\% C = \frac{MW_C * \text{Number } MW_C \times 100}{\text{Total Molecular weight}} \quad (\text{B.3})$$

$$\% H = \frac{MW_H * \text{Number } MW_H \times 100}{\text{Total Molecular weight}} \quad (\text{B.4})$$

$$\% N = \frac{MW_N * \text{Number } MW_N \times 100}{\text{Total Molecular weight}} \quad (\text{B.5})$$

**C/N ratio is calculated as:**

$$\text{C/N ratio} = \frac{(\% C / MW)}{(\% N / MW)} \quad (\text{B.6})$$

N : Number of atom

MW : Molecular weight

**Calculation turnover number (TON)**

$$\text{TON} = \frac{\text{glycerol conversion}}{\text{mol of Au}} \quad (\text{B.7})$$

Au/C:

mol of Au:

$$\begin{aligned} \text{weight of catalyst} & 99.4 \text{ g gold} = 0.6 \text{ g} \\ \text{weight of catalyst} & 0.611 \text{ g gold} = \frac{(0.6 * 0.611)}{100} \\ & = 0.0039 \text{ g} \end{aligned}$$

mole of Au:

$$\begin{aligned} \text{mol of Au} & = \frac{0.0039}{196.9} \\ & = 1.87 * 10^{-5} \text{ mol} \end{aligned}$$

glycerol conversion:

$$\begin{aligned} \text{glycerol conversion} &= \text{Mole reactant in} - \text{Mole reactant out} \\ &= 0.005 - 0.00416 \\ &= 0.84 \times 10^{-3} \text{ mol} \end{aligned}$$

$$\begin{aligned} \text{TON of Au/C} &= \frac{0.84 \times 10^{-3}}{1.87 \times 10^{-5}} \\ &= 44.85 \end{aligned}$$

**Table A-1 Calculation turnover number (TON)**

Catalyst	TON
Au/C	44.8
Au/SiO <sub>2</sub>	29.1
Au/Amido-SiO <sub>2</sub>	37.6
Au/MCM-41	21.1
Au/Amido-MCM-41	24.0
Au/SBA-15	32.0
Au/Amido-SBA-15	19.0

สถาบันวิทยบริการ  
จุฬาลงกรณ์มหาวิทยาลัย

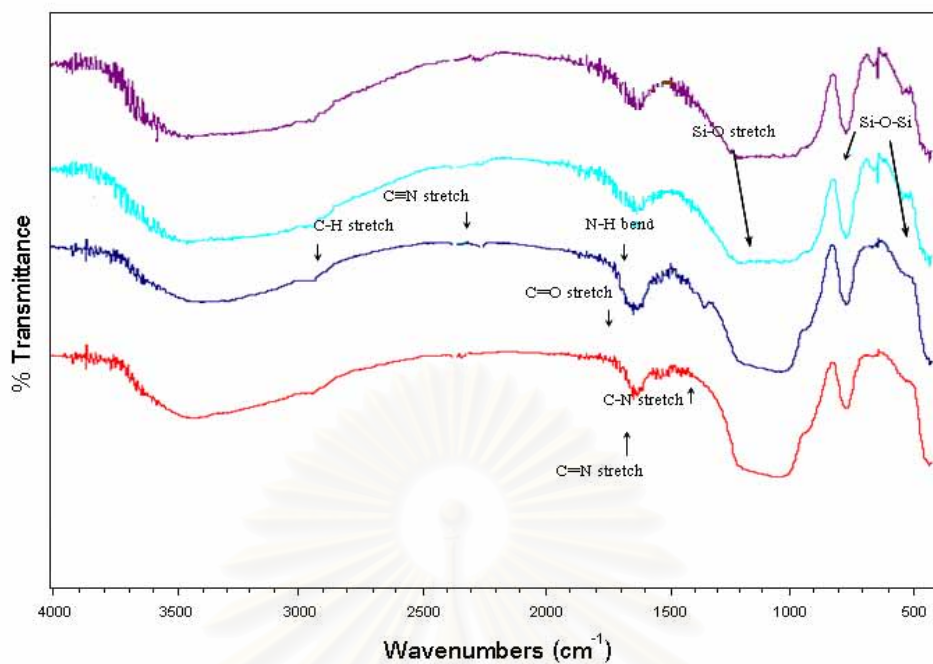


**Figure 4.1** FT-IR spectra of SBA-15, AP- SBA-15, CA- SBA-15 and Amido- SBA-15 in KBr.

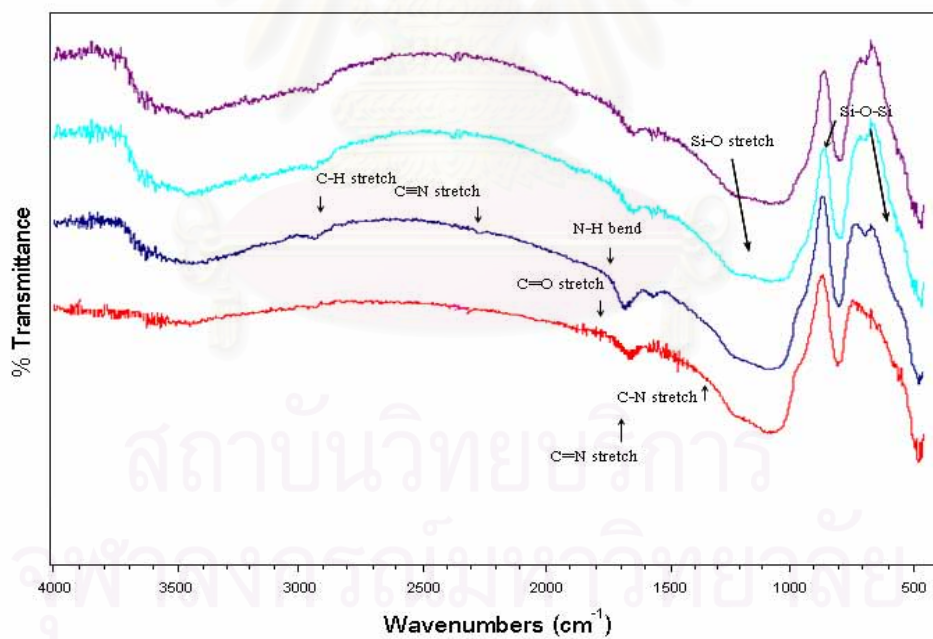


**Figure 4.2** FT-IR spectra of MCM-41, AP- MCM-41, CA- MCM-41 and Amido-MCM-41 in KBr.



## Appendix B

### Experimental data

Sample: Au/C

### BET Surface Area Report

BET Surface Area:	$646.6439 \pm 8.8984 \text{ m}^2/\text{g}$
Slope:	$0.006764 \pm 0.000092 \text{ g/cm}$
Y-Intercept:	$-0.000033 \pm 0.000012 \text{ g/}$
C:	-207.121140
Qm:	$148.5445 \text{ cm}^3/\text{g STP}$
Correlation Coefficient:	0.9997239
Sectional Area:	$0.1620 \text{ nm}^2$

**Table B-1** BET Surface Area Report

Relative Pressure (P/Po)	Quantity Adsorbed (cm <sup>3</sup> /g STP)	1/[Q(Po/P - 1)]
0.069	167.927	0.0004
0.081	170.562	0.0005
0.121	177.299	0.0008
0.161	183.163	0.0011
0.200	188.051	0.0014

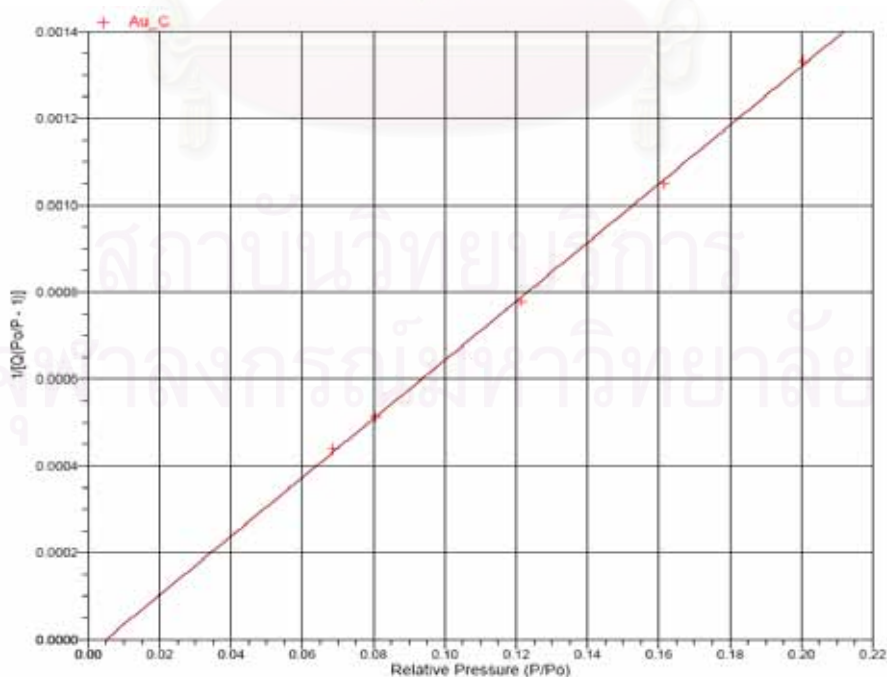


**Figure B-1** BET Surface Area Report of Au/C

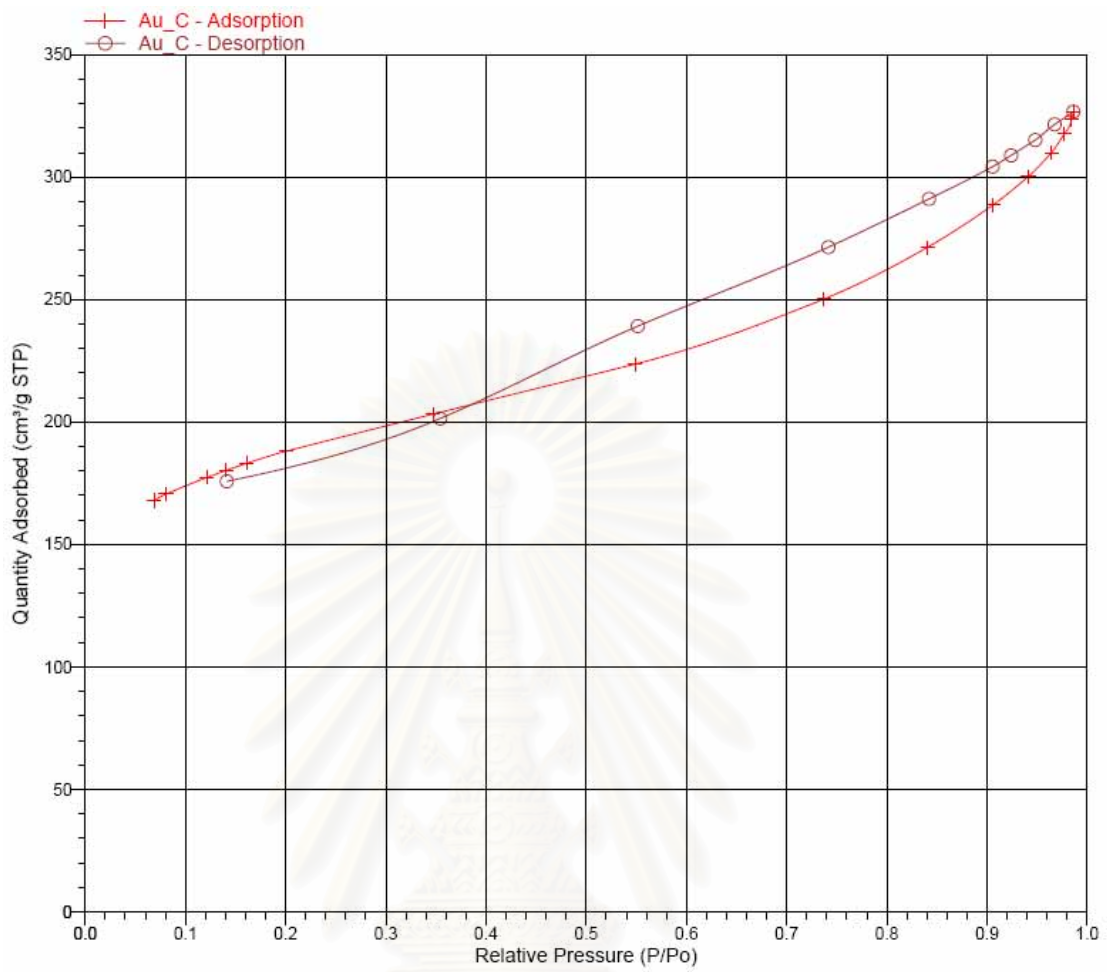


**Figure B-2** Isotherm Linear Plot of Au/C

สถาบันวิทยบริการ  
จุฬาลงกรณ์มหาวิทยาลัย

Sample: Au/SiO<sub>2</sub>

### BET Surface Area Report

BET Surface Area: 631.8551 ± 2.1298 m<sup>2</sup>/g  
 Slope: 0.006797 ± 0.000023 g/cm<sup>3</sup> STP  
 Y-Intercept: 0.000092 ± 0.000003 g/cm<sup>3</sup> STP  
 C: 74.794946  
 Qm: 145.1473 cm<sup>3</sup>/g STP  
 Correlation Coefficient: 0.9999828  
 Molecular Cross-Sectional Area: 0.1620 nm<sup>2</sup>

**Table B-2** BET Surface Area Report

Relative Pressure (P/Po)	Quantity Adsorbed (cm <sup>3</sup> /g STP)	1/[Q(Po/P - 1)]
0.066	130.906	0.0005
0.079	136.614	0.0006
0.121	149.880	0.0009
0.160	161.438	0.0012
0.199	172.130	0.0014

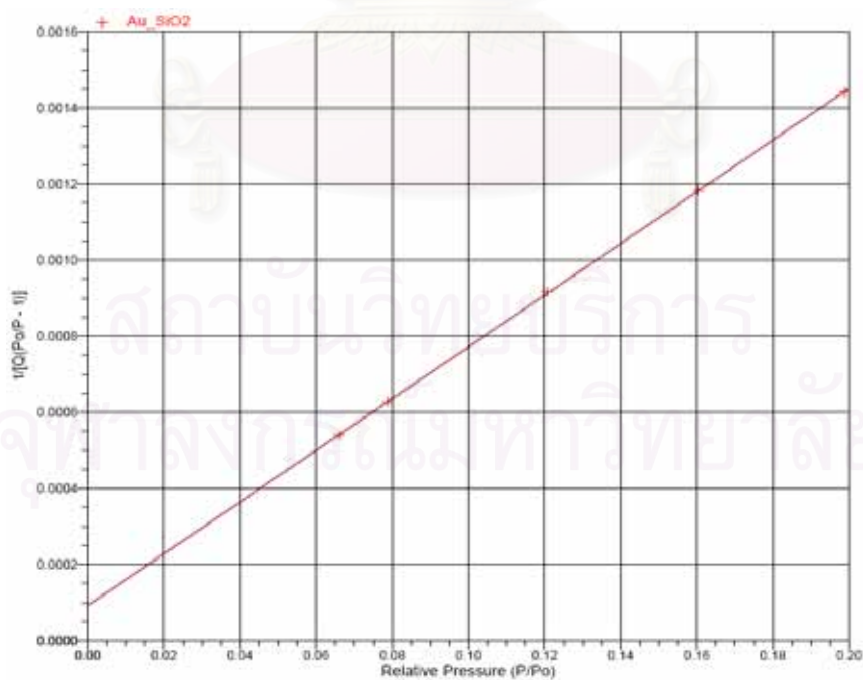


**Figure B-3** BET Surface Area Report of Au/SiO<sub>2</sub>

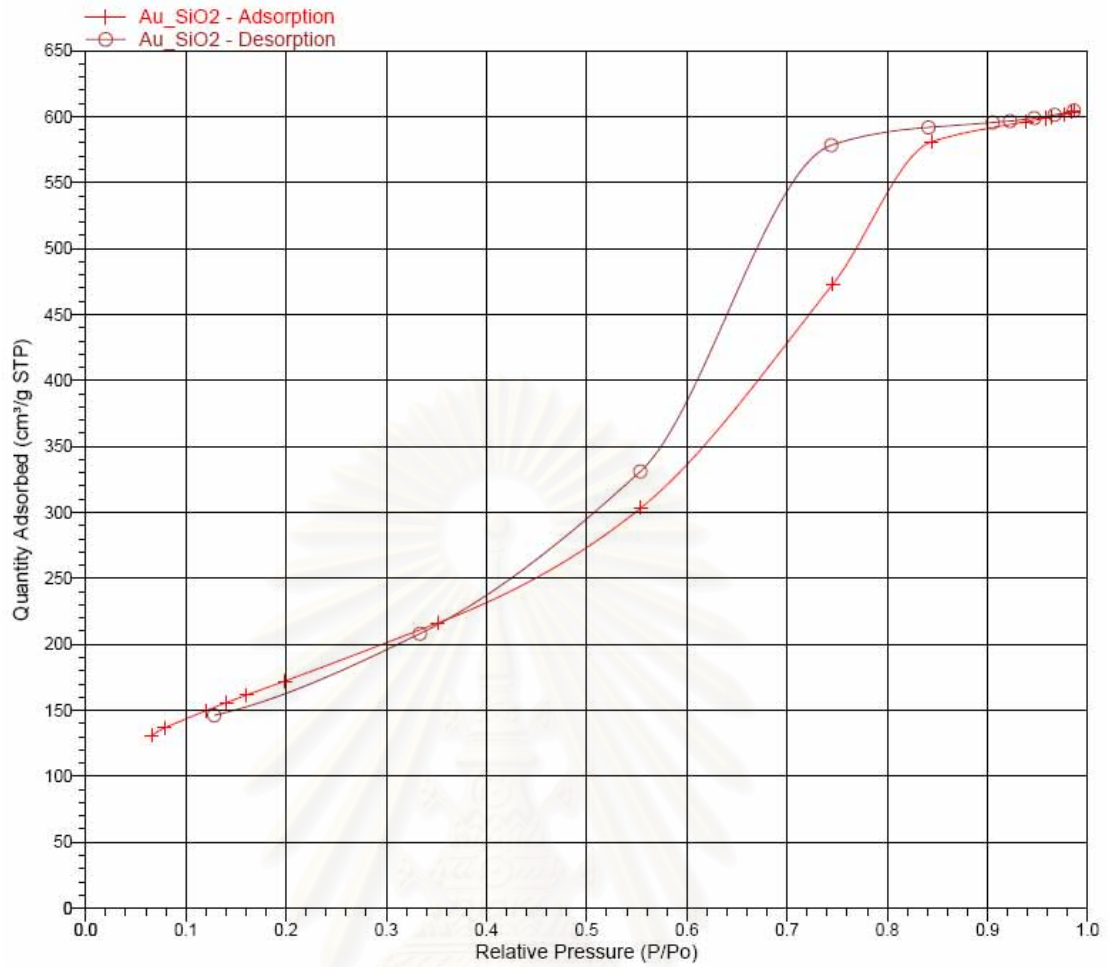


**Figure B-4** Isotherm Linear Plot of Au/SiO<sub>2</sub>

สถาบันวิทยบริการ  
จุฬาลงกรณ์มหาวิทยาลัย

**Sample: Au/Amido-SiO<sub>2</sub>**

**BET Surface Area Report**

BET Surface Area: 305.5857 ± 2.2549 m<sup>2</sup>/g  
 Slope: 0.013971 ± 0.000104 g/cm<sup>3</sup> STP  
 Y-Intercept: 0.000274 ± 0.000014 g/cm<sup>3</sup> STP  
 C: 51.926380  
 Qm: 70.1980 cm<sup>3</sup>/g STP  
 Correlation Coefficient: 0.9999166  
 Molecular Cross-Sectional Area: 0.1620 nm<sup>2</sup>

**Table B-3** BET Surface Area Report

Relative Pressure (P/Po)	Quantity Adsorbed (cm <sup>3</sup> /g STP)	1/[Q(Po/P - 1)]
0.066	59.425	0.0012
0.080	62.436	0.0014
0.120	69.423	0.0020
0.160	75.758	0.0025
0.200	81.741	0.0031

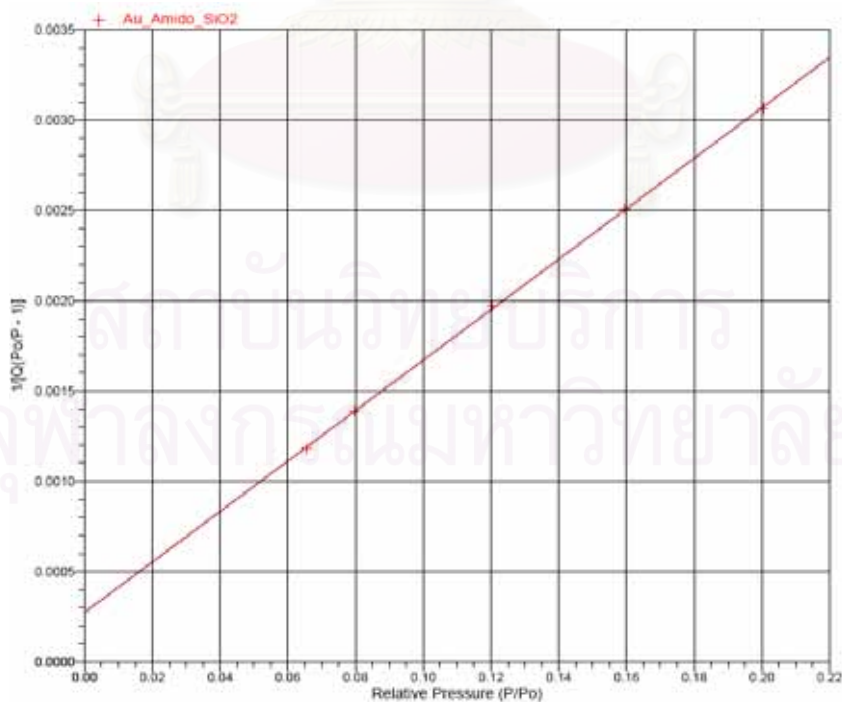


**Figure B-5** BET Surface Area Report of Au/Amido-SiO<sub>2</sub>

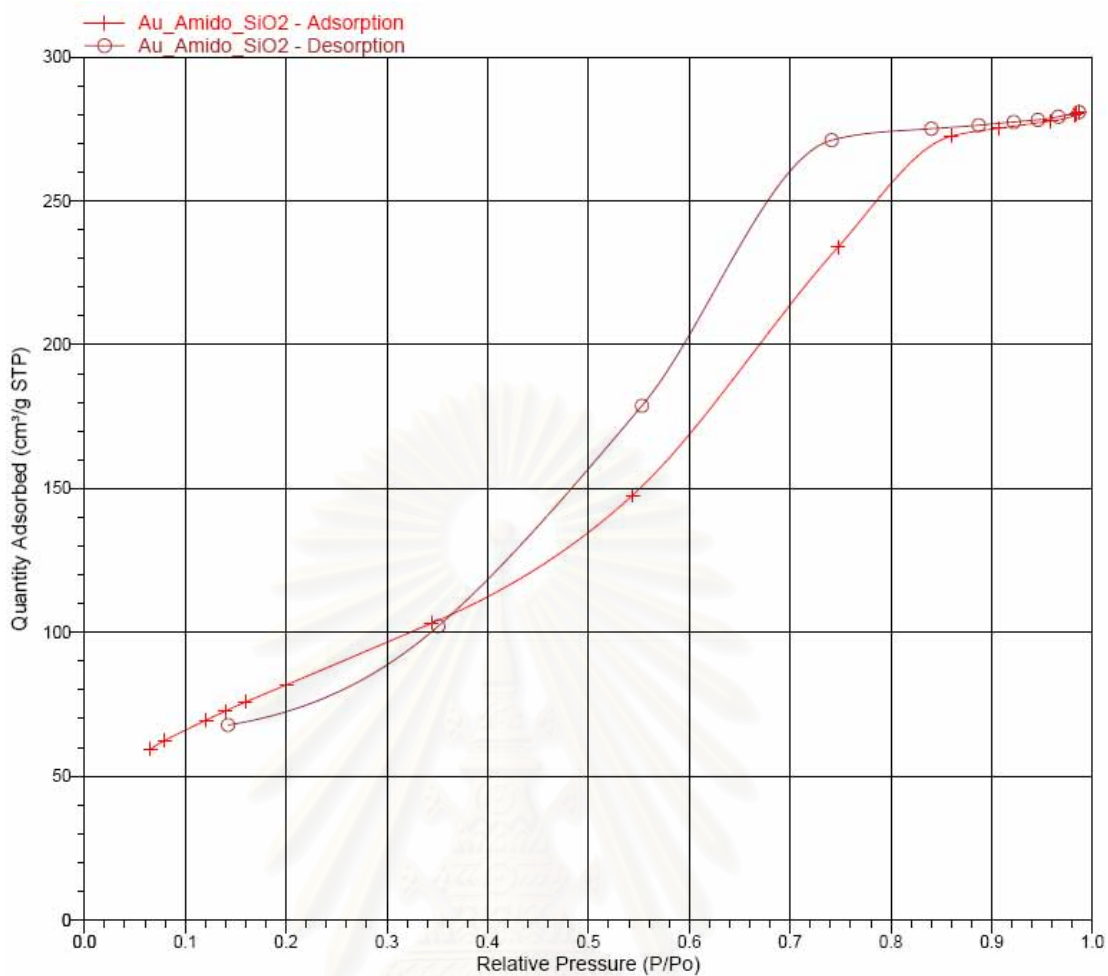


**Figure B-6** Isotherm Linear Plot of Au/Amido-SiO<sub>2</sub>

สถาบันวิทยบริการ  
จุฬาลงกรณ์มหาวิทยาลัย

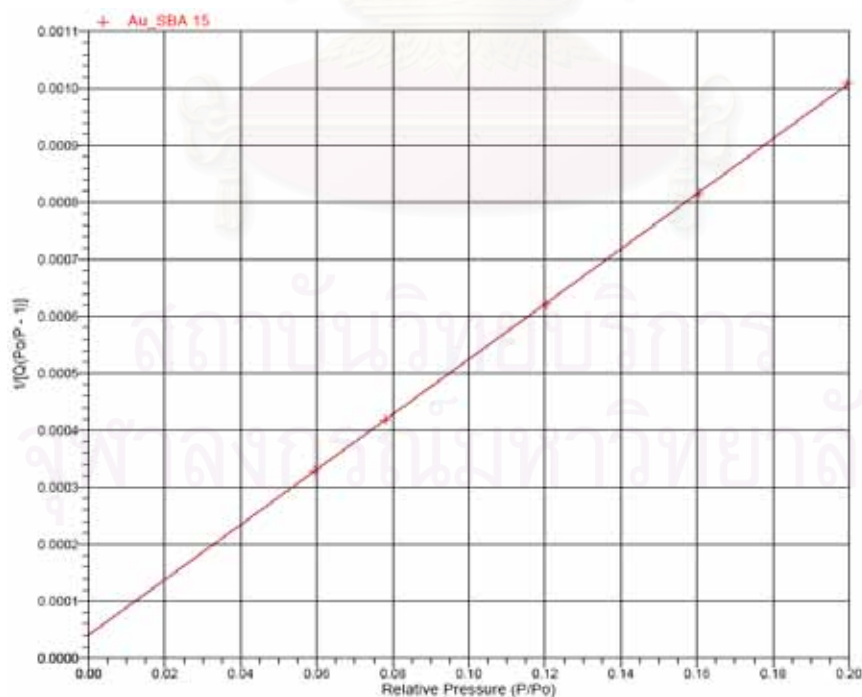


**Sample: Au/SBA-15****BET Surface Area Report**

BET Surface Area:  $892.0126 \pm 4.1269 \text{ m}^2/\text{g}$   
 Slope:  $0.004839 \pm 0.000022 \text{ g}/\text{cm}^3 \text{ STP}$   
 Y-Intercept:  $0.000041 \pm 0.000003 \text{ g}/\text{cm}^3 \text{ STP}$   
 C: 119.015544  
 Qm:  $204.9097 \text{ cm}^3/\text{g STP}$   
 Correlation Coefficient: 0.9999679  
 Molecular Cross-Sectional Area:  $0.1620 \text{ nm}^2$

**Table B-4** BET Surface Area Report

Relative Pressure (P/Po)	Quantity Adsorbed (cm <sup>3</sup> /g STP)	1/[Q(Po/P - 1)]
0.059	191.502	0.0003
0.078	201.785	0.0004
0.120	220.186	0.0006
0.160	234.542	0.0008
0.199	246.956	0.0010

**Figure B-7** BET Surface Area Report of Au/SBA-15

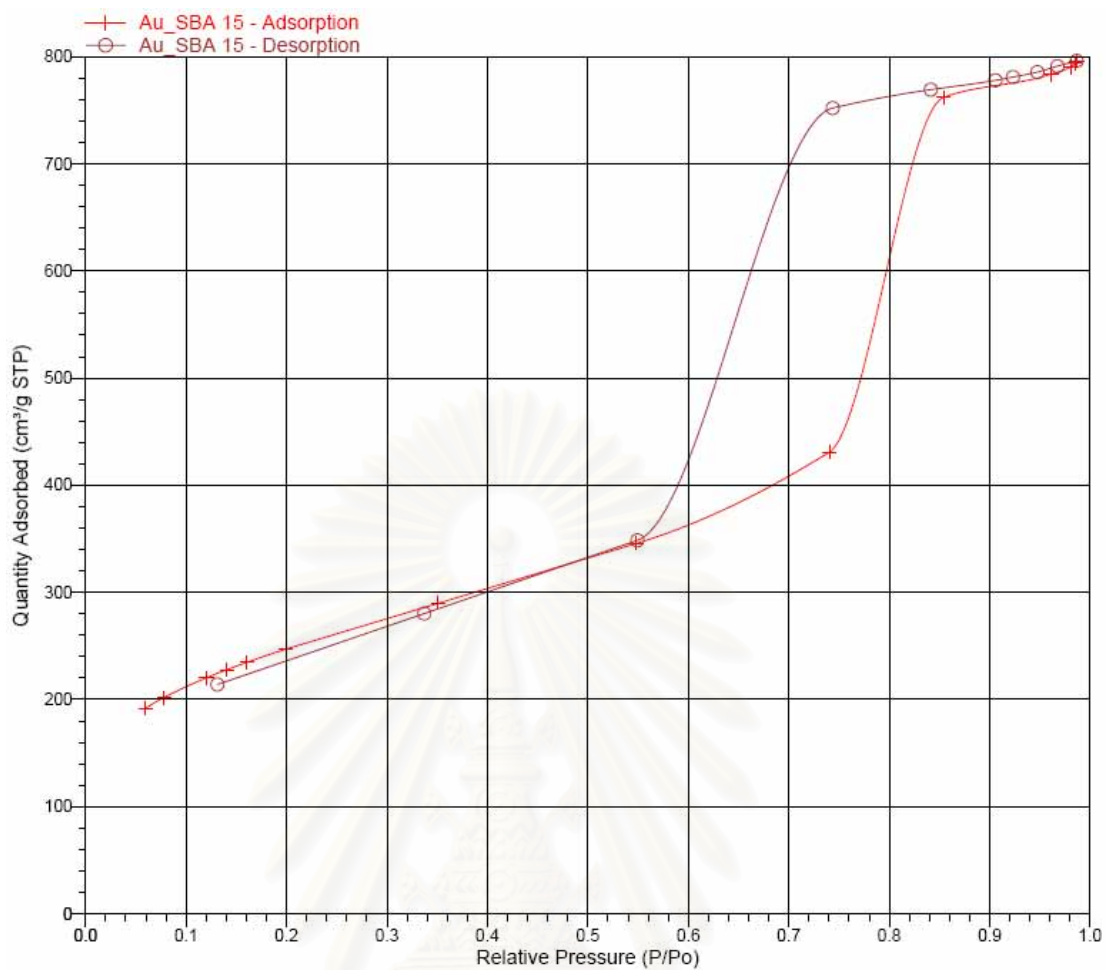


**Figure B-8** Isotherm Linear Plot of Au/SBA-15

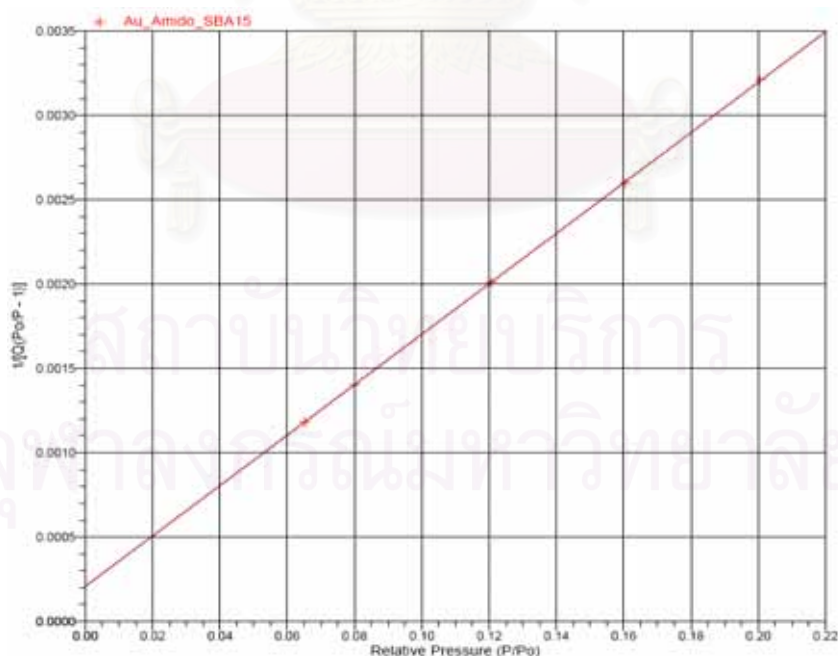
สถาบันวิทยบริการ  
จุฬาลงกรณ์มหาวิทยาลัย

**Sample: Au/Amido-SBA-15****BET Surface Area Report**

BET Surface Area:	287.1902 ± 0.6734 m <sup>2</sup> /g
Slope:	0.014950 ± 0.000035 g/cm <sup>3</sup> STP
Y-Intercept:	0.000208 ± 0.000005 g/cm <sup>3</sup> STP
C:	72.852951
Qm:	65.9722 cm <sup>3</sup> /g STP
Correlation Coefficient:	0.9999917
Molecular Cross-Sectional Area:	0.1620 nm <sup>2</sup>

**Table B-5** BET Surface Area Report

Relative Pressure (P/Po)	Quantity Adsorbed (cm <sup>3</sup> /g STP)	1/[Q(Po/P - 1)]
0.065	59.006	0.0012
0.080	61.847	0.0014
0.120	68.145	0.0020
0.160	73.471	0.0026
0.200	78.152	0.0032

**Figure B-9** BET Surface Area Report of Au/Amido-SBA-15

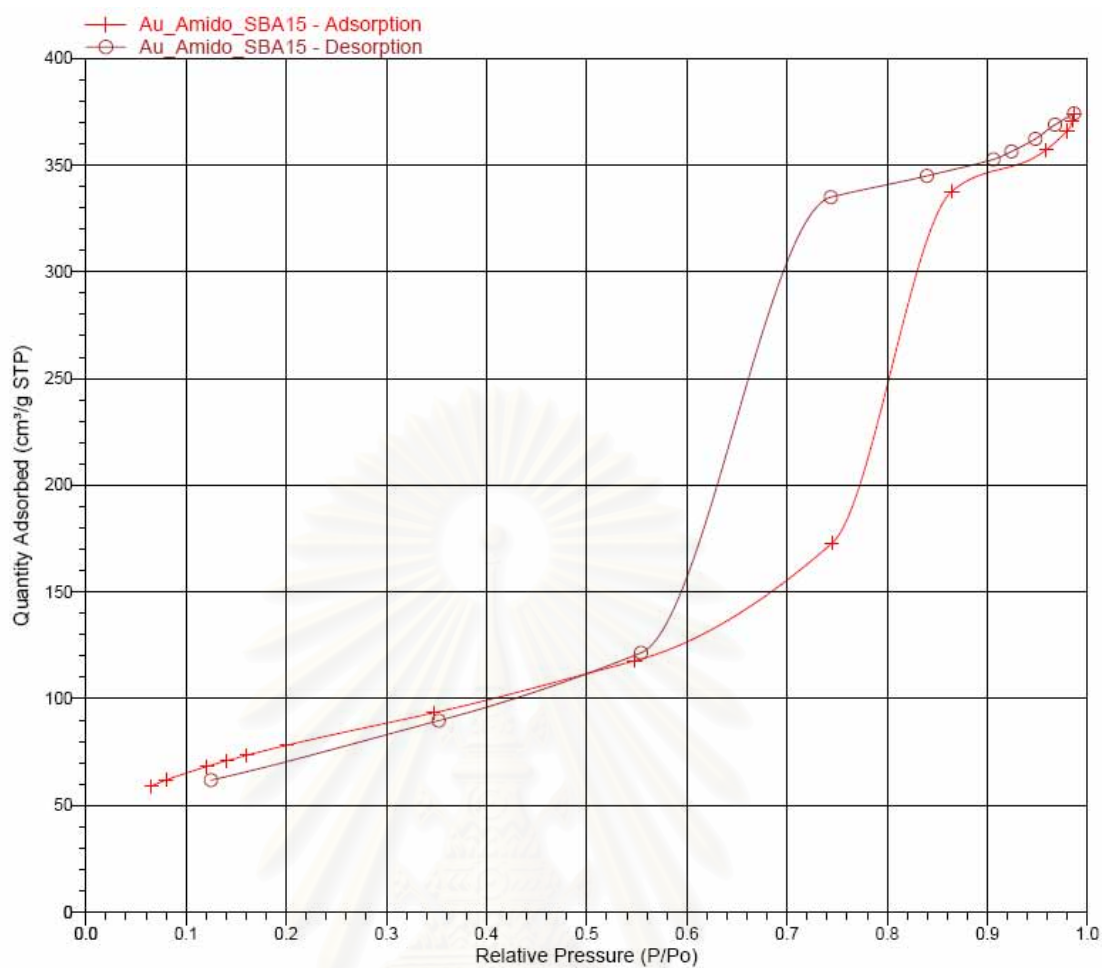


**Figure B-10** Isotherm Linear Plot of Au/Amido-SBA-15

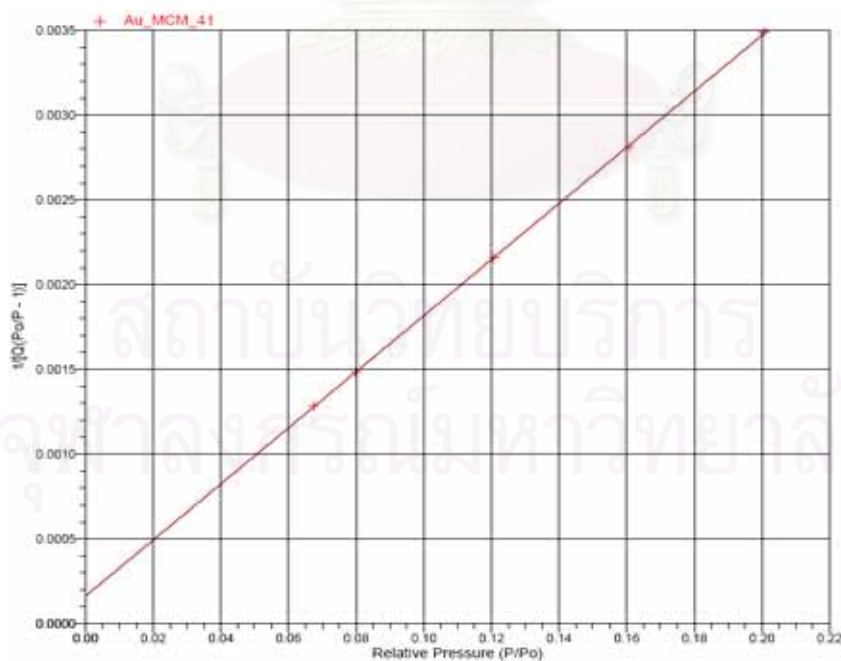
สถาบันวิทยบริการ  
จุฬาลงกรณ์มหาวิทยาลัย

**Sample: Au/MCM-41****BET Surface Area Report**

BET Surface Area:	$760.5478 \pm 1.1271 \text{ m}^2/\text{g}$
Slope:	$0.016545 \pm 0.000072 \text{ g}/\text{cm}^3 \text{ STP}$
Y-Intercept:	$0.000163 \pm 0.000010 \text{ g}/\text{cm}^3 \text{ STP}$
C:	102.636034
Qm:	$59.8520 \text{ cm}^3/\text{g STP}$
Correlation Coefficient:	0.9999719
Molecular Cross-Sectional Area:	$0.1620 \text{ nm}^2$

**Table B-6** BET Surface Area Report

Relative Pressure (P/Po)	Quantity Adsorbed (cm <sup>3</sup> /g STP)	1/[Q(Po/P - 1)]
0.067	56.448	0.0012
0.080	58.431	0.0015
0.121	63.587	0.0022
0.161	68.121	0.0028
0.201	71.914	0.0035

**Figure B-11** BET Surface Area Report of Au/MCM-41

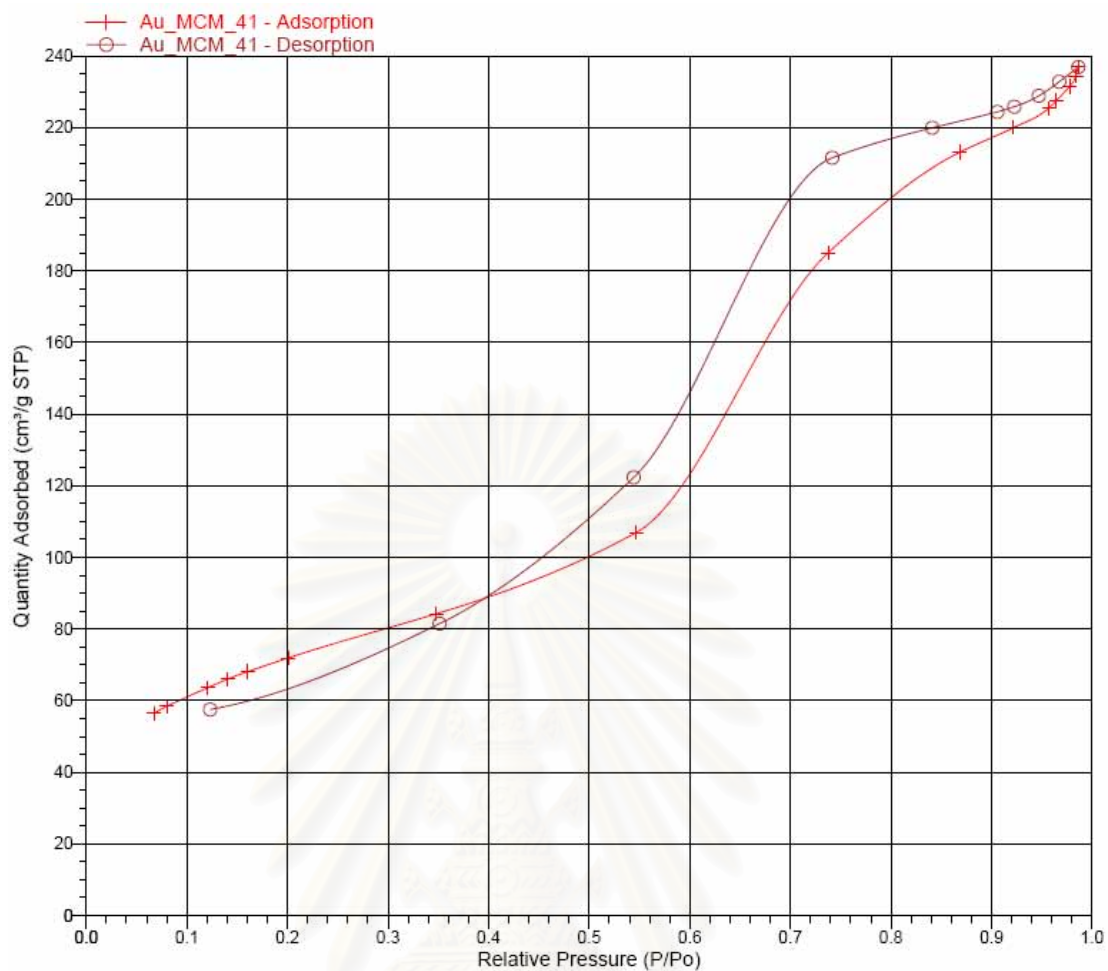


**Figure B-12** Isotherm Linear Plot of Au/MCM-41

สถาบันวิทยบริการ  
จุฬาลงกรณ์มหาวิทยาลัย

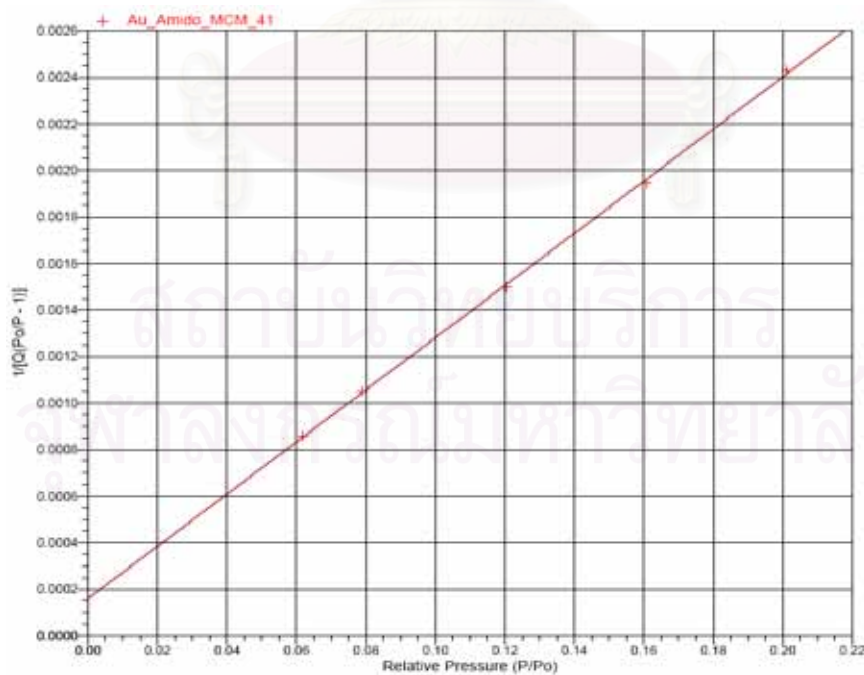


**Sample: Au/Amido-MCM-41****BET Surface Area Report**

BET Surface Area:	$382.9538 \pm 4.4870 \text{ m}^2/\text{g}$
Slope:	$0.011207 \pm 0.000132 \text{ g}/\text{cm}^3 \text{ STP}$
Y-Intercept:	$0.000160 \pm 0.000018 \text{ g}/\text{cm}^3 \text{ STP}$
C:	70.830869
Qm:	$87.9707 \text{ cm}^3/\text{g STP}$
Correlation Coefficient:	0.9997920
Molecular Cross-Sectional Area:	$0.1620 \text{ nm}^2$

**Table B-7** BET Surface Area Report

Relative Pressure (P/Po)	Quantity Adsorbed (cm <sup>3</sup> /g STP)	1/[Q(Po/P - 1)]
0.062	76.669	0.0009
0.079	81.567	0.0011
0.120	91.307	0.0015
0.161	98.447	0.0019
0.201	103.598	0.0024

**Figure B-13** BET Surface Area Report of Au/Amido-MCM-41

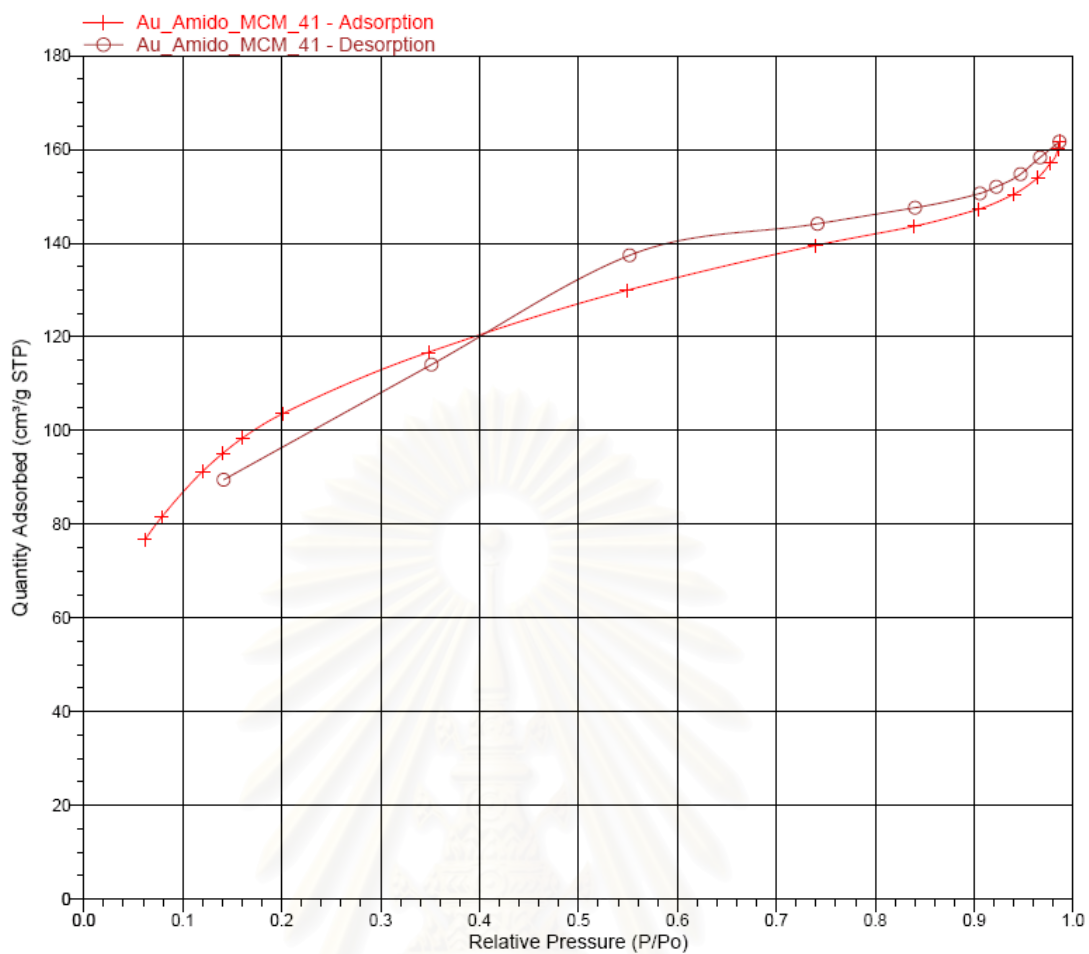


**Figure B-14** Isotherm Linear Plot of Au/Amido-MCM-41

สถาบันวิทยบริการ  
จุฬาลงกรณ์มหาวิทยาลัย

## XRD analysis of MCM-41

### Sample of name MCM-41

X-ray: Cu/ 40kv/ 20mA  
Sampling Width: 0.02 deg.  
Scanning Speed: 1.000 deg./min.  
Divergence Slit: 1 deg.  
Scattering Slit : 1 deg.  
Scan range: 0.500 – 8.000 deg.

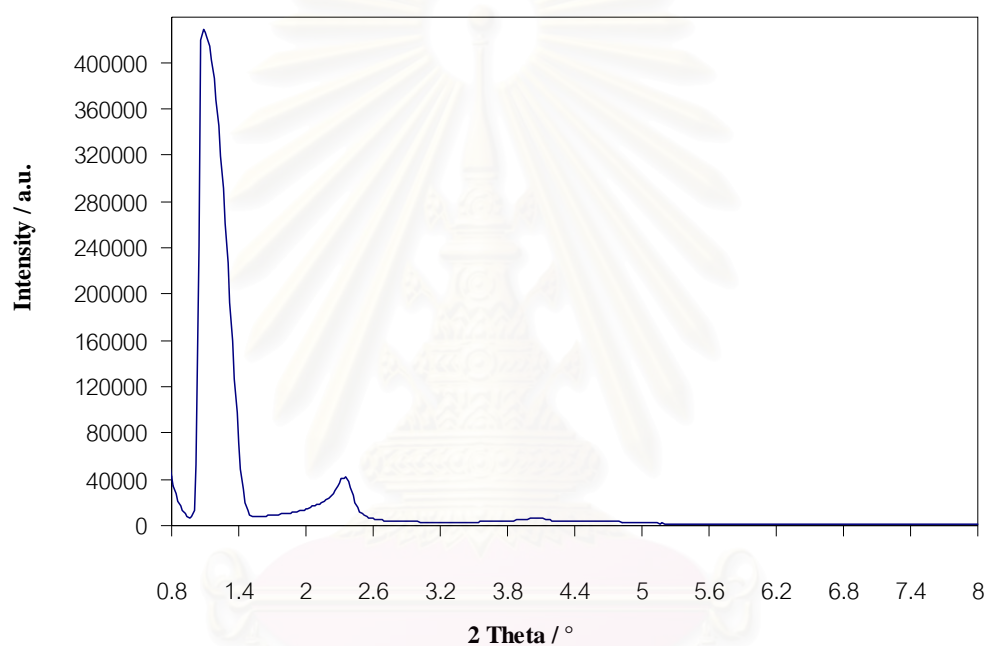


**Figure B-15** XRD pattern of MCM-41.

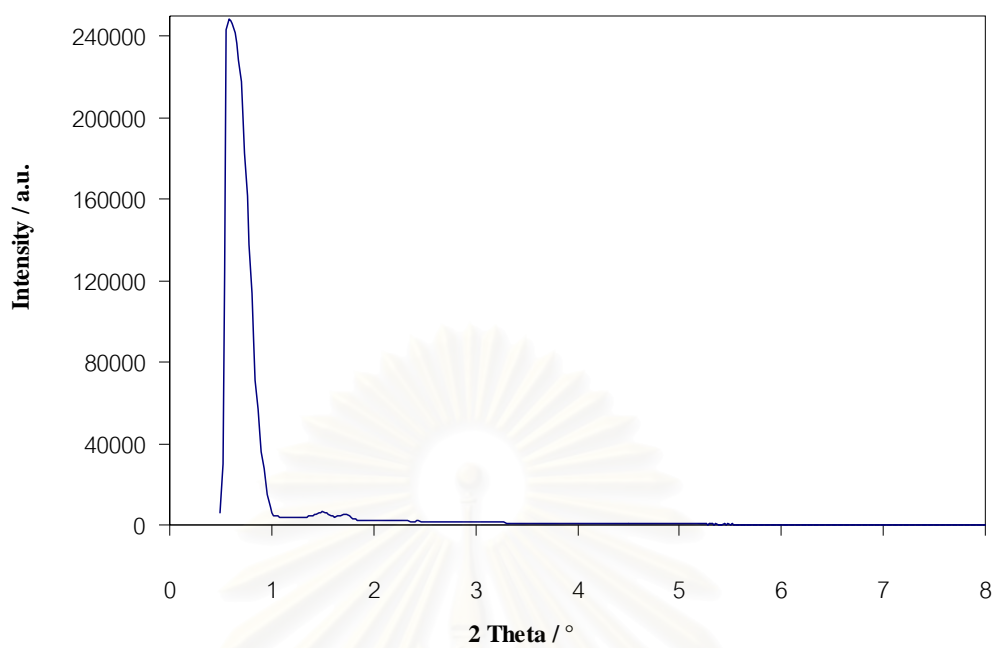


**Figure B-16** XRD pattern of SBA-15.

สถาบันวิทยบริการ  
จุฬาลงกรณ์มหาวิทยาลัย

## APPENDIX C

**Table C-1** Retention time of possible products from glycerol oxidation by HPLC condition listed in Table 4.3 at 245 nm

Products	Retention time (min)			
	UV detector		RI detector	
	Salt	Acid	Salt	Acid
Acid products				
Glyoxylic acid	6.94	10.99	s/p	11.42
Glyceric acid	7.24	12.32	7.6	12.87
Glycolic acid	7.95	14	s/p	14.38
Oxalic acid	8.22	14.34	8.68	14.97
Tartronic acid	9.37	15.83	10.3	16.2
Non-acid products				
Glyceraldehyde	12.93		13.2	
Dihydroxyacetone	15.3		15.73	

## APPENDIX D

## Calibration curve and Chromatogram analysis by HPLC

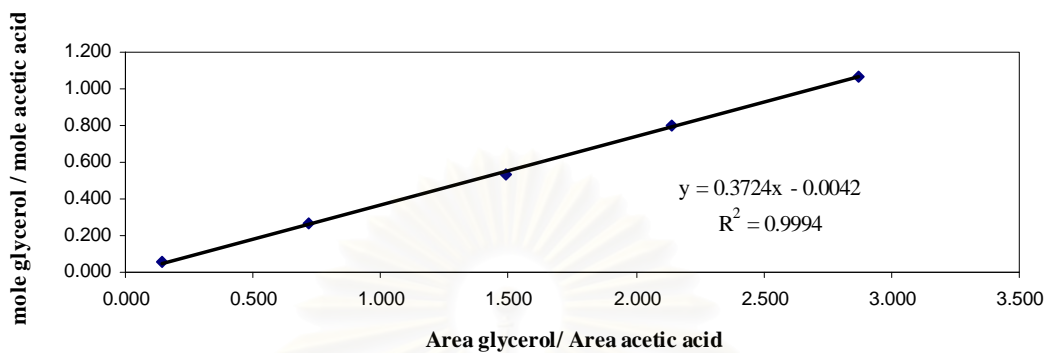


Figure D-1 A chromatogram of Calibration curve glycerol

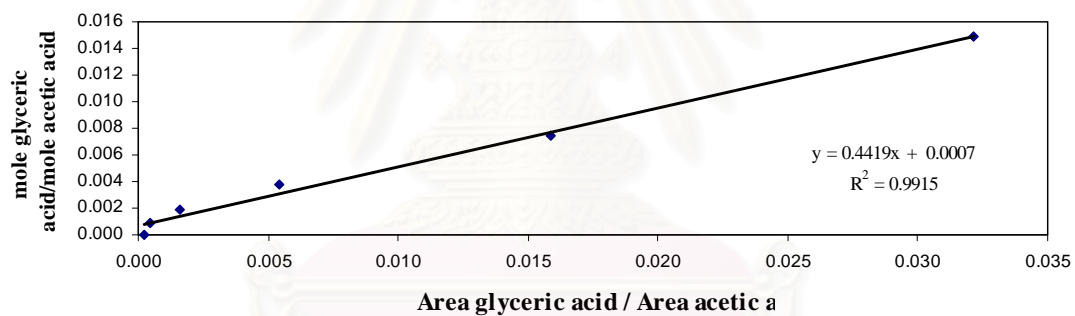
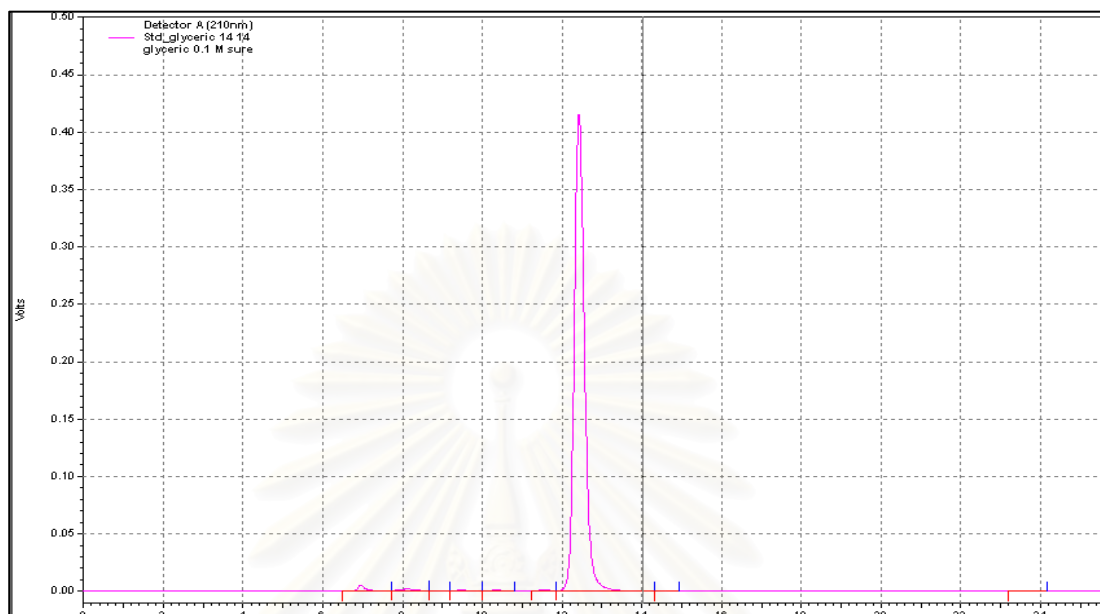


Figure D-2 A chromatogram of Calibration curve glyceric acid

สถาบันวิทยบริการ  
จุฬาลงกรณ์มหาวิทยาลัย



**Chromatogram of possible products from glycerol oxidation by HPLC condition listed in Table 4.3 at 245 nm**



**Figure D-3** A chromatogram of Glyceric acid in UV detector

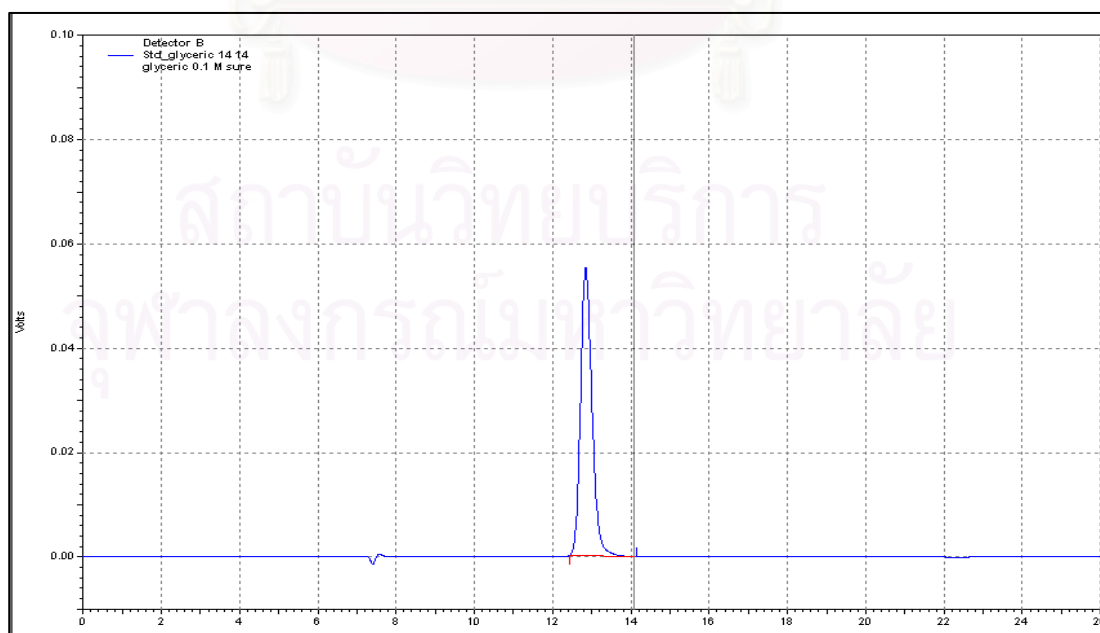


**Figure D-4** A chromatogram of Glyceric acid in RI detector

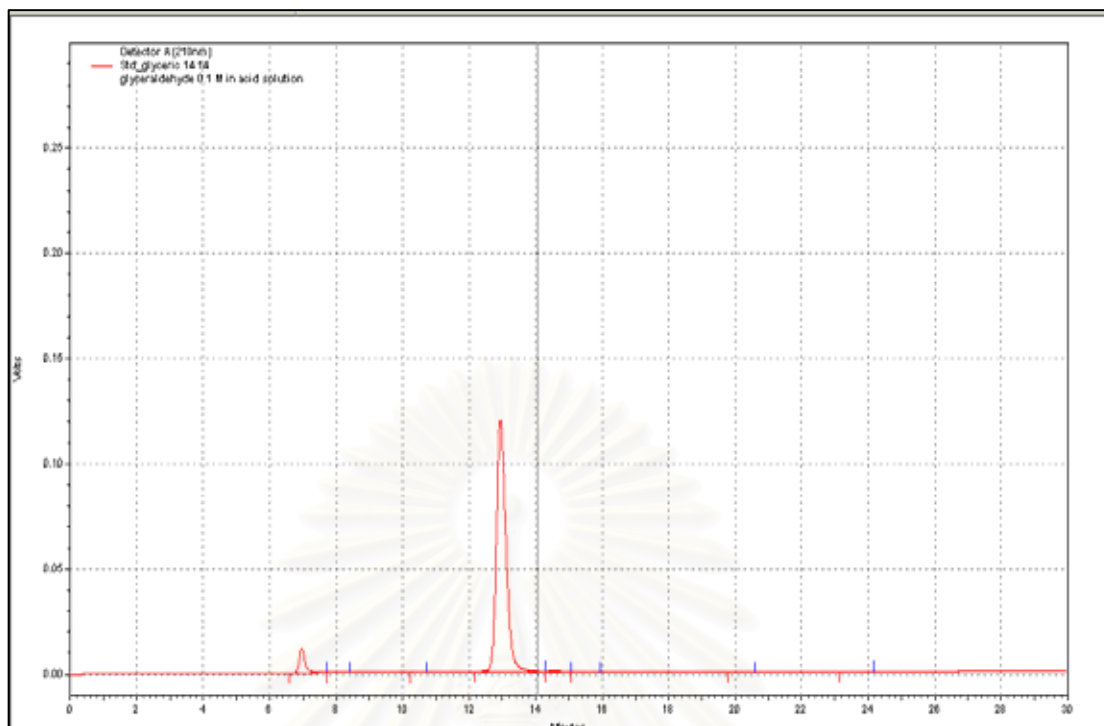


**Figure D-5** A chromatogram of Glyceraldehyde in UV detector

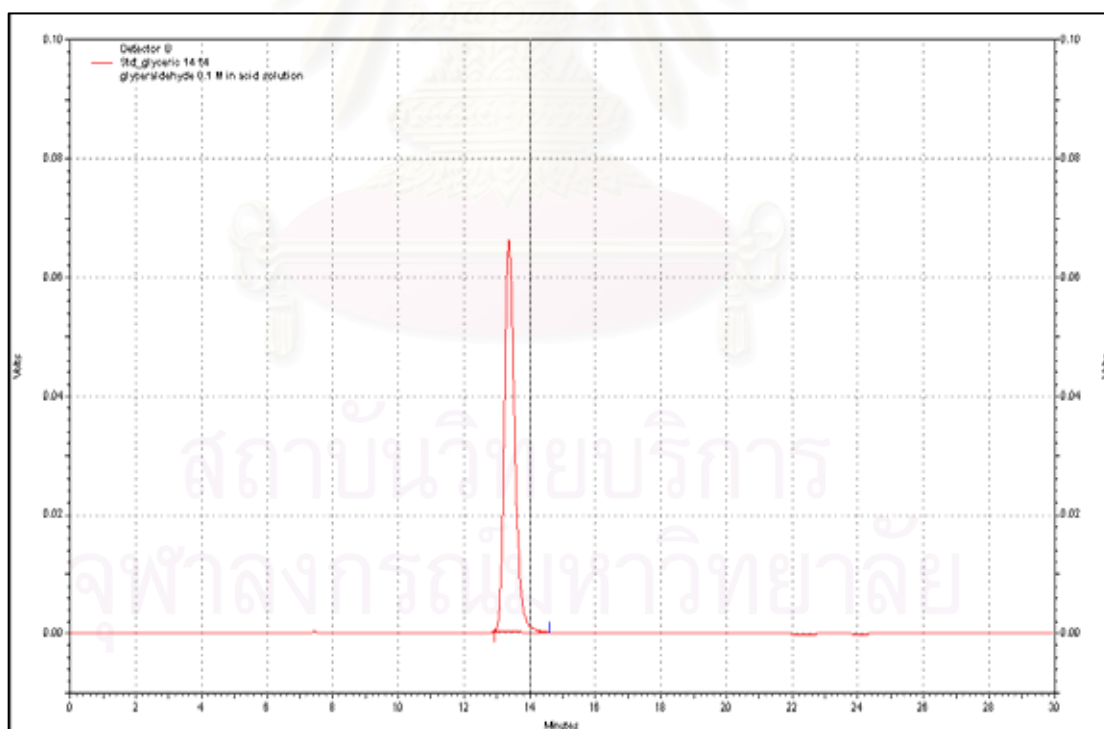


**Figure D-6** A chromatogram of Glyceraldehyde in RI detector

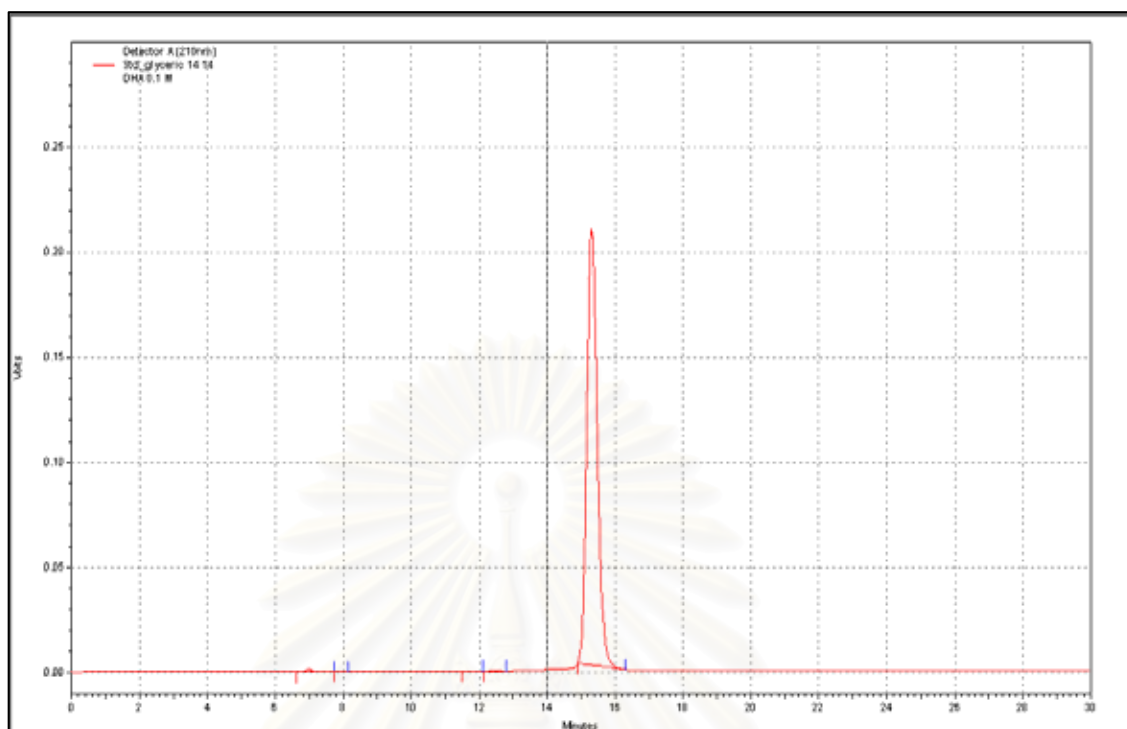


**Figure D-7** A chromatogram of Dihydroxyacetone in UV detector

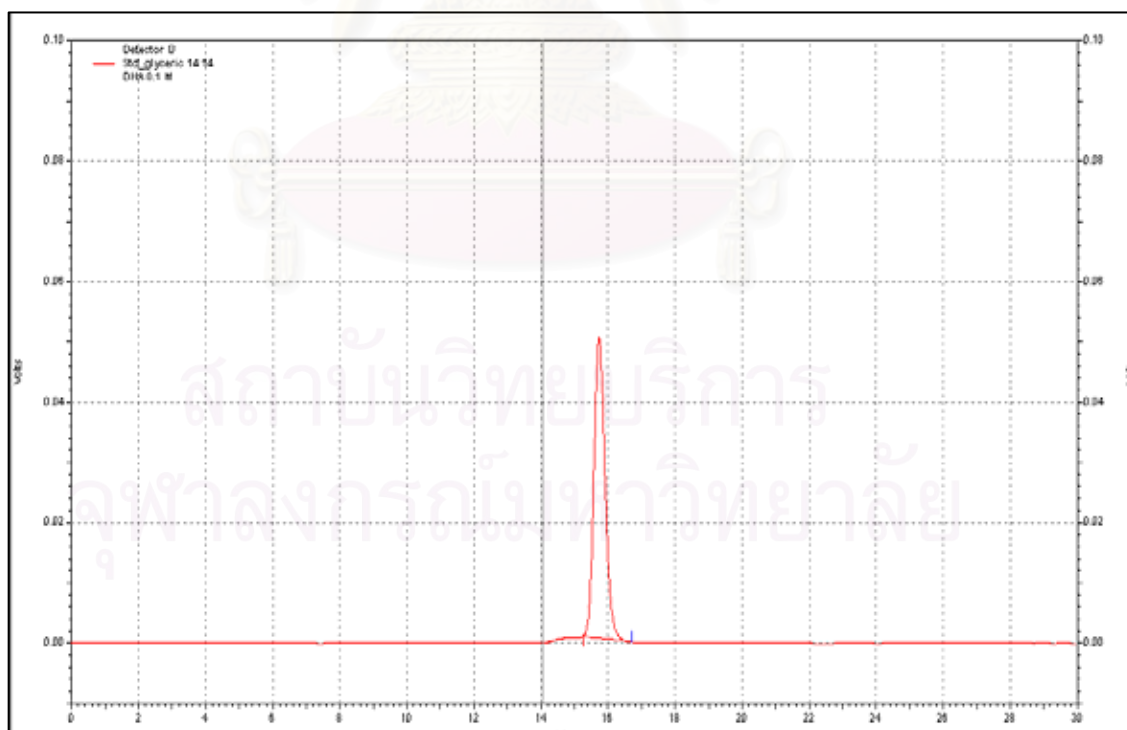


**Figure D-8** A chromatogram of Dihydroxyacetone in RI detector

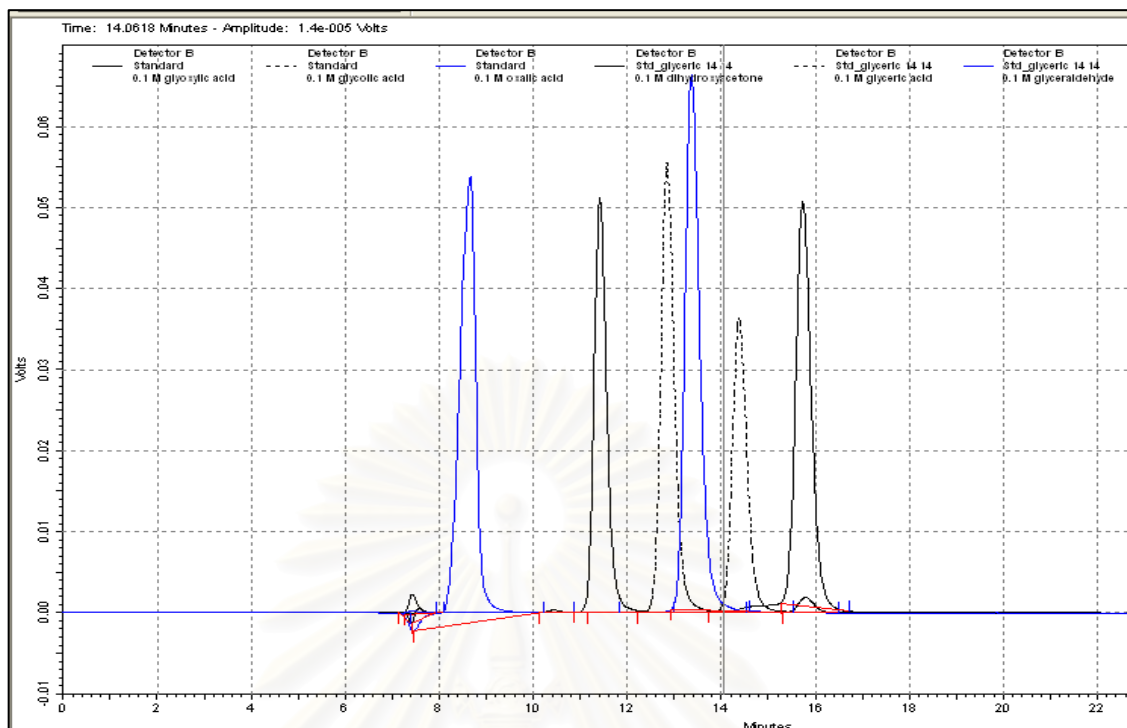


Figure D-9 A chromatogram of products in UV detector

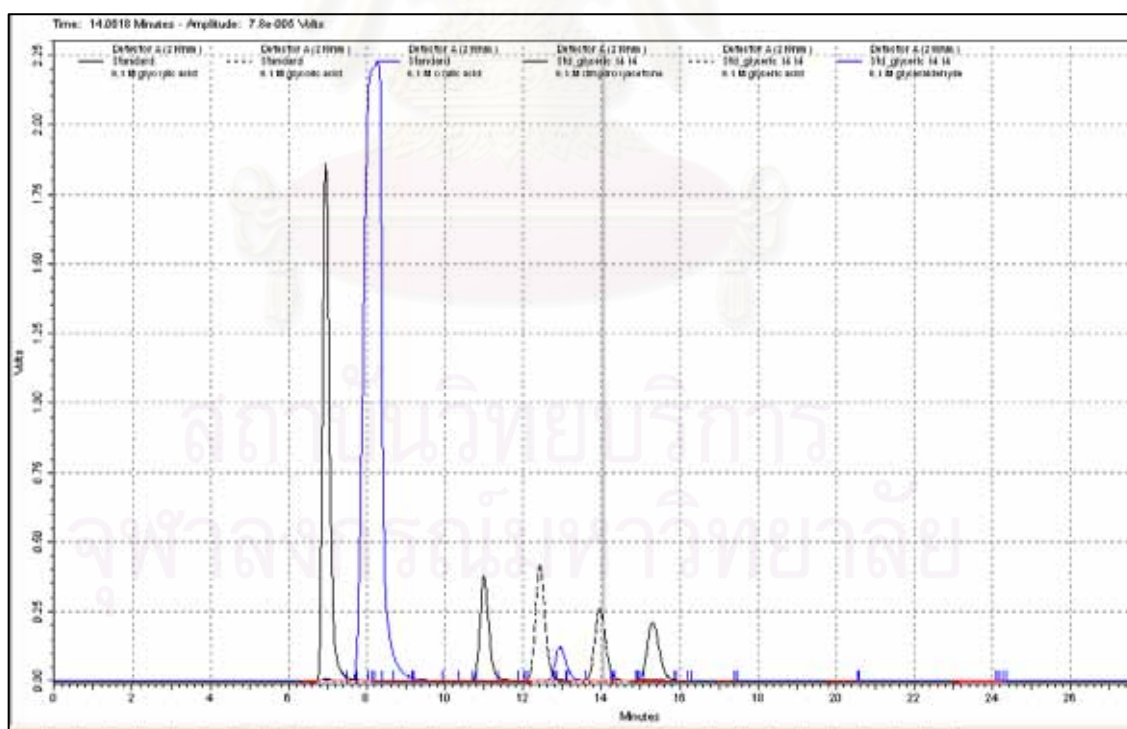


Figure D-10 A chromatogram of products in RI detector

## VITA

Mr. Taweechai Bainumngern was born on January 11, 1983 in Bangkok, Thailand. He received his Bachelor degree of Science in Industry Chemical from King Mongkut's Institute of Technology Ladkrabang in 2005. After that, he has been a graduate student at the Master study in Program of Petrochemistry and Polymer Science, Faculty of Science, Chulalongkorn University in 2005 and completed the program. The present address is 74/5 Soi Sukumvit 63, Ekkamai Road, Wattana, Bangkok, Thailand, 10110. Contact number is 087-7070903.



สถาบันวิทยบริการ  
จุฬาลงกรณ์มหาวิทยาลัย